

CALIFORNIA CURRENT INTEGRATED ECOSYSTEM ASSESSMENT (CCIEA) CALIFORNIA CURRENT ECOSYSTEM STATUS REPORT, 2021

A report of the NOAA CCIEA Team to the Pacific Fishery Management Council, March 10, 2021.

*Editors: Dr. Chris Harvey (NWFSC), Dr. Toby Garfield (SWFSC), Mr. Greg Williams (PSMFC),
and Dr. Nick Tolimieri (NWFSC)*

1 INTRODUCTION

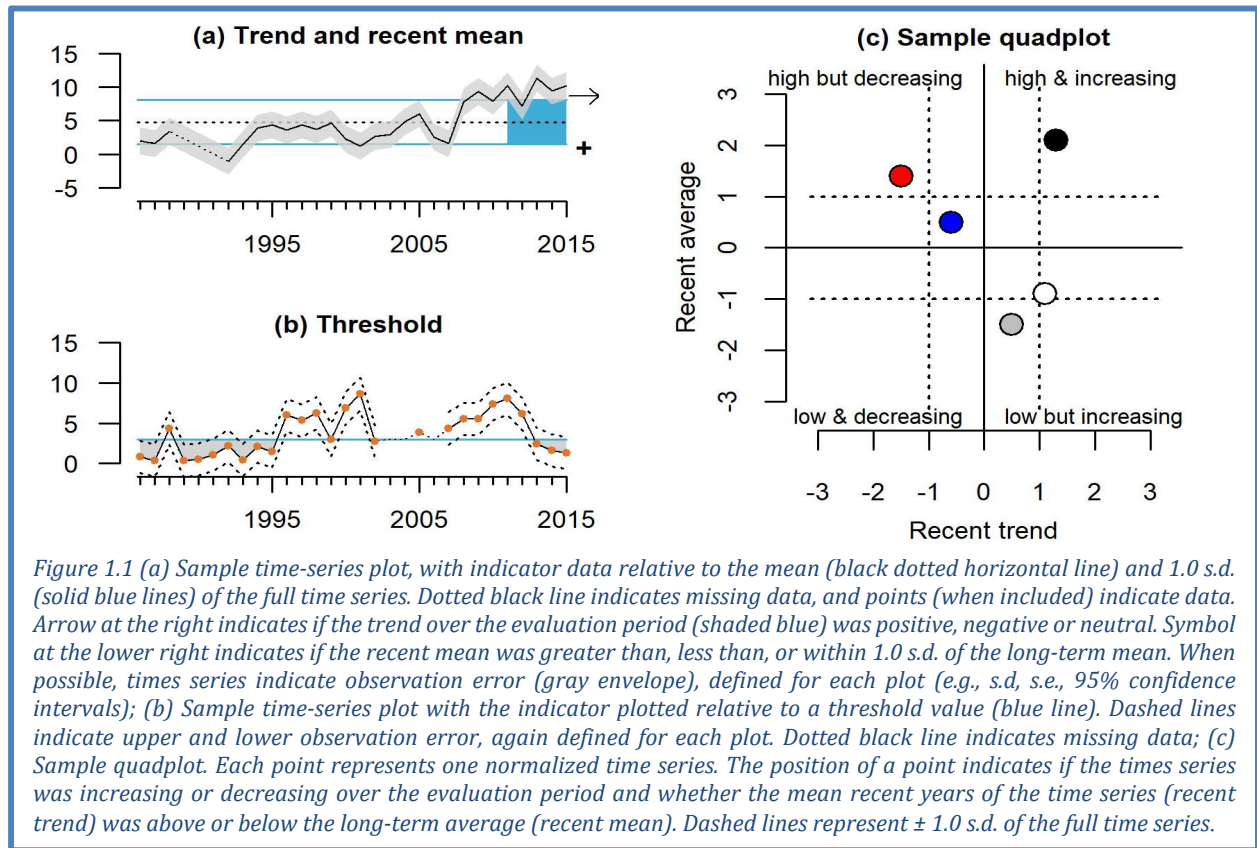
Section 1.4 of the 2013 Fishery Ecosystem Plan (FEP) established a reporting process wherein NOAA provides the Pacific Fishery Management Council (Council) with a yearly update on the status of the California Current Ecosystem (CCE), as derived from environmental, biological, economic and social indicators. NOAA's California Current Integrated Ecosystem Assessment (CCIEA) team is responsible for this report. This is our 9th report, with prior reports in 2012 and 2014-2020.

This report summarizes CCE status based on data and analyses that generally run through 2020. Highlights are summarized in Box 1.1. Appendices provide additional information or clarification, as requested by the Council, the Scientific and Statistical Committee (SSC), or other advisory bodies.

Box 1.1: Highlights of this report

- West Coast research efforts in 2020 were heavily impacted by the COVID-19 pandemic. While care should always be exercised in interpreting ecosystem indicators, that is especially true this year. As always, the CCIEA team is available to advise.
- 2020 saw a transition from El Niño conditions and positive PDO signals to La Niña conditions and a negative PDO for the first time in many years. These conditions are generally associated with higher productivity in the CCE.
- The second largest marine heatwave observed in the North Pacific occurred in 2020, but mostly stayed offshore.
- The system experienced low snowpack, drought, and catastrophic wildfires in 2020.
- Strong winter upwelling preceded the start of an average to above-average upwelling season, providing a good nutrient supply to the base of the food web.
- Foraging conditions appeared to be above average, based on measures of the zooplankton community, continued high abundance of anchovies, and production of offspring at seabird and sea lion colonies.
- Signs of concern included widespread harmful algal blooms, continued presence of species associated with warmer waters, and mixed outlooks for returns of Chinook salmon in 2021.
- Fishery landings and revenues appear to be substantially lower in 2020 compared to 2019, and the COVID-19 pandemic is one of many possible contributing factors.
- We introduce or update several analyses of coastal communities, revenue dynamics, and fishing networks that may help us understand how fishing communities respond to change.

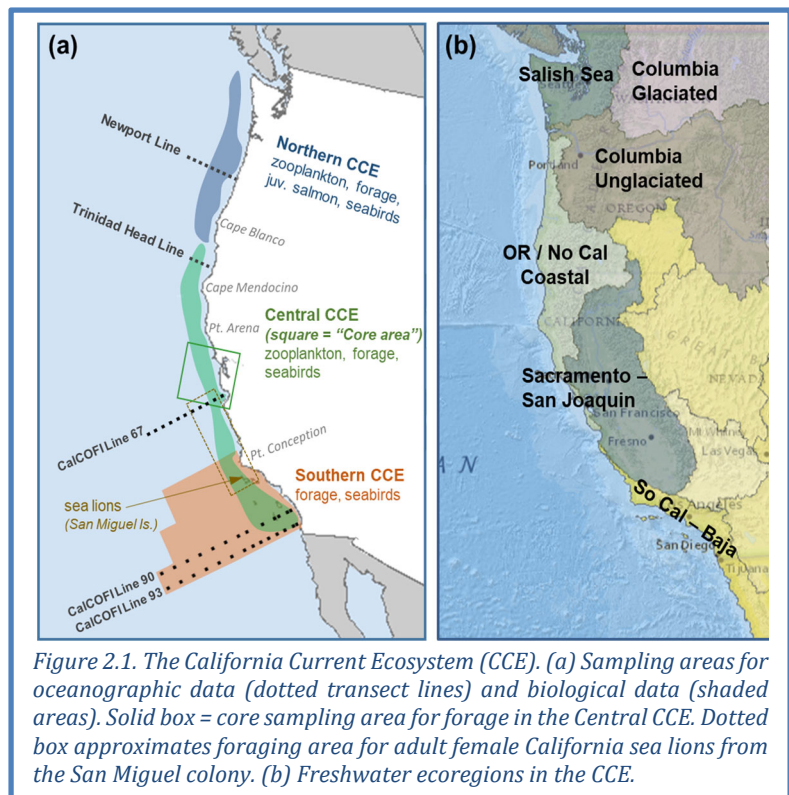
Throughout this report, most indicator plots follow the formats illustrated in Figure 1.1.



2 SAMPLING LOCATIONS

We generally refer to areas north of Cape Mendocino as the “Northern CCE,” Cape Mendocino to Point Conception as the “Central CCE”, and areas south of Point Conception as the “Southern CCE.” Figure 2.1a shows sampling areas for most regional oceanographic data. Key transects are the Newport Line off Oregon, the Trinidad Head Line off northern California, and CalCOFI lines further south. This sampling is complemented by basin-scale observations and models. Figure 2.1a also shows sampling areas for most biological indicators.

Freshwater ecoregions in the CCE are shown in Figure 2.1b, and are the basis by which we summarize indicators for snowpack, flows, and stream temperatures.



Box 2.1: COVID impacts on data—The COVID-19 pandemic impacted most West Coast survey programs in 2020, resulting in reduced data availability for many time series:

- Surveys that were cancelled completely in 2020 included NOAA’s coastwide Coastal Pelagic Species cruise and West Coast Groundfish Bottom Trawl Survey.
- Survey efforts were severely scaled back for forage species (particularly cancellations or effort reductions of critical spring cruises) and also for marine mammals and seabirds.
- Ship-based survey reductions resulted in far fewer measurements of dissolved oxygen.
- Sample processing has been delayed for many surveys.

COVID-related effects on data are noted throughout the report, and we recommend taking additional care in interpreting findings from this year’s report. As always, the CCIEA team is available to advise.

3 CLIMATE AND OCEAN DRIVERS

Climate and ocean signals showed signs of transition in 2020. Weak El Niño conditions and a positive PDO gave way to a La Niña and a negative PDO, conditions not experienced since before the 2013-2016 marine heatwave (the “Blob”). Moderate to strong upwelling north of Point Conception expanded cool coastal waters and mostly kept a new and very large marine heatwave offshore. Harmful algal blooms were widespread, while reduced snowpack and streamflow in some regions contributed to severe drought conditions. These dynamics are detailed further in the sections below.

3.1 BASIN-SCALE INDICATORS

We use three satellite-derived indices to describe large-scale physical ecosystem states. The Oceanic Niño Index (ONI) describes the equatorial El Niño Southern Oscillation (ENSO). An ONI above 0.5°C indicates El Niño conditions, which often lead to lower primary production, weaker upwelling, poleward transport of equatorial waters and species, and more southerly storm tracks in the CCE. An ONI below -0.5°C means La Niña conditions, which usually lead to higher productivity. The Pacific Decadal Oscillation (PDO) describes north Pacific sea surface temperature (SST) anomalies that may persist for many years. Positive PDOs are associated with warmer SST and lower productivity in the CCE, while negative PDOs indicate cooler SST and higher productivity. The North Pacific Gyre Oscillation (NPGO), an index of sea surface height, indicates changes in circulation that affect source waters for the CCE. Positive NPGOs are associated with strong equatorward flow and higher salinity, nutrients, and chlorophyll-*a*. Negative NPGOs are associated with decreased subarctic source water and lower CCE productivity.

Basin-scale indices suggest a return to average or above-average conditions for productivity in 2020: the ONI and PDO turned negative, while the NPGO remained negative. The ONI indicated that weak El Niño conditions, which had mostly persisted since late 2018, began to diminish in March 2020. ONI values were negative by June and La Niña conditions have existed since August 2020 (Figure 3.1.1, top). In November, ONI dropped to -1.3°C , its lowest value since 2011. NOAA forecasts a 95%

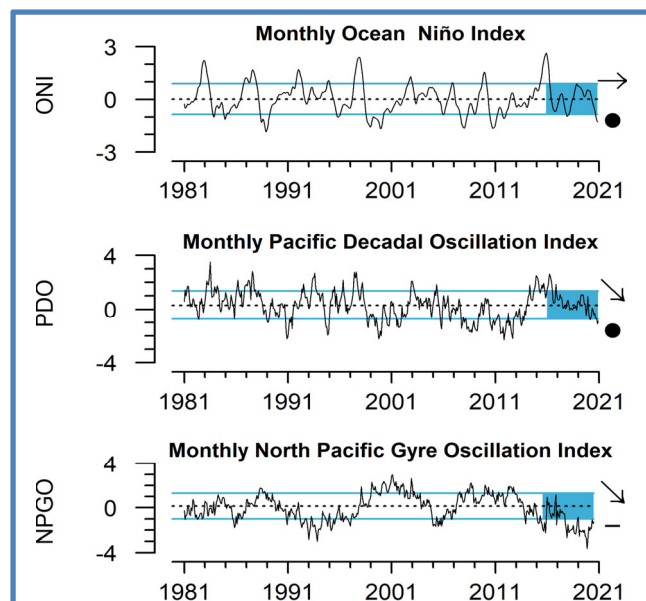
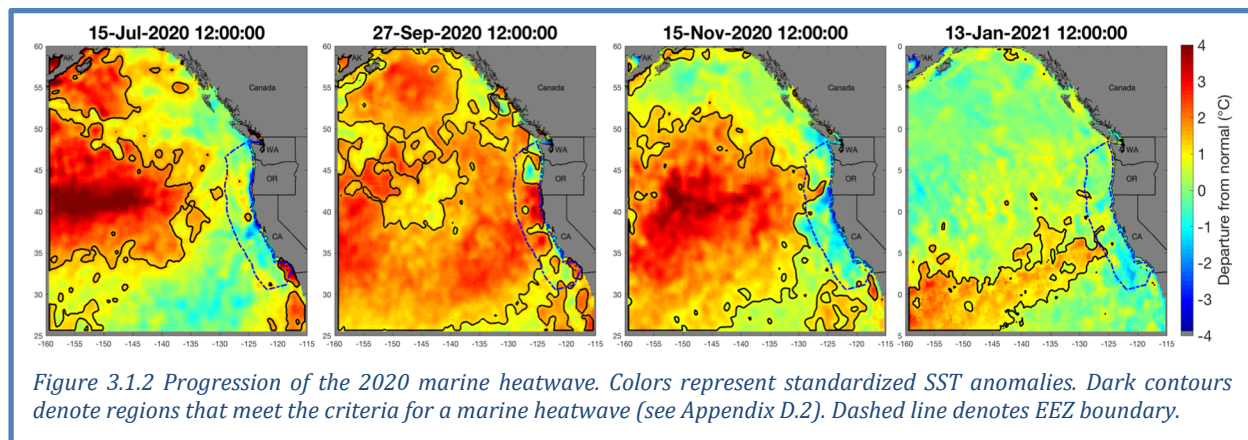


Figure 3.1.1 Monthly values of the Ocean Niño Index (ONI), Pacific Decadal Oscillation (PDO), and the North Pacific Gyre Oscillation (NPGO) from 1981-2020. Mean and s.d. for 1981-2010. Lines, colors, and symbols are as in Fig. 1.1.

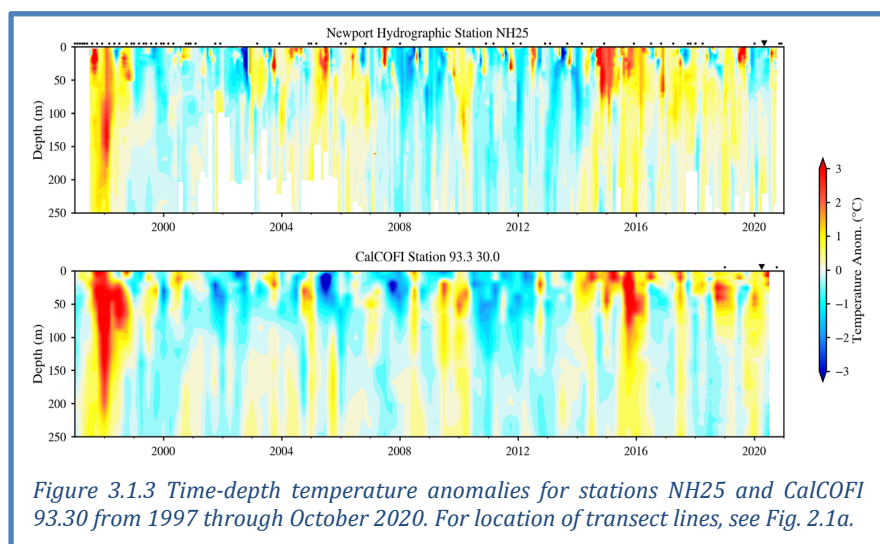
chance of La Niña remaining through winter and a 65% chance of continuing through spring 2021. The PDO continued a 5-year trend of decreasing values since 2016 (Figure 3.1.1, middle). PDO was negative for most of 2020, the longest string of negative values since before the 2013-2016 marine heatwave, and the November value (-1.12) was the lowest since 2013. NPGO remained in the negative state it has been in since late 2016, although the values were not as negative as the extreme lows at the end of 2019 (Figure 3.1.1, bottom). Seasonal values for all indices are in Appendix D.1.

The northeast Pacific continues to experience large marine heatwaves in surface waters. In January 2020, a heatwave that began in summer 2019 had receded to an offshore region in the Gulf of Alaska. A new heatwave occurred from February-June 2020 in the area where the 2019 event faltered, but it remained >1500 km from the West Coast. Then, a much larger heatwave formed offshore in June, and by mid-September it had grown to its maximum size of ~9.1M km² (Figure 3.1.2), the second largest North Pacific heatwave on record behind the 2013-2016 “Blob” (Appendix D.2). The 2020 heatwave stayed offshore until September, presumably held off by moderate to strong upwelling that occurred in the central and northern CCE for much of 2020. The heatwave lingered in coastal waters through November, particularly the northern CCE, then moved offshore, where it remains as of January 2021.



The upper portion of the water column off Newport, Oregon was relatively cool for much of 2020 (Figure 3.1.3, top). Temperatures were ~0.5°C cooler than average in the upper 50 m from winter through summer, and close to average at greater depths. The anomaly in the upper water column was the longest sustained cool period of the last 5 years. Temperatures off Newport switched to average or above-average in late summer, coincident with the arrival of the marine heatwave.

In contrast, the Southern California Bight was warm in 2020. At CalCOFI station 93.30 off San Diego, warm anomalies >1°C dominated the water column in winter and spring, particularly in the upper 50 m (Figure 3.1.3, bottom). These anomalies were likely related to the weak El Niño in early 2020. Deeper waters shifted from warm to cool anomalies in spring. Summer and fall data are as



yet unavailable from this station, but wave glider data from nearby Line 90 indicate warmer-than-average waters for most of 2020 (Appendix D.2). Similarly, a wave glider off Monterey Bay recorded average or above-average temperatures down to 250 m for most of 2020 (Appendix D.2).

3.2 REGIONAL INDICATORS

Upwelling in the CCE occurs when equatorward coastal winds move deep, cold, nutrient-rich water to the surface, fueling seasonal production. On average, upwelling peaks in late April at 33°N (near San Diego), mid June at 39°N (off Point Arena), and late July at 45°N (off Newport). Nutrient delivery by upwelling also varies by region: vertical flux of nitrate at 39°N is an order of magnitude greater than at 45°N or 33°N. Jacox et al. (2018) developed models to estimate the vertical fluxes of water (Cumulative Upwelling Transport Index; CUTI) and nitrate (Biologically Effective Upwelling Transport Index; BEUTI) in the CCE.

In 2020, there were frequent upwelling events at 39°N and 45°N, with peaks ≥ 1 s.d. above the mean, that were usually followed by relaxation events (Figure 3.2.1, left).

Upwelling events provided inputs of nitrate into the surface waters, especially the strong upwelling events in February and June at 39°N (Figure 3.2.1, right). When upwelling events are followed by relaxation, as occurred in 2020, the upwelled nutrients may be more likely to be retained and spur coastal production. Also, the large upwelling events in February may have provided an early injection of nutrients before the spring transition into the productive season for the coastal food web.

The cool, productive habitat created by upwelling can be compressed along the coast by offshore impingement, marine heatwaves, or reduced upwelling conditions, with cascading ecological effects

on marine species. Santora et al. (2020) developed the habitat compression index (HCI) to describe this physical process. HCI ranges from 0 (= complete intrusion of warm offshore water in a region) to 1 (= upwelled water fully extending 150 km from the coast). Off central California (35.5°N to 40°N), upwelled habitat has been expanding since 2015 (Figure 3.2.2), and winter and spring HCI values in 2020 were close to long-term means. HCI estimates for the rest of the West Coast indicate that seasonal upwelling habitat has generally been stable or expanding over the past five years for northern California, Oregon and Washington (Appendix D.3).

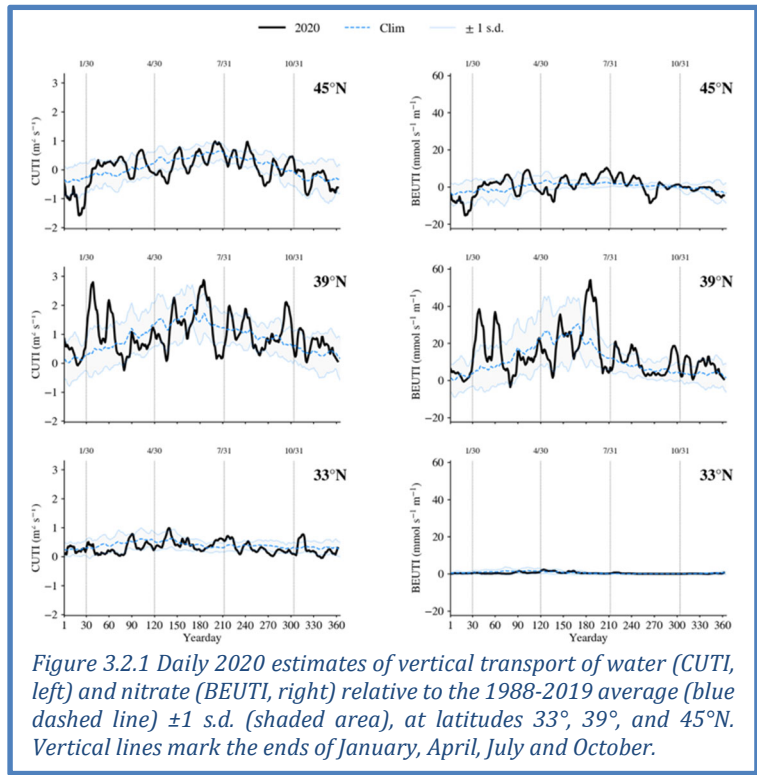


Figure 3.2.1 Daily 2020 estimates of vertical transport of water (CUTI, left) and nitrate (BEUTI, right) relative to the 1988-2019 average (blue dashed line) ± 1 s.d. (shaded area), at latitudes 33°, 39°, and 45°N. Vertical lines mark the ends of January, April, July and October.

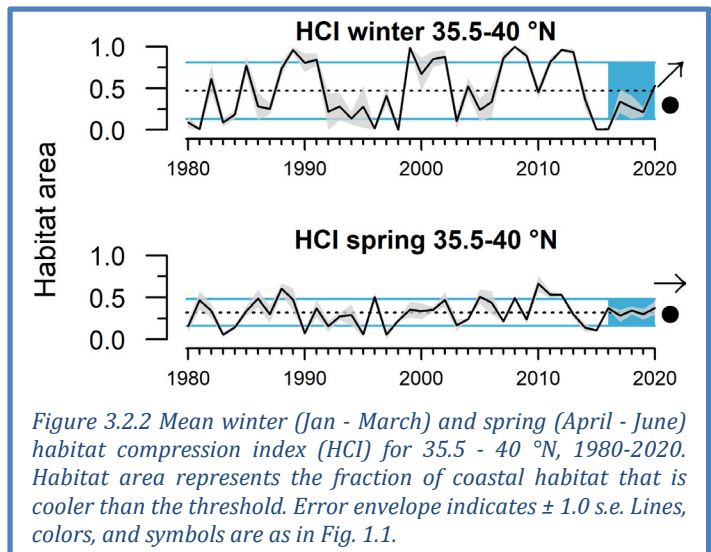
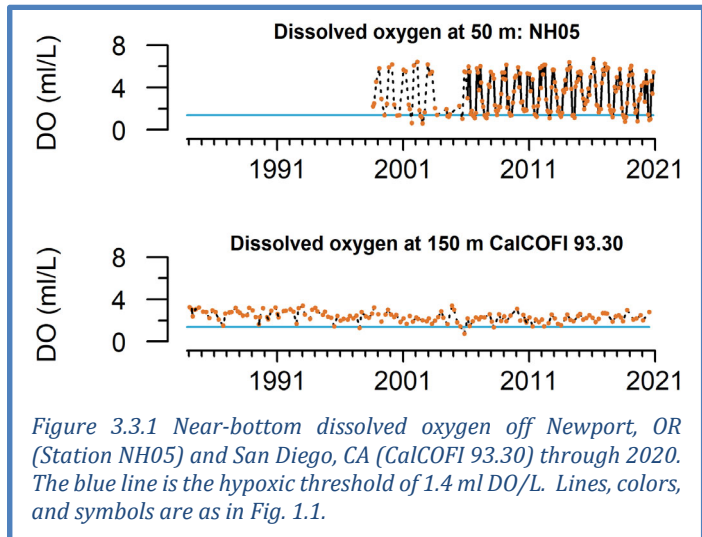


Figure 3.2.2 Mean winter (Jan - March) and spring (April - June) habitat compression index (HCI) for 35.5 - 40°N, 1980-2020. Habitat area represents the fraction of coastal habitat that is cooler than the threshold. Error envelope indicates ± 1.0 s.e. Lines, colors, and symbols are as in Fig. 1.1.

3.3 HYPOXIA AND OCEAN ACIDIFICATION

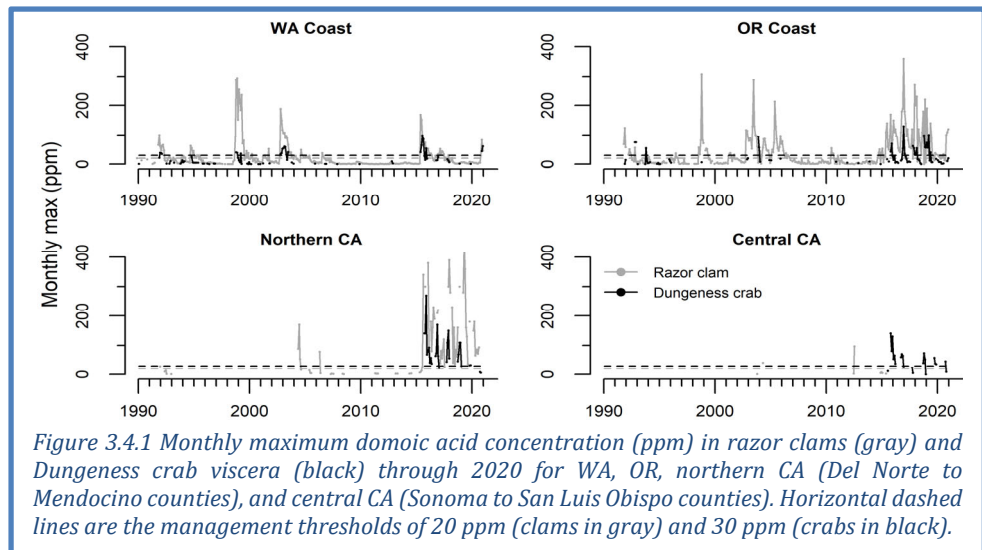
Dissolved oxygen (DO) is dependent on processes such as currents, upwelling, air-sea exchange, primary production, and respiration. Low DO can compress habitat and cause stress or die-offs for sensitive species (Chan et al. 2008). Near-bottom DO at station NH05 off Newport, Oregon fell below the hypoxia threshold in June-August 2020, and was similar in intensity to 2019 (Figure 3.3.1, top). Off San Diego at CalCOFI station 93.30, near-bottom DO was above the hypoxia threshold in winter and summer (Figure 3.3.1 bottom; no spring data), but summer DO at CalCOFI stations further offshore was generally below average, and many stations had the lowest summer DO observed since monitoring began in 1984 (Appendix D.4). DO maps and seasonal time series from Newport and CalCOFI are in Appendix D.4.

Ocean acidification, caused by increased anthropogenic CO₂, lowers pH and carbonate in seawater and can be stressful to shell-forming organisms and other species (Feely et al. 2008, Bednaršek et al. 2020). At station NH05 off Newport, levels of aragonite (a form of calcium carbonate) were favorable during spring, unlike in the previous two years, before waters became corrosive in summer and fall as is typical. Offshore at NH25, much of the water column in 2020 was corrosive. Details and plots are in Appendix D.4.



3.4 HARMFUL ALGAL BLOOMS (HABS) AND “RED TIDE”

Blooms of the diatom *Pseudo-nitzschia* can produce domoic acid, a toxin that can affect coastal food webs and lead to shellfish fishery closures when shellfish tissue levels exceed regulatory limits (Appendix E). In 2020, exceedances of domoic acid were detected in razor clams and crabs from northern California to the Canadian border (Figure 3.4.1), which caused protracted fishery closures and delays for much of the West Coast, many of which continued into early 2021. The razor clam fishery remained closed in northern California, as it has been since 2016. In Oregon, a statewide razor clam closure begun in 2019 was gradually lifted for northern (January), central (February), and southern beaches (August) before closing again over the course of the fall. A rapid rise of domoic acid in Washington closed recreational and Tribal razor clam harvests in October. Many crab fishery seasons were shortened, due in part to domoic acid but also to meat quality and to



reducing risk of whale entanglement in crab gear. Domoic acid led to closure of northern California rock crab fisheries throughout 2020, and also delayed opening of the Dungeness crab fishery from Cape Falcon to the Oregon/Washington border for all of December 2020. Domoic acid also led to closures of commercial, recreational and Tribal Dungeness crab fisheries in Washington for parts of November and December 2020. Details of the causes, locations and timings of delays and closures are in Appendix E.

Further south, an extremely dense, prolonged “red tide” of the dinoflagellate *Lingulodinium polyedra* extended from Los Angeles to Baja in spring 2020. Levels of *L. polyedra* and chlorophyll at Scripps Pier were the highest ever recorded. This highly disruptive bloom caused hypoxia, fish and invertebrate kills, and respiratory irritation among surfers and beach-goers. A toxin associated with *L. polyedra*, yessotoxin, may have played a role in the die-offs. Conditions thought to have promoted the bloom included high March-April rains, stratification due to low winds, seasonal warming, and anomalous conditions in the region since 2014. Details are in Appendix E.

3.5 HYDROLOGIC INDICATORS

Favorable freshwater conditions are critical for anadromous populations. Hydrologic indicators presented here are snowpack, streamflow and stream temperature, summarized by ecoregion (Figure 2.1b). Snow-water equivalent (SWE) is the water content in snowpack, which supplies cool freshwater to streams in spring, summer and fall. Maximum flows in winter and spring are important for habitat formation and removal of salmon parasites, but extreme discharge events can scour salmon redds. Below-average minimum flows in summer and fall can restrict habitat for juvenile salmon and migrating adults. High summer temperatures can impair physiology and cause mortality.

On April 1 2020, SWEs in the northern ecoregions (Salish Sea/WA Coast, Columbia Glaciated, Columbia Unglaciated) were close to long-term means (Figure 3.5.1). However, SWE were ~1 s.d. below average in 2020 for coastal Oregon and Northern California and Sacramento/San Joaquin, and were much lower than in 2019. Moderate to severe droughts were forecast for northern California, Oregon and parts of Washington in April 2020. These intensified to severe-extreme conditions in summer and triggered catastrophic wildfires throughout the West.

Maximum flows showed similar patterns to SWE for 2020 at ecoregional scales, with near-average values in the Salish Sea/WA Coast and both Columbia ecoregions, but below-average values in 2020 for coastal Oregon/Northern California and Sacramento/San Joaquin. Trends for the most recent 5 years are negative for Columbia Glaciated, OR/NoCA

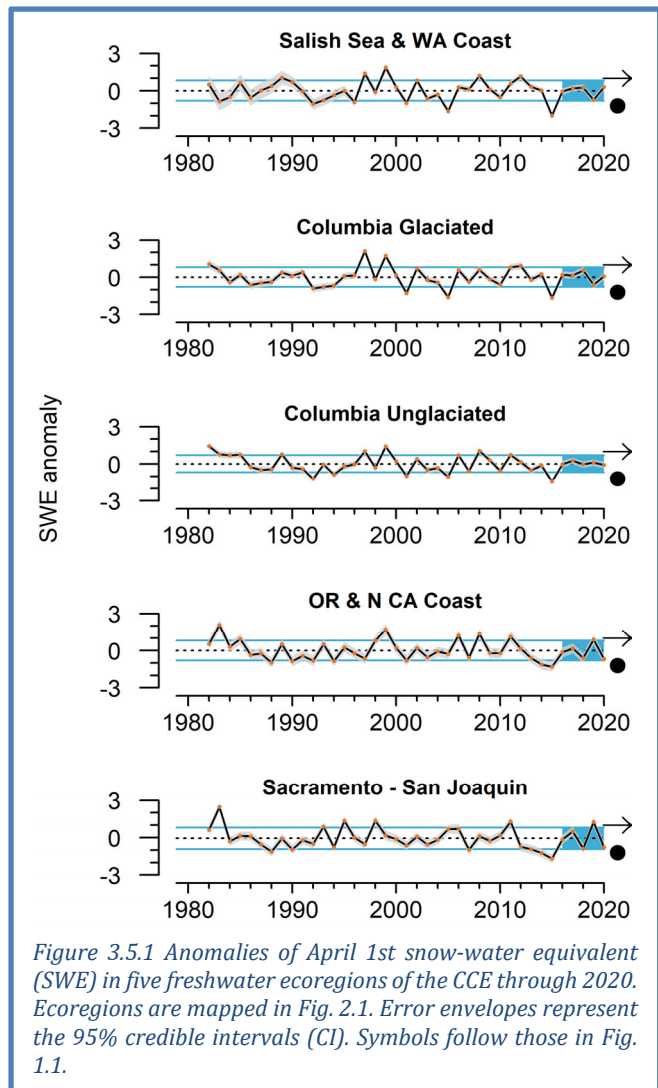
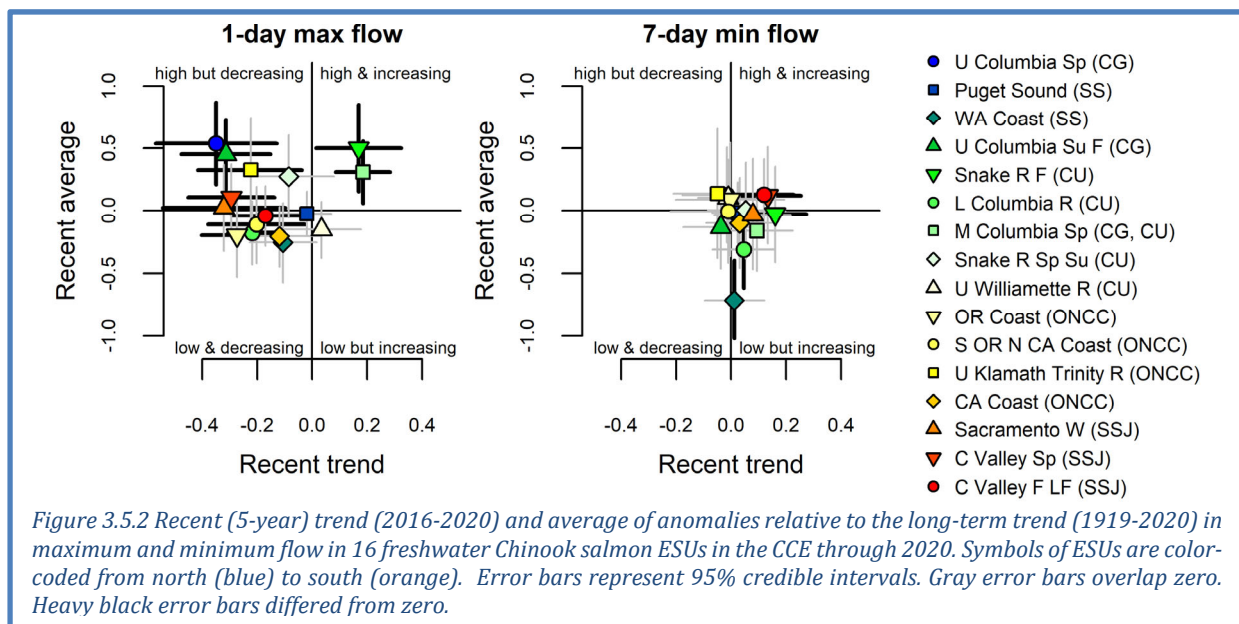


Figure 3.5.1 Anomalies of April 1st snow-water equivalent (SWE) in five freshwater ecoregions of the CCE through 2020. Ecoregions are mapped in Fig. 2.1. Error envelopes represent the 95% credible intervals (CI). Symbols follow those in Fig. 1.1.

Coast and Sacramento/San Joaquin but non-significant in other regions (see Appendix F). Minimum flows were close to long-term averages in all ecoregions in 2020, and generally have improved since 2015 (Appendix F). August stream temperatures for the Salish Sea/WA Coast were cooler in 2020 than in recent years, but the OR/NoCA Coast and Sacramento/San Joaquin ecoregions were warmer than average, and increased relative to 2019 (Appendix F).

We also summarize streamflows at the finer scale of individual Chinook salmon evolutionarily significant units (ESUs). These results are summarized in quad plots, which indicate ESUs with significant short-term trends or recent averages that differ from long-term means. With the exception of two ESUs in the Columbia system, maximum flows had either declining or non-significant trends from 2016-2020; in general, maximum flows were close to or above average during that period (Figure 3.5.2, left; Appendix F). Because high winter maximum flows are generally beneficial for juvenile salmon in southerly populations, the negative winter trends in southern ecoregions, driven by low values in 2018 and 2020, suggest worsening recent conditions for egg and alevin incubation. Minimum flows were generally close to long-term averages, but some ESUs experienced increasing minimum flows over the past five years, including the Snake River Fall and both Central Valley ESUs (Figure 3.5.2, right; Appendix F). Minimum flows in the Washington Coast and Lower Columbia ESUs have been below average in recent years.



Because SWE typically peaks in early spring, the last official measure of SWE will be on April 1, 2021. As of January 31st 2021, SWE is mixed. Most stations in northern Washington and northern Idaho are average or above average, while eastern Oregon and central/southern Idaho are mixed. Stations in western Oregon and in California are mostly below average. Drought persists in nearly all of California, much of Oregon, and parts of Idaho and Washington (Appendix F).

4 FOCAL COMPONENTS OF ECOLOGICAL INTEGRITY

The CCIEA team examines many indicators related to the abundance and condition of key species and the dynamics of ecological interactions. Preliminary data suggest average to above-average feeding conditions in 2020 in much of the CCE, with signs of improved abundance of nutritious zooplankton, high abundance of anchovy, and positive productivity signals for top predators. Signals for Chinook salmon returns in 2021 are mixed. Sections below should be interpreted with care because survey effort was reduced in 2020 due to COVID-19, and many samples have yet to be processed.

4.1 COPEPOD BIOMASS AND KRILL SIZE

Copepod biomass anomalies represent variation in northern copepods (cold-water zooplankton species rich in wax esters and fatty acids) and southern copepods (smaller species with lower fat content and nutritional quality). In summer, northern copepods usually dominate the zooplankton community along the Newport Line (Figure 2.1a), while southern copepods dominate in winter. Positive values of northern copepods correlate with stronger returns of Chinook salmon to Bonneville Dam and coho salmon to coastal southern Oregon (Peterson et al. 2014). El Niño events and positive PDO regimes can increase southern copepods (Keister et al. 2011, Fisher et al. 2015).

In 2020, northern copepods continued an overall increasing trend since the extreme lows during the 2014-2016 heatwave. They were >1 s.d. above the mean in spring-summer 2020 before their regular seasonal decline in the fall (Figure 4.1.1, top). The spring-summer anomaly was among the highest of the time series. Southern copepods were below-average for much of 2020, continuing a decline since the heatwave (Figure 4.1.1, bottom). These values suggest above-average feeding conditions for pelagic fishes off central Oregon in 2020, with late-spring/summer copepod ratios the most favorable observed since before the 2014-2016 heatwave, and in nearly a decade. The biweekly survey that collects these data lost only two sampling dates due to COVID-19, both in spring.

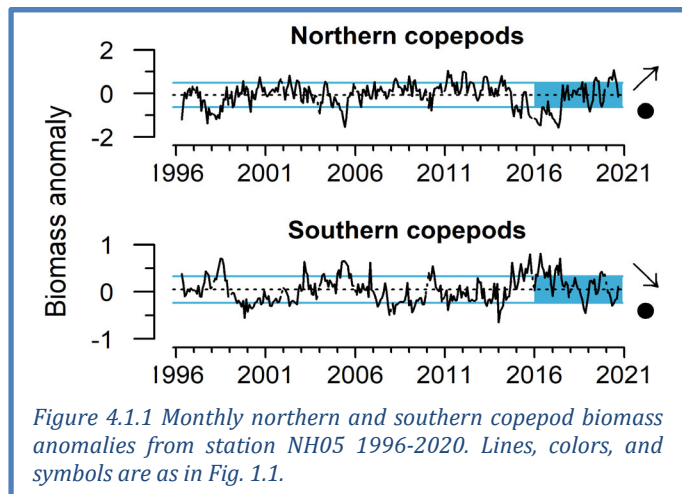


Figure 4.1.1 Monthly northern and southern copepod biomass anomalies from station NH05 1996-2020. Lines, colors, and symbols are as in Fig. 1.1.

Krill are among the most important prey for fishes, mammals and seabirds in the CCE. The key species *Euphausia pacifica* is sampled year-round off Trinidad Head (Figure 2.1a). Mean length of adult *E. pacifica* is an indicator of krill as a prey resource. *E. pacifica* grow from short individuals in winter to longer individuals by summer. *E. pacifica* lengths in spring and summer of 2020 were above average (Figure 4.1.2), and much greater than in 2019 when krill growth may have been negatively affected by El Niño conditions in the 2018-2019 winter. The overall trend for krill lengths has been increasing since poor growth at the onset of the 2014-2016 heatwave. COVID-19 led to some cancelled cruises and delayed sample processing at Trinidad Head, but the 2020 data are from stations that are highly representative of *E. pacifica* lengths in the region (Robertson and Bjorkstedt 2020). A spring survey that has produced estimates of krill biomass and distribution off Oregon and Washington since 2011 (Brodeur et al. 2019) was cancelled in 2020 due to COVID-19.

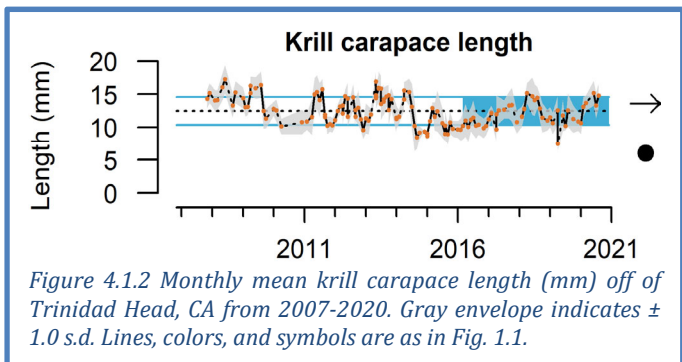


Figure 4.1.2 Monthly mean krill carapace length (mm) off of Trinidad Head, CA from 2007-2020. Gray envelope indicates ± 1.0 s.d. Lines, colors, and symbols are as in Fig. 1.1.

4.2 REGIONAL FORAGE AVAILABILITY

Our ability to understand dynamics of the CCE's diverse forage community was impacted by COVID-19, which disrupted regional forage surveys and sample processing. We typically use multivariate analyses to compare the timing and nature of forage community shifts across the three regions, but are unable to do so this year, due to data limitations. Instead, we present some time series that we

believe to be most representative of times and locations that were surveyed in 2020, with additional time series in Appendix G along with explanations of methodological changes, which were reviewed by the Council SSC-Ecosystem Subcommittee in January 2021.

Northern CCE: The Northern CCE survey off Washington and Oregon (Figure 2.1a) targets juvenile salmon in surface waters, and also samples surface-oriented fishes, squid and jellies. Due to COVID-19, processing of samples from 2020 was delayed and only recently completed. Among 2020 samples that we have had time to evaluate, the most striking observation is unprecedented catches of YOY sablefish (Figure 4.2.1). Other time series for this survey are in Appendix G.1. Juvenile salmon data are shown in the next section.

Central CCE: Data shown here are from the “Core area” of a survey (Figure 2.1a) that targets pelagic juvenile rockfishes, but also samples other pelagic species. Due to COVID-19, survey effort in 2020 was sharply reduced (15 trawls, compared to the usual >60 trawls). We analyzed data from 1998-2020 at just these stations (see methods in Appendix G.2). Adult anchovy remained highly abundant at these stations in 2020, while YOY rockfish catches were well below average and continued declining recent trends (Figure 4.2.2). Other available time series are in Appendix G.2.

Southern CCE: Forage data for the Southern CCE (Figure 2.1a) come from CalCOFI larval fish surveys. The spring larval survey was cancelled in 2020 due to COVID-19, so here we present results from winter larval surveys, conducted annually in January-February (see Appendix G.3). The southern forage community appeared to experience a shift from 2019 to 2020. Larval anchovy decreased from 2019 to 2020, but were still above the long-term average (Figure 4.2.3). Southern mesopelagic fishes also decreased from 2019 to 2020. Rockfishes were uncommon in 2020, as were larval flatfishes and sardines (Appendix G.3).

Pyrosomes: Pyrosomes, a warm-water pelagic tunicate, were highly abundant in the Central CCE and as far north as Trinidad Head in 2020, as they have frequently been since anomalous warming began in 2014. Small pyrosomes began to show up on the Newport Line and on Oregon beaches in late 2020, possibly after being forced north by seasonal currents and early winter storms.

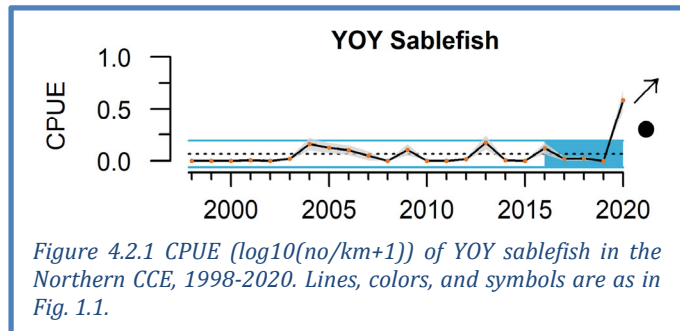


Figure 4.2.1 CPUE ($\log_{10}(\text{no}/\text{km}+1)$) of YOY sablefish in the Northern CCE, 1998-2020. Lines, colors, and symbols are as in Fig. 1.1.

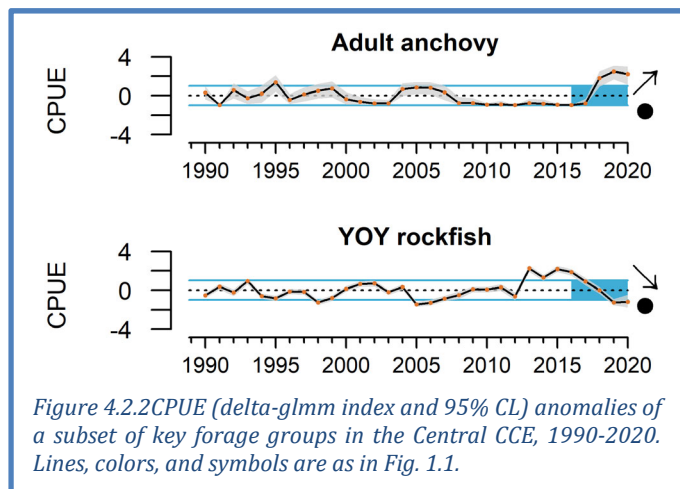


Figure 4.2.2 CPUE (Δ -glm index and 95% CL) anomalies of a subset of key forage groups in the Central CCE, 1990-2020. Lines, colors, and symbols are as in Fig. 1.1.

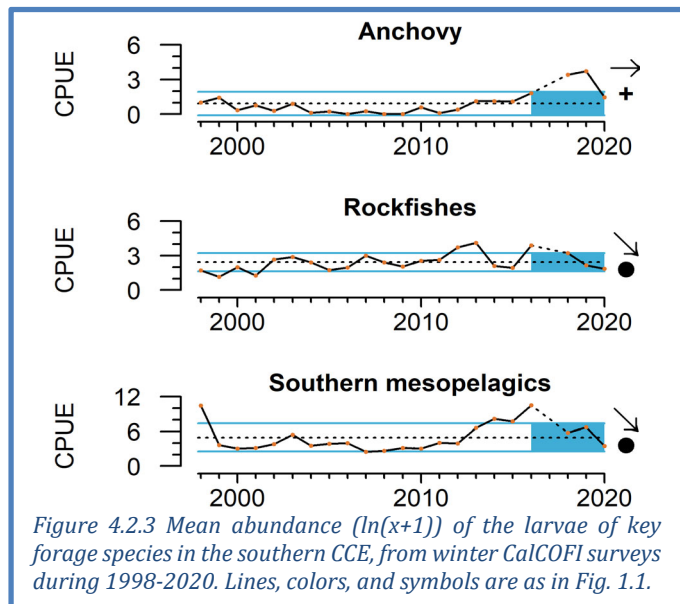


Figure 4.2.3 Mean abundance ($\ln(x+1)$) of the larvae of key forage species in the southern CCE, from winter CalCOFI surveys during 1998-2020. Lines, colors, and symbols are as in Fig. 1.1.

4.3 SALMON

Escapement: We examine trends in natural escapement from different populations of Chinook and coho salmon to compare status and coherency in production dynamics across their range. We summarize escapement in quad plots; time series are shown in Appendix H. Chinook salmon escapements are updated through 2018, while coho data mostly are updated through 2019.

Escapements of California Chinook salmon from 2009-2018 were within 1 s.d. of long-term means (Figure 4.3.1, top), though 2018 escapements were among the lowest on record in several ESUs, especially in the Central Valley (Appendix H.1). California escapement trends were neutral for the last decade, though those trends mask increases followed by declines during that time period (Appendix H.1). In the Northwest, most mean escapements in the past decade were within 1 s.d. of average (Figure 4.3.1, top); the exception was above-average Snake River Fall Chinook escapements. Escapement trends over the past decade were neutral for most Northwest ESUs except for Willamette Spring Chinook (increasing) and Snake River Spring-Summer Chinook (decreasing). Details are in Appendix H.2.

Escapement data available for coho salmon show a declining trend for Oregon Coast coho and neutral trends for other ESUs (Figure 4.3.1, bottom). Available ESUs have recent averages that are close to time series averages. Details are in Appendix H.3.

Juvenile salmon abundance: Catches of juvenile coho and Chinook salmon from surveys during June in the Northern CCE (Figure 2.1a) are indicators of salmon survival during their first few weeks at sea. In 2020, juvenile subyearling Chinook salmon catches were higher than the previous two years, but were within 1 s.d. of the long-term average (Figure 4.3.2). Juvenile yearling Chinook salmon catches declined in 2020, and were ~1 s.d. below average. Yearling coho salmon catches were similar to 2019, and were within 1 s.d. of the time series average.

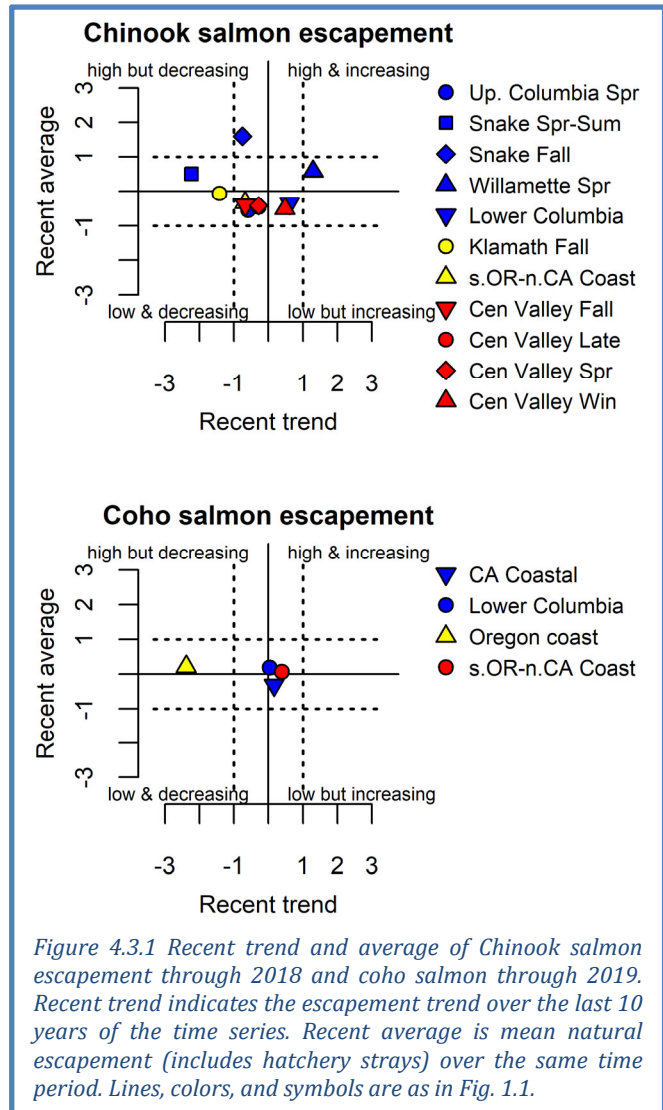


Figure 4.3.1 Recent trend and average of Chinook salmon escapement through 2018 and coho salmon through 2019. Recent trend indicates the escapement trend over the last 10 years of the time series. Recent average is mean natural escapement (includes hatchery strays) over the same time period. Lines, colors, and symbols are as in Fig. 1.1.

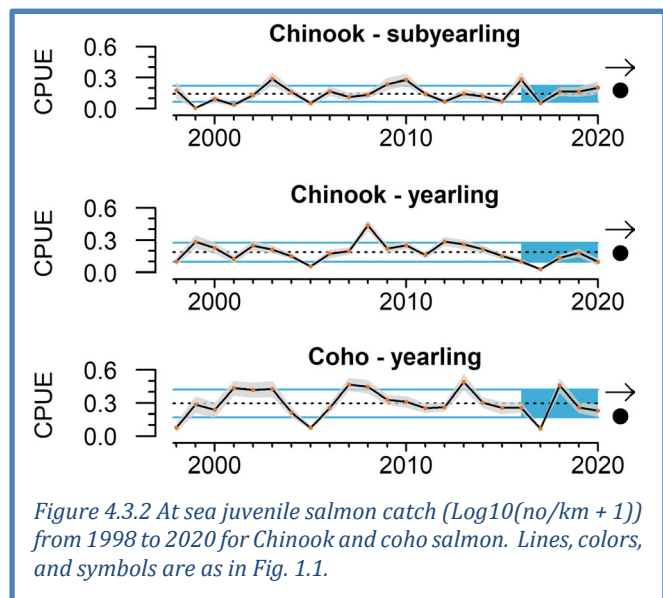


Figure 4.3.2 At sea juvenile salmon catch (Log10(no/km + 1)) from 1998 to 2020 for Chinook and coho salmon. Lines, colors, and symbols are as in Fig. 1.1.

Stoplight tables: Long-term associations between oceanographic conditions, food web structure, and salmon productivity (Burke et al. 2013, Peterson et al. 2014) support qualitative outlooks of returns of Chinook salmon to Bonneville Dam and smolt-to-adult survival of Oregon Coast coho salmon. This suite of indicators is depicted in the “stoplight chart” in Table 4.3.1, and includes many indicators shown elsewhere in this report (PDO, ONI, SSTa, deep temperature, copepods, juvenile salmon catch). For coho salmon returning to the Oregon coast in 2021, ecosystem indicators for the dominant smolt year (2020) suggest a mix of good, intermediate and poor relative conditions. For Chinook salmon returning to the Columbia Basin in 2021, indicators for the dominant smolt year (2019) mostly reflect a mix of intermediate and poor conditions. A related quantitative model that incorporates these indicators into outlooks for Chinook salmon returns estimates a probability of relatively poor counts of both Spring and Fall Chinook at Bonneville Dam in 2021 (Appendix H.4).

Table 4.3.1 “Stoplight” table of conditions for smolt years 2017-2020 and qualitative outlooks for adult returns in 2021 for coho salmon returning to coastal Oregon and Chinook salmon returning to the Columbia Basin. Green/circle = “good,” yellow/square = “intermediate,” and red/diamond = “poor,” relative to the long-term time series.

Scale of indicators	Smolt year				Adult return outlook	
	2017	2018	2019	2020	Coho, 2021	Chinook, 2021
Basin-scale						
PDO (May-Sept)	■	■	◆	■	■	◆
ONI (Jan-Jun)	■	●	◆	◆	◆	◆
Local and regional						
SST anomalies	■	■	◆	■	■	◆
Deep water temp	◆	◆	◆	◆	◆	◆
Deep water salinity	■	●	■	◆	◆	■
Copepod biodiversity	◆	■	■	●	●	■
Northern copepod anomaly	◆	■	●	●	●	●
Biological spring transition	◆	◆	■	●	●	■
Winter ichthyoplankton biomass	■	■	◆	●	●	■
Winter ichthyoplankton community	◆	◆	◆	■	■	◆
Juvenile Chinook catch (Jun)	◆	■	■	■	■	■
Juvenile coho catch (Jun)	◆	●	■	■	■	■

In last year’s report, we introduced an indicator-based outlook for Chinook salmon in California. Friedman et al. (2019) found that Central Valley Fall Chinook salmon returns were correlated with natural-area spawning escapement of parent generations; fall egg incubation temperature and February streamflow in the Sacramento River; and a marine predation index based on the abundance and diet of common murrelets at Southeast Farallon Island. For adult salmon returning in 2021, signals are mixed, both within and across age classes. The dominant age class (age-3, from the 2018 brood year) experienced unfavorable parent escapement and egg incubation temperature, but favorable winter flows for newly hatched juveniles (Table 4.3.2).

Table 4.3.2 Conditions for naturally produced Central Valley Fall Chinook salmon returning in 2021, from brood years 2016-2019. Indicators reflect each cohort’s parent generation escapement, egg incubation temperature, flow during juvenile stream residence, and seabird predation in the early marine phase. Heavy outline and bold type indicates age-3 Chinook salmon, the dominant age class returning to the Central Valley.

Spawning Escapement (t=0)	Incubation Temperature (Oct-Dec t=0)	February Median Flow (t+1)	Seabird Marine Predation Index (t+1)	Chinook Age in Fall 2021
2016: 56,000 (low)	11.8°C (poor)	48,200 cfs (very high)	Near average	5
2017: 18,000 (very low)	11.8°C (poor)	5,525 cfs (very low)	Near average	4
2018: 72,000 (low)	11.7°C (poor)	21,700 cfs (high)	Near average	3
2019: 120,400 (met goal)	11.2°C (suboptimal)	6,030 cfs (very low)	Near average	2

Age-4 fish are the progeny of a very low escapement year (2017) and experienced both poor egg incubation temperature in the 2017-2018 winter and very low streamflow for juveniles. Age-5 fish (produced in 2016) have mixed signals thanks to better juvenile flow regimes.

The Council’s Habitat Committee, Salmon Technical Team, and others including CCIEA scientists have begun developing more comprehensive stoplight tables for Sacramento River Fall Chinook and Klamath River Fall Chinook, both of which were the focus of rebuilding plans following recent determinations of overfishing. The stoplight tables feature indicators related to the egg incubation, freshwater, early marine, and spawning phases, as well as hatchery releases. These new stoplight charts build on the effort shown in Table 4.3.2, and are presented and described in Appendix H.5. They show that both stocks experienced below-average freshwater and marine conditions in two of the three brood years defined in the rebuilding plans (2012-2014); in the years since, freshwater conditions have improved for Sacramento River Fall Chinook, but not for Klamath River Fall Chinook, while marine conditions have declined for both (Appendix H.5).

4.4 GROUND FISH STOCK ABUNDANCE AND DISTRIBUTION

Except for Pacific hake, there were no groundfish assessment updates in 2020, so indices for the status of groundfish biomass and fishing pressure are essentially unchanged from last year’s report. We will update that figure in next year’s report following the upcoming assessment cycle.

Changes in abundance and spatial distribution of groundfish may affect fishing opportunities in different locations. We are analyzing data from the NOAA groundfish bottom trawl survey to determine if groundfish stock availability is changing at different spatial and temporal scales (Selden et al 2020; details in Appendix I). Here we focus on three key target stocks—sablefish, petrale sole and yellowtail rockfish—and how relative availability of their biomass has changed over time for four ports (Figure 4.4.1).

Availability of the three species has generally increased since ~2010, with some variability in recent years (Figure 4.4.1). These overall increases are due at least in part to increasing stock biomass. Availability of all three species was higher for Astoria than for the more southerly ports, potentially reflecting larger core habitat area farther north. The center of gravity of these three stocks varies over time, but there is no clear evidence that the populations are steadily shifting in a single latitudinal direction (Appendix I). Sablefish have experienced both northerly and southerly changes in center of gravity of 2-3° latitude in the span of years, while petrale sole and yellowtail rockfish centers of gravity have been more stable, suggesting that biomass increase is a more important cause of the availability increase (Figure 4.4.1). Future work to understand the relative roles of climate, recruitment, stock size,

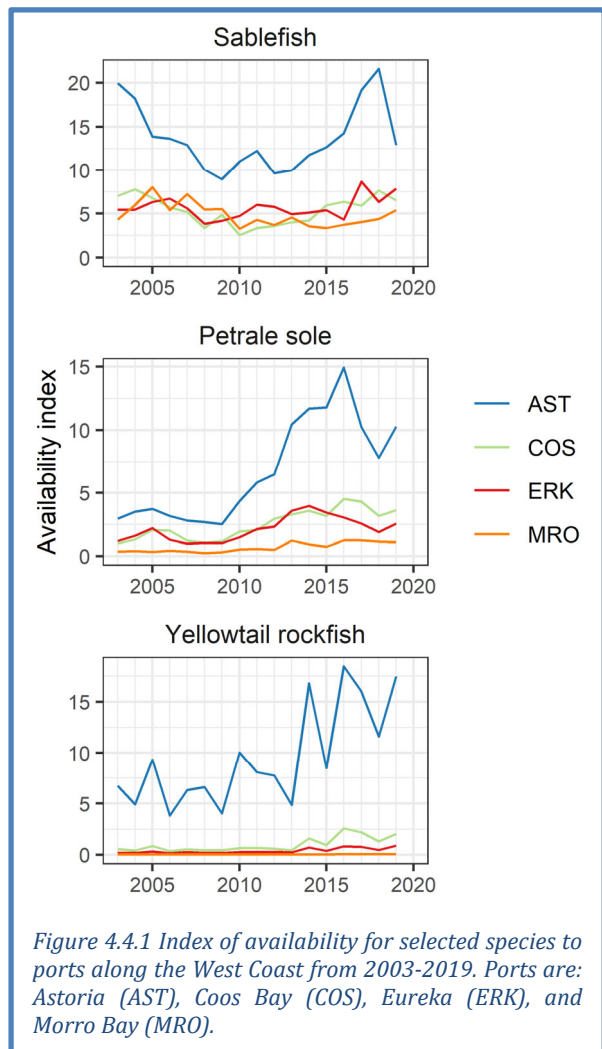
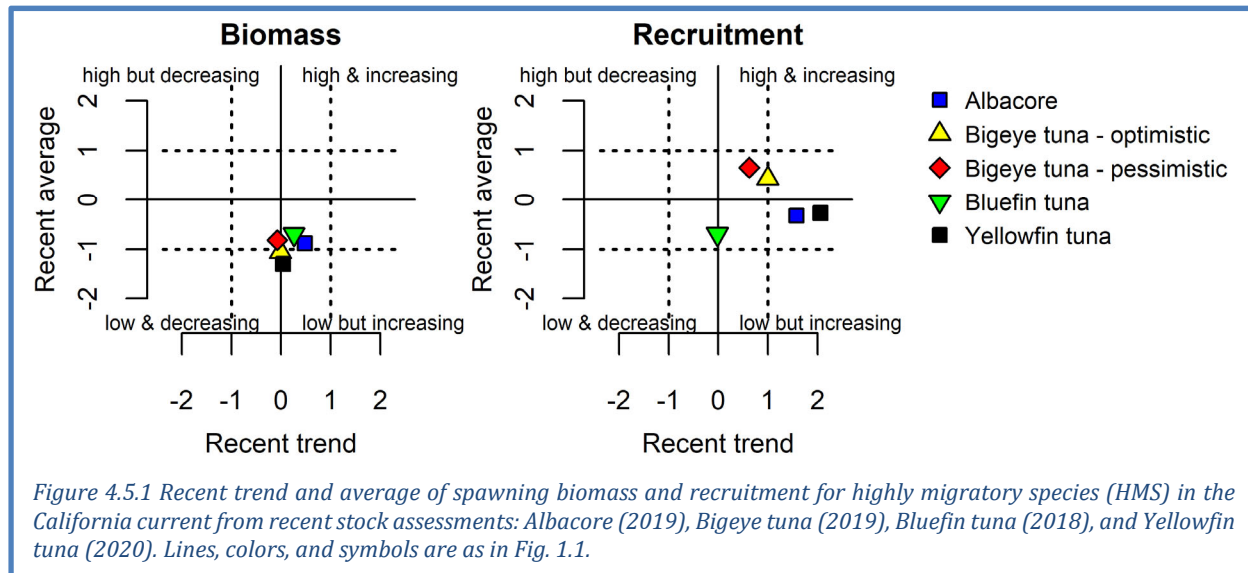


Figure 4.4.1 Index of availability for selected species to ports along the West Coast from 2003-2019. Ports are: Astoria (AST), Coos Bay (COS), Eureka (ERK), and Morro Bay (MRO).

fisheries removals, and other factors would help to explain observed variation in center of gravity. Details and analyses with additional ports and groundfish species, including lingcod, skates and other rockfishes, are in Appendix I.

4.5 HIGHLY MIGRATORY SPECIES

Several highly migratory species (HMS) targeted by West Coast fisheries have had recent updates to their assessments, including information on stock biomass and recruitment. Here we present stocks that have been updated as quad plots summarizing recent short-term averages and trends of biomass and recruitment; time series and summaries of stock condition for these stocks, as well as stocks that have not been recently assessed (e.g., swordfish, blue marlin, skipjack) are presented in Appendix J.

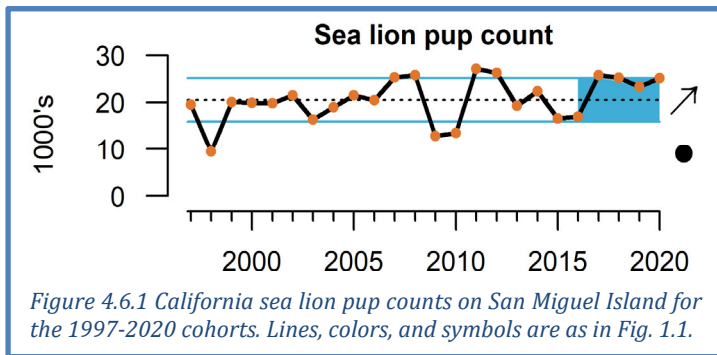


Biomasses of recently assessed HMS stocks appeared to be below average relative to the full assessment periods, and biomass trends ranged from weakly negative to weakly positive (Figure 4.5.1 left; Appendix J). HMS recruitment estimates from recent assessments are within ± 1 s.d. of long-term averages, and several stocks experienced apparent increases in recruitment the most recent five years (Figure 4.5.1 right), although these estimates should be interpreted cautiously given their high uncertainty (Appendix J). The relationships between these indicators and different attributes of population condition (e.g., target and limit reference points) are complicated and differ by species, as summarized in Appendix J; for example, bigeye tuna estimates are drawn from 44 separate reference models that broadly group into two outlooks, one relatively “optimistic” and one relatively “pessimistic.” We will continue to improve on HMS indicators in future reports.

4.6 MARINE MAMMALS

Sea lion production: California sea lions are sensitive indicators of prey availability and composition in the central and southern CCE: research has shown that pup counts and condition at the San Miguel Island colony are positively correlated with seasonal prey availability, and that pup counts and growth can be especially high when higher quality prey such as sardines, anchovy or mackerels have high occurrence in adult female sea lion diets (Melin et al. 2012a). Sea lion pup count relates to prey availability and nutritional status for gestating females from October to June, while pup growth from birth to age 7 months is related to prey availability to lactating females from June to February. These metrics have been shown to be good indicators of forage quality and abundance even when the sea lion population is at or near carrying capacity (Appendix K).

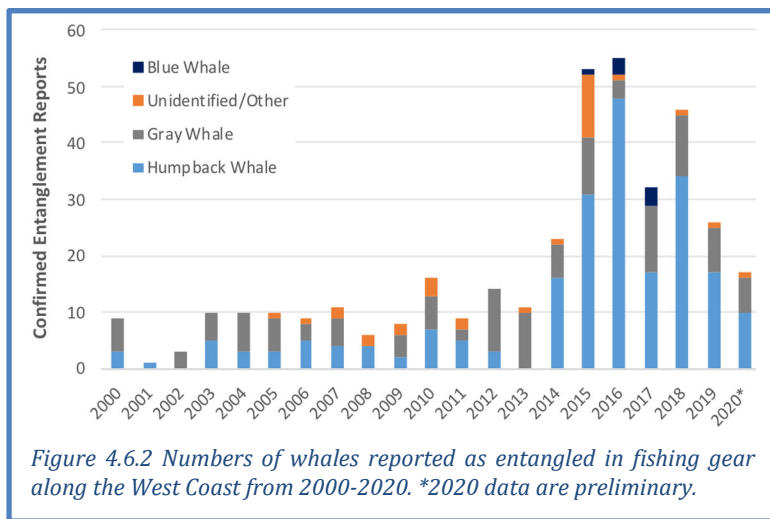
In 2020, NOAA scientists were able to conduct counts of sea lion pups via aerial surveys. The 2020 cohort was the fourth consecutive year of above-average pup counts (Figure 4.6.1), and continued the positive trend since the relatively low counts in 2015-2016. The relatively high pup count in 2020 implies abundant and high-quality prey for adult female sea lions in their foraging area (rectangle in Figure 2.1a), and is consistent with the estimates of high anchovy abundance derived from the limited sampling of forage communities of the Central and Southern CCE in 2020 (Section 4.2).



We usually report sea lion pup growth from fall and winter, but researchers could not assess pup growth or condition in 2020 due to COVID-19 restrictions. However, based on threshold analyses relating sea lion pup growth to PDO, conditions in 2020 are consistent with normal to above-normal pup growth. Details of this analysis are in Appendix K.

Whale entanglement: Reports of whale entanglements along the West Coast increased in 2014 and even more in the next several years, particularly for humpback whales. While ~50% of reports cannot be attributed to a specific source, Dungeness crab gear has been the most common source identified in this period. The dynamics of entanglement risk and reporting are complex, and are affected by shifts in ocean conditions and prey fields, changes in whale populations, changes in distribution and timing of fishing effort, and improved reporting due to increased public awareness.

Based on preliminary data, West Coast entanglement reports were again higher in 2020 than pre-2014, although fewer confirmed reports were received than in any year since 2013 (Figure 4.6.2; note that COVID-19 reduced reporting capability, with fewer vessels available to assist with sighting and documentation). Humpback whales continued to be the most common species reported entangled. As in previous years, the majority of reports were in California, though entanglements were known to include gear from all three West Coast states. Confirmed sources included commercial and recreational Dungeness crab,



commercial rock crab, and gillnet fisheries. No confirmed entanglements occurred in sablefish fixed gear. Significant actions were taken in 2020 to address entanglement risk, including closures and delays of Dungeness crab seasons in California, and late-season reductions of allowable Dungeness crab gear and new line marking requirements in Washington. In Oregon, newly adopted regulations that restrict depths and amount of Dungeness crab gear that can be fished will be implemented in 2021. While these actions are expected to reduce entanglement risks, other factors will continue to present obstacles to risk reduction. These include exposure of whales to derelict gear, foraging in nearshore waters during certain ecosystem conditions, and growth of some whale populations.

4.7 SEABIRDS

Seabird indicators (densities, productivity, diet, and mortality) are a portfolio of metrics that reflect population health and condition of seabirds, as well as links to lower trophic levels and other conditions in the CCE. To highlight the status of different seabird guilds and their ecological relationships multiple focal species are monitored throughout the CCE. The species we report on here and in Appendix L represent a breadth of foraging strategies, life histories, and spatial ranges.

Seabird colonies on Southeast Farallon Island off central California experienced mixed productivity in 2020 (Figure 4.7.1). Several species experienced improved fledging production relative to 2019. Cassin's auklets, which feed on krill, bounced back strongly in 2020, consistent with higher amounts of krill in their diets (Appendix L). Pigeon guillemots and rhinoceros auklets experienced near-average productivity in 2020, an increase from 2019. Anchovies again dominated diets of piscivorous birds at this colony (Appendix L). Anchovies may have been too large for some chicks to ingest, leading to poor fledgling rates, especially in common murres.

Further north at Yaquina Head, Oregon, fledgling production in 2020 was above-average for two cormorant species, suggesting good feeding conditions; colony failure of common murres at Yaquina Head was likely due to extreme disturbance by bald eagles rather than to poor feeding conditions (data not shown; see Appendix L).

Monitoring of stranded birds on beaches, often done by citizen scientists, provides information on unusual mortality events linked to ecosystem conditions. There were no reports of large mortality events ("wrecks") during 2020, although data were not available from some parts of central and southern California, and sampling was also substantially reduced due to COVID-19 (Appendix L.2).

5 FISHERY LANDINGS AND REVENUE

5.1 COASTWIDE LANDINGS BY MAJOR FISHERIES

Commercial fishery landings data are >90% complete through the end of 2020 for the three coastal states. Coastwide total landings have declined by 8-9% per year each year since 2017, largely tracking changes in hake and market squid (Figure 5.1.1). Salmon, CPS, HMS, and non-hake groundfish are at or near lows for the time series. Ocean conditions, wildfires, and COVID-related effects on supply and demand all likely contributed to the overall decrease in landings in 2020. COVID-related restrictions contributed to decreased demand, particularly from restaurants and export markets. Additionally, COVID outbreaks on some Pacific hake vessels may have reduced ability to harvest available quota (NMFS 2021). State-by-state landings are presented in Appendix M. *We will provide further updates in the March 2021 presentation to the Council.*

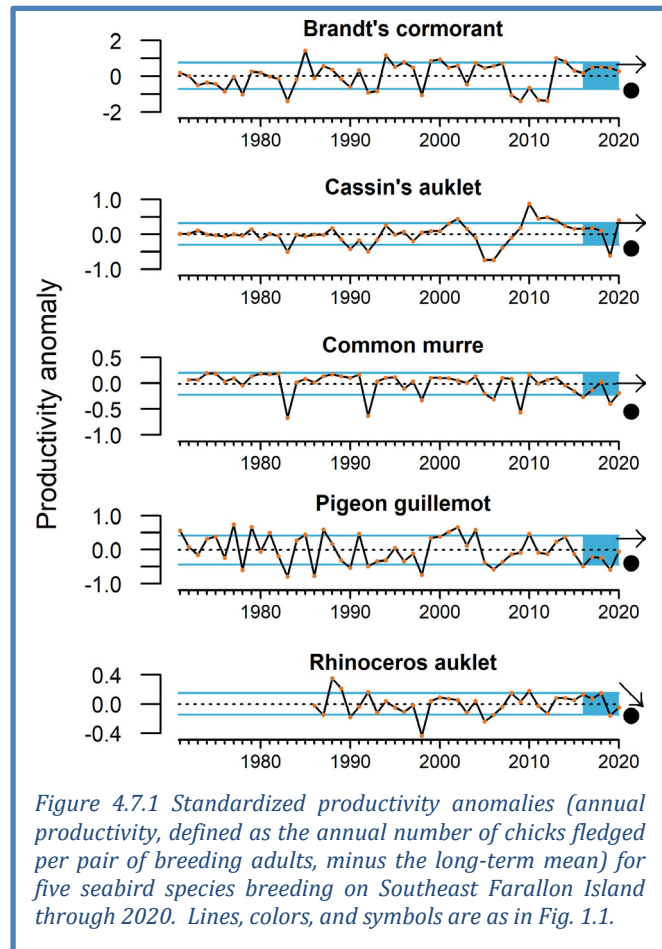
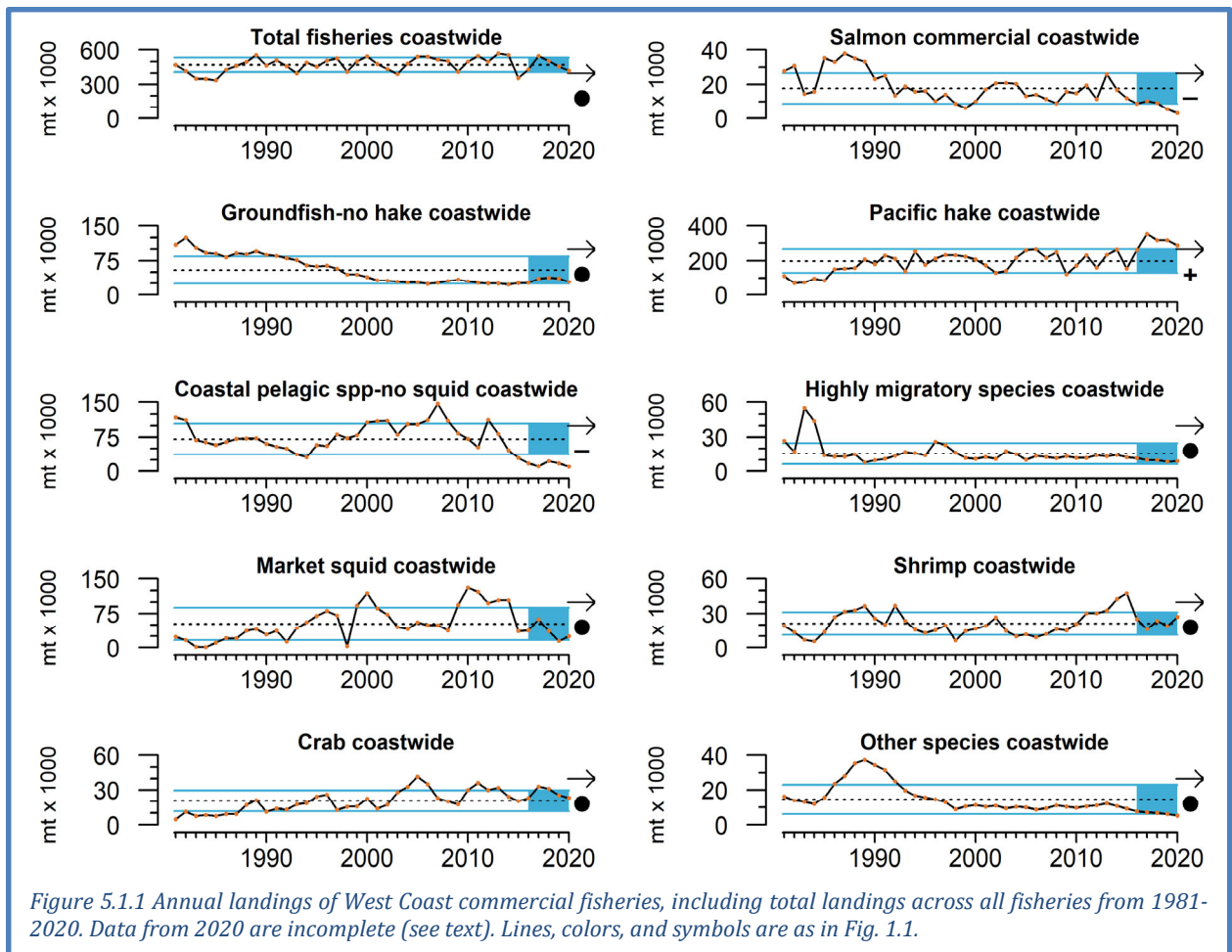
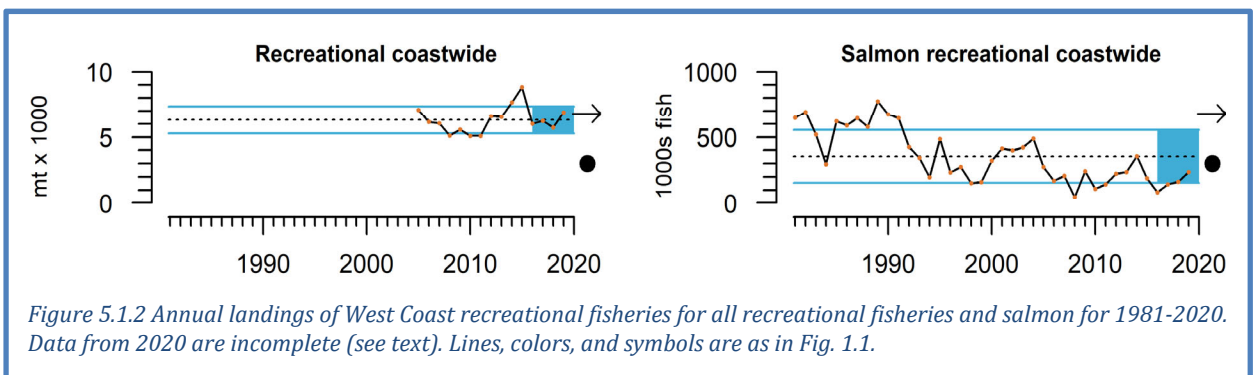


Figure 4.7.1 Standardized productivity anomalies (annual productivity, defined as the annual number of chicks fledged per pair of breeding adults, minus the long-term mean) for five seabird species breeding on Southeast Farallon Island through 2020. Lines, colors, and symbols are as in Fig. 1.1.



Recreational landings data (excluding salmon and Pacific halibut) are complete at the coastwide level through 2019, and were close to the time series average, as they had been since 2016 (Figure 5.1.2). Large increases in recreational albacore landings in 2019 contributed to an overall increase in recreational landings relative to 2018. Recreational landings of Chinook and coho salmon at a coastwide level increased each year from 2017-2019, though they remained low relative to the 1980s and 1990s. Recreational landings data available thus far for 2020 suggest declines relative to 2019, although recreational HMS landings data were not yet available for California and Washington, and albacore are a major component of recreational landings. Albacore landings in Oregon were dramatically lower in 2020, likely due in part to cool coastal conditions (see Figure 3.1.3). COVID-19 likely caused disruptions to recreational fishing opportunities, including restrictions on charter boat trips. State-by-state recreational landings and details are in Appendix M.



Total revenue for West Coast commercial fisheries decreased from 2016–2019, and is 22% lower in 2020 than in 2019, based on data currently available (see Appendix M.2). Revenue for 8 of 9 target groups currently show decreases in 2020 compared to 2019: CPS finfish (-45%), Pacific hake (-38%), non-hake groundfish (-37%), salmon (-33%), other species (-14%), crab (-13%), HMS (-10%), and shrimp (-6%). Market squid currently show greater revenue in 2020 than in 2019 (+91%). Ocean conditions, wildfires, compressed Dungeness crab fishing seasons, and COVID-related effects on supply and demand all likely contributed to the apparent decrease in total revenue in 2020. In addition, vessels and processors may have experienced increased operational costs due to overcoming COVID outbreaks and implementing protective measures. Coastwide and state-level revenue data are presented in Appendix M.2; *we will update these data in our March presentation.*

5.2 GEAR CONTACT WITH SEAFLOOR

We track the amount of contact by groundfish bottom trawl gear with the seafloor on the shelf and slope. For space considerations, we have moved this analysis, updated through 2019, to Appendix N.

6 HUMAN WELLBEING

We include several indicators of human wellbeing in fishing communities, which relate to the risk profiles and adaptive capacities of coastal communities in the face of various pressures. We are working to develop a suite of indicators that helps track progress toward meeting National Standard 8 (NS-8) of the Magnuson-Stevens Act. NS-8 states that fisheries management measures should “provide for the sustained participation of [fishing] communities” and “minimize adverse economic impacts on such communities.”

6.1 SOCIAL VULNERABILITY

Coastal community vulnerability indices are generalized social-economic vulnerability metrics. The Community Social Vulnerability Index (CSVl) is derived from social vulnerability data (demographics, poverty, housing, labor force structure, etc.; Jepson and Colburn 2013). We monitor CSVl in communities that are highly reliant upon fishing. The commercial fishing reliance index reflects *per capita* engagement in commercial fishing (landings, revenues, permits, processing, etc.) in each West Coast fishing community (n ≈ 250).

Figure 6.1.1 plots CSVl updated through 2018 against commercial fishing reliance for communities that are among the most reliant on commercial fishing in different regions of the West Coast. Communities above and to the right of the dashed lines are those with relatively high CSVl (horizontal line) and commercial fishing reliance (vertical line). Multiple ports in Washington and Oregon are in that upper right portion of the plot, scoring relatively

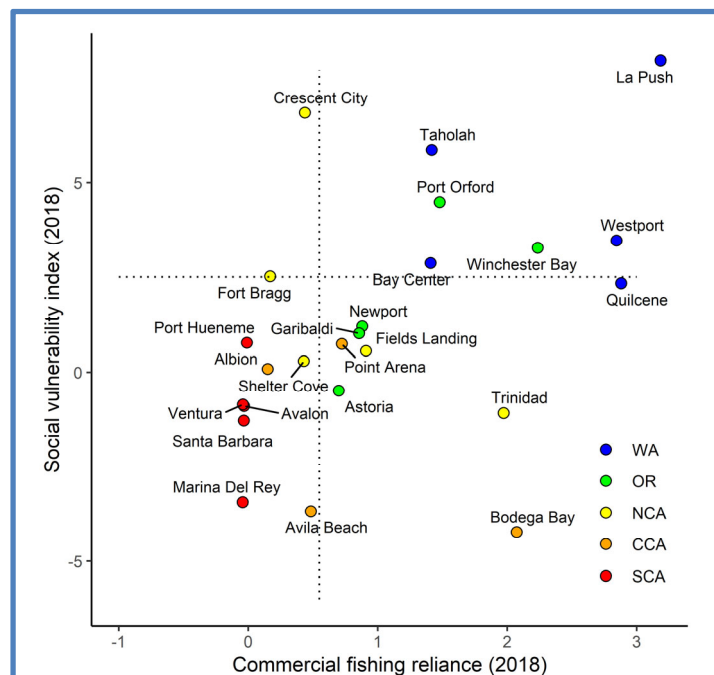


Figure 6.1.1 Commercial fishing reliance and social vulnerability scores as of 2018, plotted for twenty-five communities from each of the five regions of the California Current: WA, OR, Northern, Central, and Southern California. The top five highest scoring communities for fishing reliance were selected from each region. Black dotted lines denote one s.d. above the mean for communities with landings data. Note, the points for Avalon and Ventura overlap.

high for both reliance and CSVI compared to other coastal communities. Communities that are outliers in both indices may be especially socially vulnerable to downturns in commercial fishing. We note, however, that commercial fishing reliance can be volatile, and communities may move left on the x-axis during years with reduced landings. The communities may thus appear to be less dependent on commercial fishing when in fact they have actually just experienced a difficult year; thus, these results should be interpreted with care, and we will work to improve this analysis in the future. Additional details are in Appendix O.

6.2 DIVERSIFICATION OF FISHERY REVENUES

According to the Effective Shannon Index that we use to measure diversification of revenues across different fisheries (see Appendix P), the fleet of 28,000 vessels that fished the West Coast and Alaska in 2019 was less diverse on average than at any time in the prior 38 years (Figure 6.2.1a, solid gray line). Diversification rates for most categories of vessels fishing on the West Coast have been trending down for several years, but there were slight increases in 2019 for several categories of vessels with West Coast landings (Figure 6.2.1b-d). California, Oregon and Washington fleets all saw small increases in average diversification in 2019. The long-term declines are due both to entry and exit of vessels and changes for individual vessels. Less diversified vessels have been more likely to exit; vessels that remain have become less diversified, at least since the mid-1990s; and newer entrants generally have been less diversified than earlier entrants. Within the average trends are wide ranges of diversification levels and strategies, and some vessels remain highly diversified.

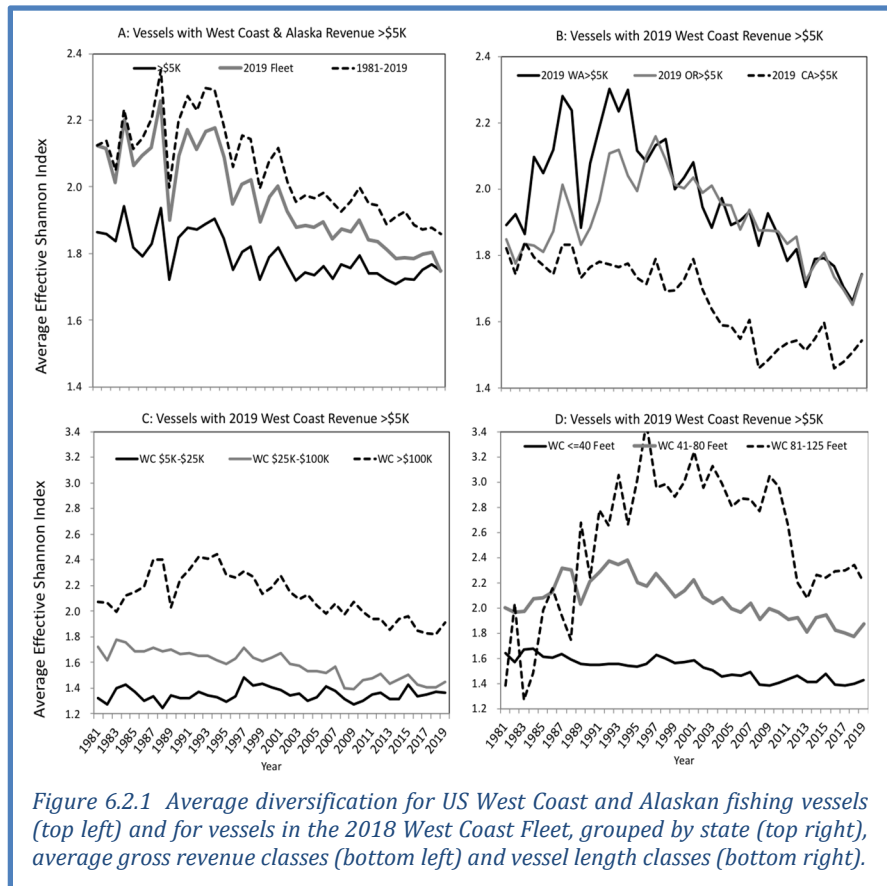


Figure 6.2.1 Average diversification for US West Coast and Alaskan fishing vessels (top left) and for vessels in the 2018 West Coast Fleet, grouped by state (top right), average gross revenue classes (bottom left) and vessel length classes (bottom right).

Port-level diversification is presented in Appendix P. Trends vary widely by port, even ports within the same region. As with individual vessels, the variability of landed value at the port level is reduced with greater diversification. Port-level diversification is variable from year to year, particularly in ports highly dependent upon Dungeness crab.

Port-level diversification is presented in Appendix P. Trends vary widely by port, even ports within the same region. As with individual vessels, the variability of landed value at the port level is reduced with greater diversification. Port-level diversification is variable from year to year, particularly in ports highly dependent upon Dungeness crab.

6.3 REVENUE CONSOLIDATION

In last year's report (see Harvey et al. 2020), we introduced port-level consolidation of fishing revenue as an exploratory indicator. With guidance from the SSC, we have updated that analysis for this report. The updated approach uses a metric called the Theil Index to estimate geographic concentration of revenue at the scale of the 21 port groups previously established for the economic

input-output model for Pacific Coast fisheries (IO-PAC; Leonard and Watson 2011). The Theil Index estimates the difference between observed revenue concentrations and what they would be if they were distributed with perfect equality across port groups.

We produced annual Theil Index values for revenue distribution of total fisheries and of different fishery management groups. In Figure 6.3.1 top, the Theil Index for each management group is shown, where positive values indicate revenue concentration greater than the long-term average, and negative values indicate revenue concentration closer to equality across the port groups. All fisheries combined (Figure 6.3.1 top, upper left) show small deviations and little variability over time, suggesting that total revenue has not exhibited high levels or extended trends of geographic concentration. This is shown in the maps in Figure 6.3.1 bottom, where the sizes of the bubbles, representing inflation-adjusted revenue from all commercial fisheries in each port-group, are fairly consistent over time. Separate fishery management groups show much clearer fluctuations in revenue concentration (Figure 6.3.1 top). For example, Theil Index values for groundfish have been gradually increasing due to greater concentration of revenues in northern port groups (see Appendix Q). In contrast, HMS revenues present a U-shaped trend, where geographic concentration of revenues was skewed to southern ports early in the time series, then decreased through the middle part of the time period, and then increased again in recent years as revenues became more concentrated in the north (Appendix Q). CPS, salmon and shrimp show high short-term or decadal variability.

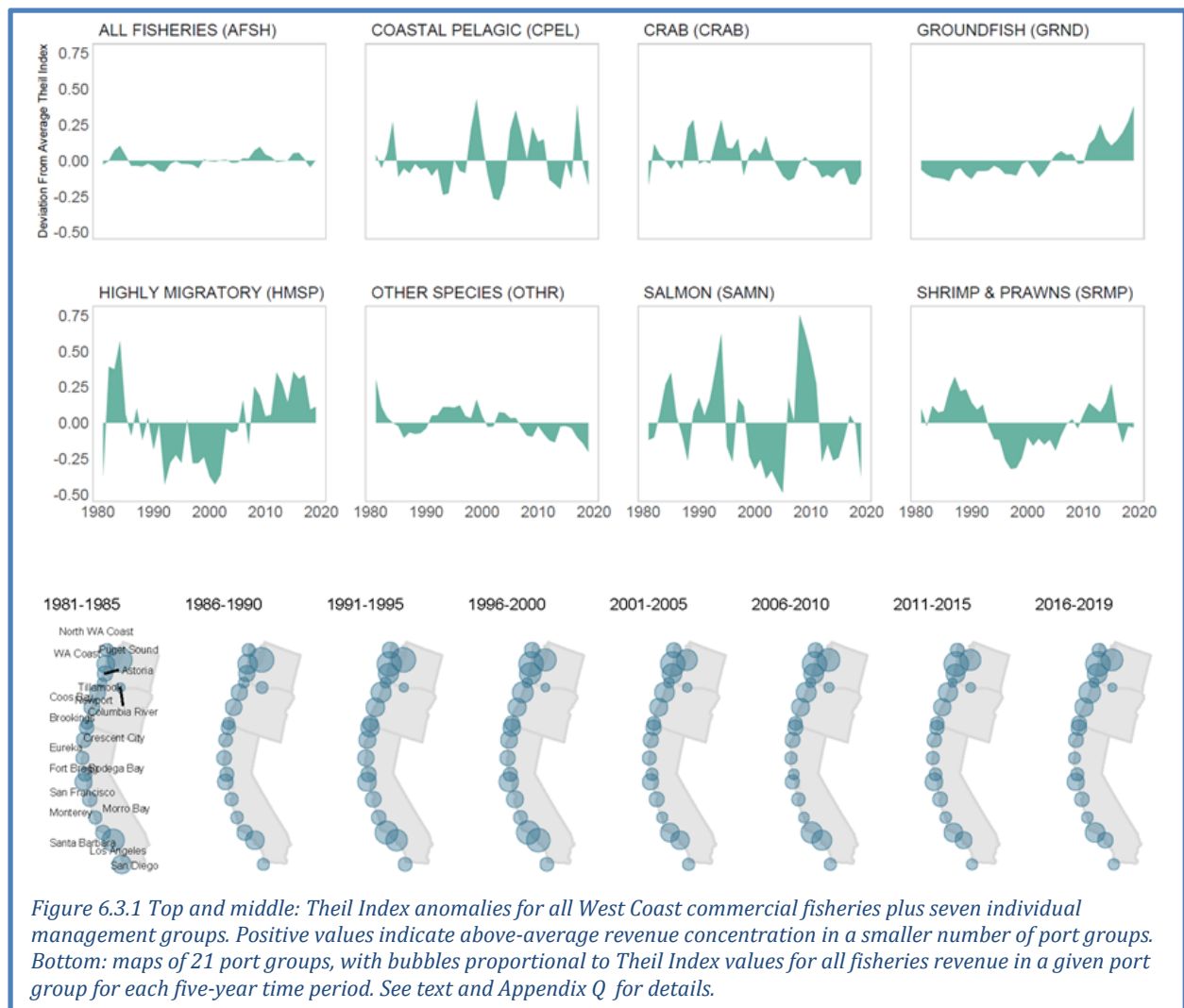


Figure 6.3.1 Top and middle: Theil Index anomalies for all West Coast commercial fisheries plus seven individual management groups. Positive values indicate above-average revenue concentration in a smaller number of port groups. Bottom: maps of 21 port groups, with bubbles proportional to Theil Index values for all fisheries revenue in a given port group for each five-year time period. See text and Appendix Q for details.

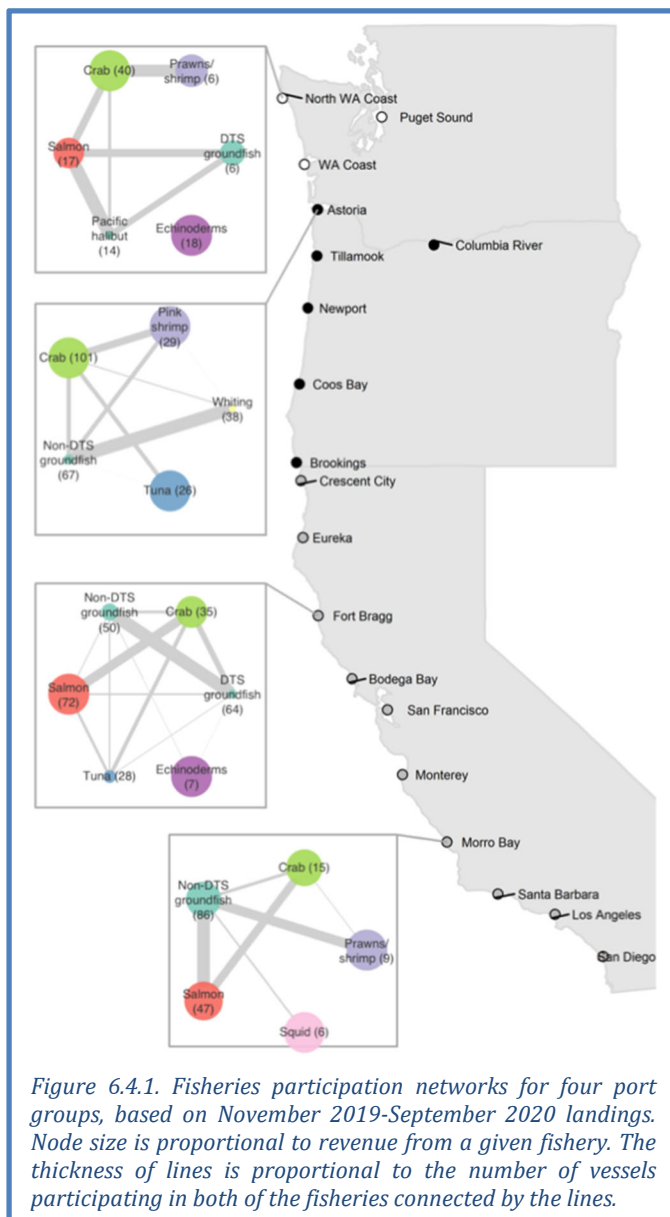
We have not attempted to interpret the Theil Index with respect to NS-8, or to link changes to specific causes. We will work with Council advisory bodies to develop recommendations for further analyses.

6.4 FISHERIES PARTICIPATION NETWORKS

As fishers diversify their harvest portfolios, they create links between fisheries, even when ecological links between the harvested species are weak or absent. This creates networks of alternative sources of income, which can be described on a variety of spatial and temporal scales. Fisheries participation networks offer one way to represent this information visually, as nodes in a network represent fisheries, and pairs of nodes are connected by lines (“edges”) that indicate the relative number of vessels that participate in both fisheries. These networks therefore add a level of detail to the diversification indices, and context to the Theil indices, presented earlier in this report.

In IO-PAC port groups, networks consist of 1 to 8 fisheries, with 0-16 links between the fisheries within each network (see Appendix R). Some fisheries, like crab and groundfish, are represented at nearly all port groups while others, like squid, are represented at fewer. Figure 6.4.1 shows four example networks from 2019-2020. In each network, nearly all fisheries are connected to at least one other fishery, indicating that most vessels participate in multiple fisheries over the course of a year. (Echinoderms in the North Washington Coast port group are an exception). Notably, many Council-managed fisheries connect to fisheries under state jurisdictions. The prime example from Washington south to Morro Bay is the crab fishery, which accounts for a large proportion of fishing revenue (large node size) and is highly connected to other fisheries that generate less revenue in each port group. The crab, salmon, and groundfish nodes involve consistently heavy levels of cross-fishery participation across port groups (Figure 6.4.1). In the southern three port groups (Santa Barbara, Los Angeles, San Diego; see Appendix R), echinoderms and shellfish generate the majority of revenue, but compared to crab in the northern ports, there is less connectivity between these fisheries and others in the same port group.

Differences in the make-up of port group networks in part reflect differences in the ecology of adjacent coastal habitats and waters, and in part the legacy of management, market, and other factors that vary geographically. The networks demonstrate that individual fisheries do not operate in vacuums, just as species do not, and part of an ecosystem approach to fisheries management is to consider species and fisheries as



interactive entities rather than in piecemeal fashion. Thus, these networks may provide context for understanding and interpreting indicators of human activities and wellbeing presented in these reports. Further, tracking changes in the networks themselves may support the Council's Climate and Communities Initiative and other activities by providing insight into how fishing communities are changing and potentially adapting to external forces such as changing stock availabilities, climate, regulations, and economic and social systems.

7 SYNTHESIS

Accurately summarizing the status of the CCE in 2020 will be a challenge, now and going forward, due to the negative impacts of COVID-19: fisheries that depend on California Current stocks were badly disrupted, research effort was cut or delayed, and fewer eyes from the fishing, management, research, and public sectors were on the water to develop a collective sense of the state of the system. Despite those challenges, we can best summarize the past year as follows:

Evidence points to a return to average or above-average productivity in the CCE in 2020. Many indicators suggested good foraging conditions in different regions, including the high abundance of nutritious northern copepods off Oregon, large krill in plankton nets and seabird diets in northern and central California, continued abundance of anchovies, and generally good production of offspring by seabirds and sea lions at the colonies being monitored. More information on abundance and condition of key species may come available as 2020 samples continue to be processed.

Some of these results are continuations of past years' dynamics, such as the now years-long resurgence of the anchovy population. Others may have benefited from shifts in climate and ocean conditions that occurred in 2020, including a transition to La Niña and negative PDO conditions that are often associated with cooler and more productive years in the CCE. Local upwelling/relaxation strength and timing, particularly off central California, may have helped boost productivity, and also may have helped the CCE avoid some of the effects of another very large marine heatwave in 2020. We await to see if La Niña, negative PDO and positive upwelling will persist further into 2021.

The past year was not without concerning signals: we continue to see relatively warm water, offshore in the form of heatwaves, and alongshore, particularly in the southern CCE and to a lesser extent the central CCE. Harmful algal blooms were an issue in all three coastal states. Salmon outlooks remain mixed based on past years' indicators. Much of the West is facing drought in the year ahead and recovering from traumatic wildfires. And of course, fishing communities have been through the unprecedented stress test of the COVID-19 pandemic, which affected landings, revenues, operations and markets for many fisheries, and added a new layer of uncertainty to the fishing profession. As with any ecosystem shock, this one will reverberate and its full effects will take time to understand.

SUPPLEMENTARY MATERIALS TO THE CALIFORNIA CURRENT INTEGRATED ECOSYSTEM ASSESSMENT (CCIEA) CALIFORNIA CURRENT ECOSYSTEM STATUS REPORT, 2021

Appendix A LIST OF CONTRIBUTORS TO THIS REPORT, BY AFFILIATION

NWFSC, NOAA Fisheries

Mr. Kelly Andrews
Ms. Katie Barnas
Dr. Brian Burke
Dr. Jason Cope
Dr. Correigh Greene
Dr. Thomas Good
Dr. Marie Guldin
Dr. Chris Harvey (co-editor)
Dr. Daniel Holland
Dr. Mary Hunsicker
Dr. Kym Jacobson
Dr. Stephanie Moore
Dr. Stuart Munsch
Dr. Karma Norman
Dr. Jameal Samhour
Dr. Kayleigh Somers
Dr. Erin Steiner
Dr. Nick Tolimieri (co-editor)
Ms. Ashley Vizek
Mr. Curt Whitmire
Ms. Margaret Williams

Pacific States Marine Fishery Commission

Ms. Amanda Phillips
Mr. Gregory Williams (co-editor)

Oregon State University

Ms. Jennifer Fisher
Ms. Cheryl Morgan
Ms. Samantha Zeman

AFSC, NOAA Fisheries

Dr. Stephen Kasperski
Dr. Sharon Melin

NOAA Fisheries West Coast Region

Mr. Dan Lawson
Ms. Lauren Saez

Point Blue Conservation Science

Dr. Jaime Jahncke
Mr. Peter Warzybok

Scripps Institute of Oceanography

Dr. Clarissa Anderson
Dr. Dan Rudnick

University of Washington

Dr. Mary Fisher

SWFSC, NOAA Fisheries

Dr. Eric Bjorkstedt
Dr. Steven Bograd
Ms. Lynn deWitt
Dr. John Field
Dr. Newell (Toby) Garfield (co-editor)
Dr. Elliott Hazen
Dr. Michael Jacox
Dr. Andrew Leising
Dr. Nate Mantua
Mr. Keith Sakuma
Dr. Jarrod Santora
Dr. Cameron Speir
Dr. Andrew Thompson
Dr. Brian Wells
Dr. Thomas Williams

University of California-Santa Cruz

Dr. Barbara Muhling
Dr. Dale Robinson
Dr. Isaac Schroeder

Humboldt State University

Ms. Roxanne Robertson

Wellesley College

Dr. Rebecca Selden

California Department of Public Health

Ms. Christina Grant
Mr. Duy Trong
Ms. Vanessa Zubkousky-White

California Department of Fish and Wildlife

Ms. Christy Juhasz

CA Office of Env. Health Hazard Assessment

Dr. Beckye Stanton

Oregon Department of Fish and Wildlife

Dr. Caren Braby
Mr. Matthew Hunter

Oregon Department of Agriculture

Mr. Alex Manderson

Washington Department of Health

Mr. Jerry Borchert
Ms. Tracie Barry

Appendix B LIST OF FIGURE AND DATA SOURCES FOR THE MAIN REPORT

Figure 3.1.1: Oceanic Niño Index data are from the NOAA Climate Prediction Center (<https://go.usa.gov/xG6NH>). PDO data are from N. Mantua, NMFS/SWFSC, derived from the University of Washington Joint Institute for the Study of the Atmosphere and Ocean (JISAO; <http://research.jisao.washington.edu/pdo/>). North Pacific Gyre Oscillation data are from E. Di Lorenzo, Georgia Institute of Technology (<http://www.o3d.org/nngo/>).

Figure 3.1.2: Standardized sea surface temperature anomaly plots were created by A. Leising, NMFS/SWFSC, using SST data from NOAA's optimum interpolation sea surface temperature analysis (OISST; <https://www.ncdc.noaa.gov/oisst>) The standardized SSTa is defined as SSTa divided by the SD of SSTa at each location calculated over 1982–2020, thus taking into account spatial variance in the normal fluctuation of SSTa.

Figure 3.1.3: Newport Hydrographic (NH) line temperature data from J. Fisher, NMFS/NWFSC, OSU. CalCOFI data from <https://calcofi.org>. CalCOFI data before 2020 are from the bottle data database, while 2020 data are preliminary from the recent conductivity, temperature, and depth (CTD) database.

Figure 3.2.1: Daily 2020 values of BEUTI and CUTI are provided by M. Jacox, NMFS/SWFSC; detailed information about these indices can be found at <https://go.usa.gov/xG6Jp>

Figure 3.2.2: Compression index estimates developed and provided by J. Santora, NMFS/SWFSC, and I. Schroeder, NMFS/SWFSC, UCSC.

Figure 3.3.1: Newport Hydrographic (NH) line dissolved oxygen data are from J. Fisher, NMFS/NWFSC, OSU. CalCOFI data from <https://calcofi.org>. CalCOFI data before 2020 are from the bottle data database, while 2020 data are preliminary from the recent CTD database.

Figure 3.4.1: WA data are provided by the Washington State Department of Health, OR data from the OR Department of Agriculture, and CA data from the California Department of Public Health.

Figure 3.5.1: Snow-water equivalent data were derived from the California Department of Water Resources snow survey (<http://cdec.water.ca.gov/>) and the Natural Resources Conservation Service's SNOTEL sites in WA, OR, CA and ID (<http://www.wcc.nrcs.usda.gov/snow/>).

Figure 3.5.2: Minimum and maximum streamflow data were provided by the US Geological Survey (<http://waterdata.usgs.gov/nwis/sw>).

Figure 4.1.1: Copepod biomass anomaly data were provided by J. Fisher, NMFS/NWFSC, OSU.

Figure 4.1.2. Krill data were provided by E. Bjorkstedt, NMFS/SWFSC and Humboldt State University (HSU), and R. Robertson, Cooperative Institute for Marine Ecosystems and Climate (CIMEC) at HSU.

Figure 4.2.1: Pelagic forage data from the Northern CCE from B. Burke, NMFS/NWFSC and C. Morgan, OSU/CIMRS. Data are derived from surface trawls taken during the NWFSC Juvenile Salmon & Ocean Ecosystem Survey (JSOES; <https://www.fisheries.noaa.gov/west-coast/science-data/ocean-ecosystem-indicators-pacific-salmon-marine-survival-northern>).

Figure 4.2.2: Pelagic forage data from the Central CCE were provided by J. Field, K. Sakuma, and J. Santora, NMFS/SWFSC, from the SWFSC Rockfish Recruitment and Ecosystem Assessment Survey (<https://go.usa.gov/xGMfR>).

Figure 4.2.3: Pelagic forage larvae data from the Southern CCE were provided by A. Thompson, NMFS/SWFSC, and derived from winter CalCOFI surveys (<https://calcofi.org/>).

Figure 4.3.1: Chinook salmon escapement data were derived from the California Department of Fish and Wildlife (<https://www.dfg.ca.gov/fish/Resources/Chinook/CValleyAssessment.asp>), PFMC pre-season reports (<https://www.pcouncil.org/safe-documents-3/>), and the NOAA NWFSC's "Salmon Population Summary" database (<https://www.webapps.nwfsc.noaa.gov/sps>), with data provided directly from the Nez Perce Tribe, the Yakama Nation Tribe, and from Streamnet's Coordinated Assessments database (cax.streamnet.org; see website for a list of all participating data-compiling agencies).

Figure 4.3.2: Data for at sea juvenile salmon provided by B. Burke, NMFS/NWFSC, with additional calculations by C. Morgan, OSU/CIMRS. Derived from surface trawls taken during the NWFSC Juvenile Salmon and Ocean Ecosystem Survey (JSOES) cruises.

Figure 4.4.1: Groundfish biomass availability index provided by B. Selden, Wellesley College, and N. Tolimieri, NMSF/NWFSC, with data derived from the NOAA/NWFSC West Coast groundfish bottom trawl survey.

Figure 4.5.1. Highly migratory species data provided by B. Muhling, NMFS/SWFSC. Data are derived from stock assessment reports for the International Scientific Committee for Tuna and Tuna-like Species in the North Pacific Ocean (ISC; http://isc.fra.go.jp/reports/stock_assessments.html) or the Inter-American Tropical Tuna Commission (IATTC; <https://www.iattc.org/PublicationsENG.htm>).

Figure 4.6.1: California sea lion data provided by S. Melin, NMFS/AFSC, with additional data collection and interpretation by E. Jaime, NMFS/AFSC, and M. Ball, Wildlands Conservation Science.

Figure 4.6.2: Whale entanglement data provided by D. Lawson and L. Saez, NMFS/WCR.

Figure 4.7.1: Seabird fledgling production data at nesting colonies on Southeast Farallon provided by J. Jahncke and P. Warzybok, Point Blue Conservation Science.

Figure 5.1.1: Data for commercial landings are from PacFIN (<http://pacfin.psmfc.org>) and NORPAC (North Pacific Groundfish Observer Program).

Figure 5.1.2: Data for recreational landings are from RecFIN (<http://www.recfin.org/>) and the CDFW Pelagic Fisheries and Ecosystem Data Sharing index).

Figure 6.1.1: Community social vulnerability index (CSVI) and commercial fishery reliance data provided by K. Norman, NMFS/NWFSC, and A. Phillips, PSMFC, with data derived from the US Census Bureau's American Community Survey (ACS; <https://www.census.gov/programs-surveys/acs/>) and PacFIN (<http://pacfin.psmfc.org>), respectively.

Figure 6.2.1: Fishery diversification estimates were provided by D. Holland, NMFS/NWFSC, and S. Kasperski, NMFS/AFSC.

Figure 6.3.1: Theil Index and annual commercial fishery revenue data provided by K. Norman, NMFS/NWFSC, and A. Phillips, PSMFC, with data derived from PacFIN (<http://pacfin.psmfc.org>).

Figure 6.4.1: Fishery Participation Network data and analyses provided by J. Samhuri, NMFS/NWFSC, M. Fisher, UW, and A. Phillips, PSMFC, with data derived from PacFIN (<http://pacfin.psmfc.org>).

Table 4.3.1: Stoplight table of indicators and projected 2021 salmon returns courtesy of B. Burke and K. Jacobson, NMFS/NWFSC, and J. Fisher, C. Morgan, and S. Zeman, OSU/CIMRS.

Table 4.3.2: Table of indicators and qualitative outlook for 2021 Chinook salmon returns to the Central Valley courtesy of N. Mantua, NMFS/SWFSC.

Appendix C CHANGES IN THIS YEAR'S REPORT

Below we summarize major changes in the 2021 Ecosystem Status Report. As in past reports, many of these changes are in response to requests and suggestions received from the Council and advisory bodies under FEP Initiative 2, "Coordinated Ecosystem Indicator Review" (March 2015, Agenda Item E.2.b), or in response to regular technical reviews of indicators and analyses that the CCIEA team has with the SSC-Ecosystem Subcommittee (SSC-ES). We also note any items we have added and information gaps that we have filled since last year's report. Finally, we note major changes that are related to the COVID-19 pandemic (due to cancelled surveys, sample processing delays, or other COVID-related disruptions).

Request/Need	Response/Location in document
<p>Description of habitat compression along the West Coast, in relation to other basin-scale climate indicators, upwelling, and habitat suitability for key species</p>	<p>In last year's report, we introduced the Habitat Compression Index (HCI) as an index of the area of cool upwelled habitat along the central California coast, as a way of understanding food web dynamics, species distribution, and conditions that can lead to whale entanglement. The SSC-ES reviewed this index in September 2020 and recommended expanding it to cover other regions of the coast. The central California HCI is presented in the main document, Figure 3.2.2, and the other regions have been added to the Supplement in Appendix D.3, along with a brief description of methods.</p>
<p>Because of COVID-19 impacts and restrictions, many surveys were cancelled or rescheduled, and/or sample processing and data analysis has been delayed, meaning that some time series could not be updated in this year's report.</p>	<p>Details of COVID-19 impacts on survey effort and data processing are noted throughout the main body, particularly in the Ecological Integrity information in Section 4 and related appendices in the Supplement.</p> <p>The regional forage surveys described in Section 4.2 were all affected by COVID-19 through delayed sampling processing (all surveys), reduced sampling effort (Central CCE survey), or cancellation of the spring sampling cruise (Southern CCE survey). CCIEA scientists met with the SSC-ES in January 2021 for a review of methods used to adapt to these circumstances and provide some forage indicators. Methods and results are outlined in Section 4.2, with additional detail in Appendix G.</p>
<p>In March 2020 (Agenda item G.1.b), the SSC recommended that the Central Valley Fall Chinook (CVFC) salmon "stoplight table" that was introduced in the 2020 ecosystem status report receive technical review by the SSC-ES.</p>	<p>The SSC-ES reviewed the CVFC stoplight table (main body, Table 4.3.2) and supported its use as a qualitative indicator for outlooks on pending returns of CVFC. The SSC-ES requested text to describe methods, distinctions between natural-origin and composite natural+hatchery escapement, and the qualitative category boundaries in the table; text has been added to Appendix H.5. The SSC-ES also requested validation of prior years' outlooks, but we did not had time to do that for this year's report.</p>

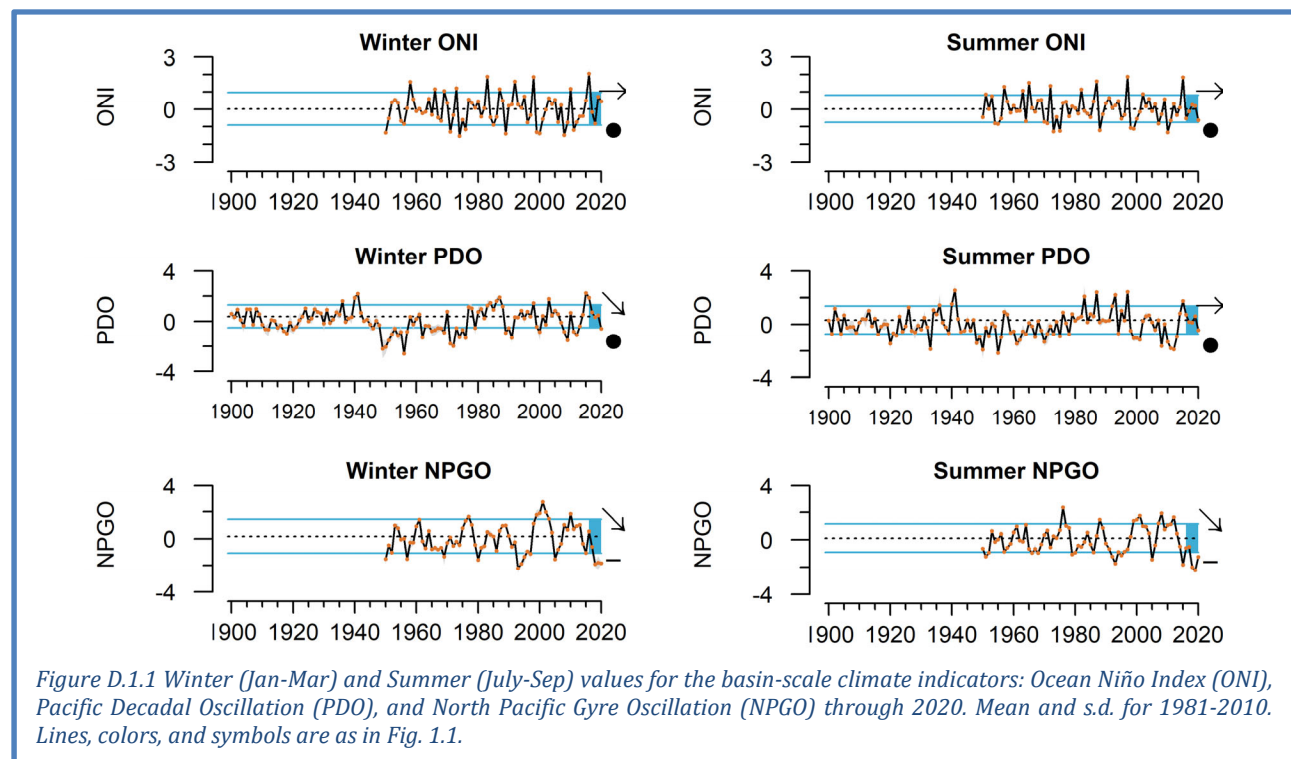
Request/Need	Response/Location in document
<p>We have received many requests for additional “stoplight table” information for salmon from California catchments, and also recommendations from the SSC-ES (from September 2016) that habitat indicators be linked spatiotemporally to life history stages of key salmon stocks</p>	<p>We have added two new stoplight tables of ecosystem conditions related to Sacramento River Fall Chinook and Klamath River Fall Chinook. These tables expand on stoplight tables for other salmon groups (including the Central Valley Fall Chinook table mentioned above) and support two stocks that are the focus of recent rebuilding plans. The tables and supporting text are in Appendix H.5 and were developed by the Council Habitat Committee and Salmon Technical Team, with participation of CCIEA team members.</p>
<p>Salmon spawning escapement counts have been limited to Chinook salmon in past reports</p>	<p>We added coho salmon escapement time series for four ESUs. Data are presented in a summary quad plot in the main body (Figure 4.3.1) and as time series in Appendix H.3.</p>
<p>Groundfish indicators have mostly been limited to stock assessment outputs in previous years, and we have not taken more advantage of data from the NMFS West Coast Groundfish Bottom Trawl Survey</p>	<p>We have updated an analysis, first presented in the 2019 report, that estimates availability of groundfish to port communities, based on Bottom Trawl Survey data, information on areas fished by vessels from different ports, and spatial analysis tools (VAST) used elsewhere for Council purposes. The approach was previously reviewed by the SSC-ES in September 2018 and the revisions were reviewed by the SSC-ES in January 2021. The analyses appear in the main body in Section 4.4 and in the Supplement in Appendix I.</p>
<p>In March 2017 (Agenda Item F.1.b), the SSC expressed concern that California sea lion indicators (pup count and pup growth at the San Miguel colony) were potentially ineffective indicators of foraging conditions when the colony is close to carrying capacity</p>	<p>The SSC-ES reviewed these indicators in September 2020. The lead CCIEA expert presented statistical modeling results showing that a sea lion population size variable was not included in any of the top-tier models to describe sea lion pup counts or sea lion pup growth, although we agree with the SSC-ES that it cannot be ruled out entirely and will continue to consider this factor as the sea lion population changes. Details are provided in Appendix K. At the SSC-ES request, we also elaborated on the ecological mechanisms we believe these indicators are representing; see Section 4.6 and Appendix K.</p> <p>Also in Appendix K, we include an analysis showing a threshold relationship between PDO and sea lion pup growth, which we were unable to measure empirically during 2020 due to COVID. The SSC-ES had reviewed this general approach in September 2017 and this particular application, briefly, in January 2021, and SSC members have recommended that we continue to explore time series of pressures and responses for the existence of threshold dynamics as evidence of possible ecosystem reference points.</p>

Request/Need	Response/Location in document
<p>In reports prior to this, we have presented fishery landings and revenue data that lagged by ~1 year because data reporting from the previous year tended to be incomplete by the time of the March briefing book deadline</p>	<p>We now report fishery landings and revenue data from the immediate prior year (in this case, 2020). At the March 2020 Council meeting, we showed an analysis to the SSC indicating that reporting of landings data to PacFIN and RecFIN in recent years had increased in efficiency, i.e., data that were available by the briefing book deadline were very highly correlated with eventual total landings and revenue for the previous year, and not substantially biased. Data and explanations are in Section 5.1 of the main body and Appendix M of the Supplement, along with clear statements of how current the data are.</p>
<p>In 2018, the Ecosystem Advisory Subpanel requested that the IEA team develop indicators of community-level fishery participation and economic status, as related to National Standard 8 (NS-8) under the Magnuson-Stevens Act.</p>	<p>In last year’s report we introduced summary statistics of revenue concentration within coastal communities. At the recommendation of the SSC, we developed that analysis further using the Theil Index to estimate revenue concentration across different fisheries, at the scale of IO-PAC port groups. The SSC-ES reviewed this analysis in September 2020. Results are shown in the main body (Section 6.3), and additional results and methods are in the Supplement (Appendix Q).</p> <p>In addition, in this year’s report we introduce fisheries participation networks to describe how vessels in different port groups participate in multiple fisheries. The SSC-ES had reviewed this general concept in September 2016, and reviewed our updated approach briefly in January 2021. Results are presented in the main body (Section 6.4) and Supplement (Appendix R). It is included as ongoing research that may be useful in assessing the impacts of external drivers (e.g., management actions, environmental variability, climate change, COVID-19) to coastal fishing communities</p>

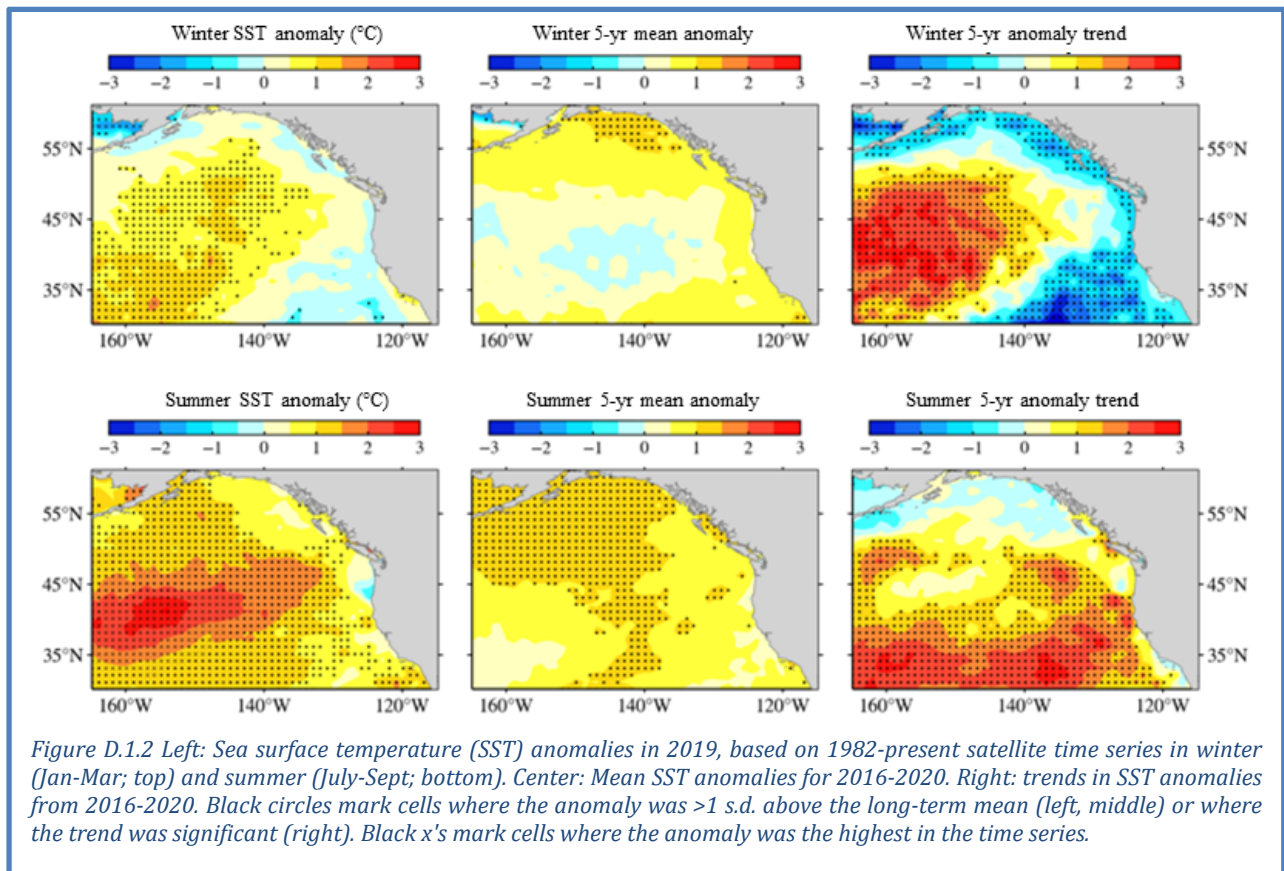
Appendix D CLIMATE AND OCEAN INDICATORS

D.1 BASIN-SCALE CLIMATE/OCEAN INDICATORS AT SEASONAL TIME SCALES

These plots show seasonal averages, short-term trends, and short-term averages of the three basin-scale climate forcing indicators shown in the main report in Figure 3.1.1. The first notable outcome is that the winter Ocean Niño Index (ONI) has a declining recent trend following the strong 2016 El Niño (Figure D.1.1). The winter 2020 ONI was positive while the summer 2020 ONI was negative, reflecting the transition of conditions that occurred over the course of the year. We expect the forthcoming winter 2021 ONI to be negative given current La Niña conditions, which are 95% likely to continue through the winter according to the NOAA Climate Prediction Center. Also, both summer and winter PDO have negative trends since 2016 (Figure D.1.1), illustrating the decline from the strong positive PDO signal of the 2013-2016 marine heatwave, and the emergence of a negative PDO during 2020. Finally, the trends in NPGO have been negative from 2016 to 2020 in both summer (Figure D.1.1), and summer NPGO has been below average over the past 5 years, including the lowest values in the time series (Figure D.1.1).

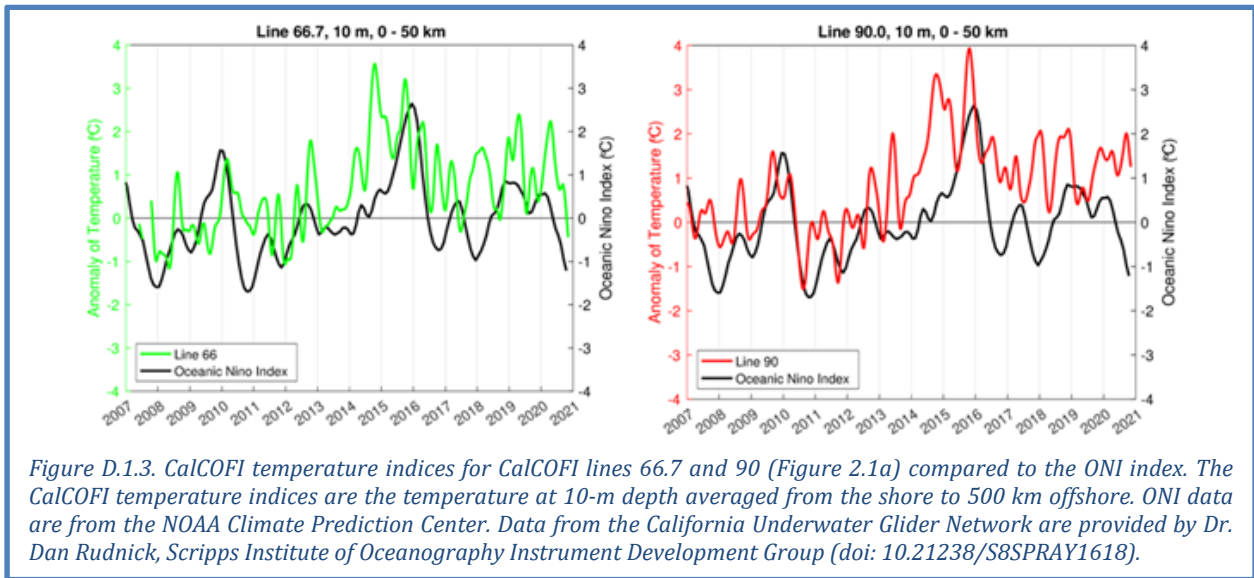


Compared to the long-term mean (1982-2020), winter sea surface temperature anomalies (SSTa) along the West Coast in 2020 were average to negative (between 0 to -0.5°C) within 150 km of the coast from Washington to northern California (Figure D.1.2, upper left). From San Francisco Bay to the Southern California Bight, SSTa during winter were mostly between 0 to 0.5°C , with larger positive anomalies between 0.5 to 1°C around Pt. Conception and the Channel Islands. Far offshore into the subtropical gyre, the winter SSTa were larger with anomalies >1 s.d. (marked with circles in Figure D.1.2 upper left). Summer SSTa along the West Coast had a similar pattern to the winter, with negative anomalies in the northern CCE and positive anomalies in the south (Figure D.1.2 lower left). Over most of the North Pacific domain, summer SSTa were >1 s.d. above average, and many locations had the largest positive anomaly since 1982 (marked with x's in Figure D.1.2 lower left). SSTa progressively increased over 2020, with fall 2020 experiencing the greatest extent of warm anomalies >1 s.d. above (data not shown).



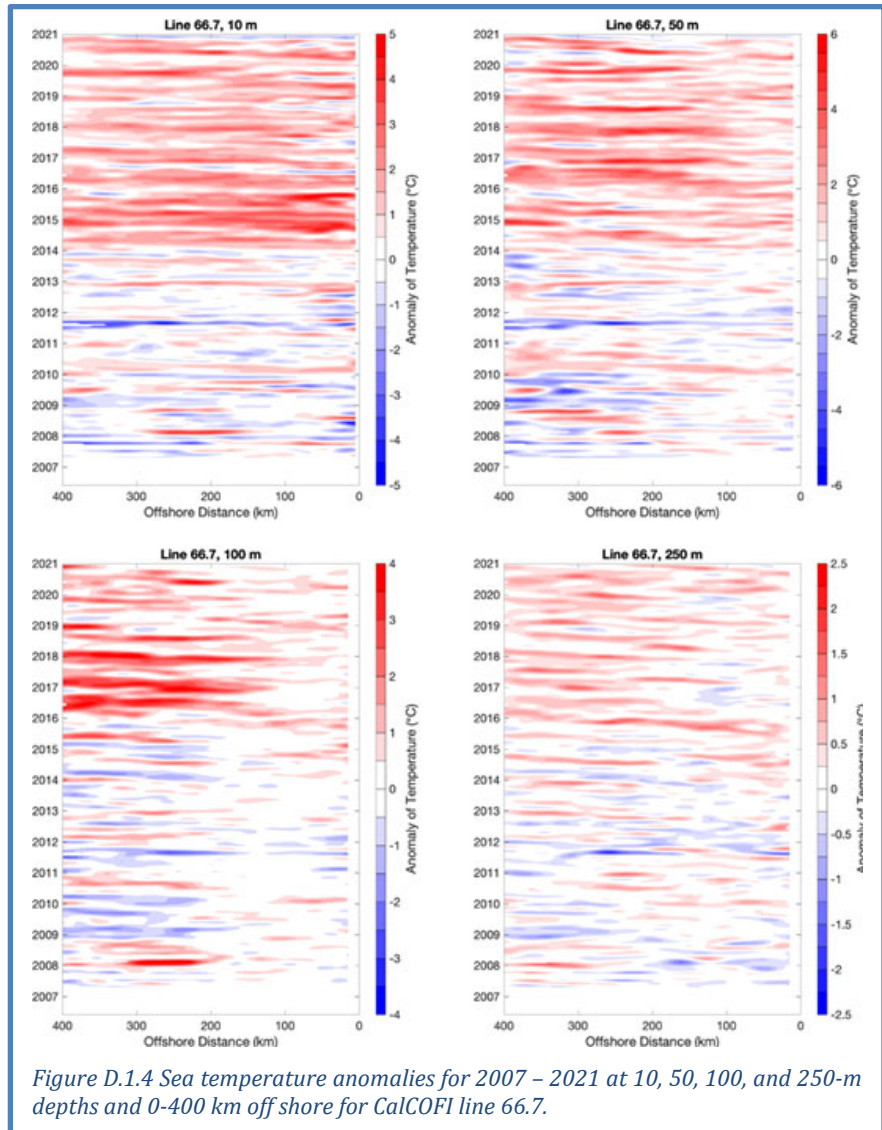
The winter 5-year mean SSTa (Figure D.1.2, top middle) was lowest along the coast from Washington to northern California, with mean anomalies no higher than 0.5 SD above the long-term average; winter mean SSTa was warmer (~1 s.d. above the long-term mean) just offshore of the northern and central CCE and in coastal waters extending down into the southern California Bight. Over most of the North Pacific, the 5-year winter means were within ± 1 s.d. of the long-term mean, except in the northern Gulf of Alaska where the 5-year means were >1 s.d. warmer than average. Winter 5-year trends (Figure D.1.2, top right) from 2016-2020 were strongly positive offshore in the subtropical gyre, but strongly negative closer to the continent and moving south into the Eastern Tropical Pacific. This reflects changes following the warm NE Pacific temperatures during the 2016 El Niño event; offshore waters have remained warm while the nearshore and subtropical gyre have returned to more average values. Summer 5-year mean SSTa (Figure D.1.2, bottom middle) along the West Coast were slightly positive from Washington to Point Conception; from Point Conception to the Mexican border the means increased with some areas exceeding 1 s.d. above the long-term average. A majority of the offshore North Pacific region had the summer 5-year mean SSTa ranging 0.5 to 1.5 s.d. above average. Summer 5-year trends (Figure D.1.2, bottom right) were positive over most of the domain south of 50°N, with the exception for the coastal region along southern California.

Jacox et al. (2017) demonstrated that El Niño events were strong predictors of CCE surface temperature. The ONI is formed from the time average of equatorial SST. In a similar manner, Rudnick et al. (2017) created indices along the autonomous glider transects on CalCOFI Lines 67 and 90 by averaging the 10 m data from the coast out 50 km. The glider data demonstrate the relatively strong correlation with the ONI prior to the 2013 marine heatwave, especially at Line 90 in the Southern California Bight (Figure D.1.3). Since then, both the Line 67 and 90 temperature indices have remained warmer than the ONI and haven't reflected the ONI cycling. Causes of this change are still being investigated.



While the figures and text above focus on near-surface temperatures, the North Pacific has stored large amounts of heat in subsurface waters over the past several years (e.g., Scannell et al. 2020).

Subsurface temperature data from glider transects provide additional information, and these data were especially valuable this year: glider data allowed for continued sampling during spring 2020 while ship-based observations were cancelled due to COVID-19 health restrictions. Gliders along CalCOFI Lines 67 and 90 (Figure 2.1a) operating since 2007 provide depth-resolved temperature and salinity data off of Monterey Bay (Line 66.7; Figure D.1.4) and Dana Point (Line 90; Figure D.1.5). Glider-based temperature data have been aggregated to construct monthly time-depth temperature anomaly figures from the coast to the offshore zone. Glider data along Line 67 (to 400 km



offshore) generally show positive temperature anomalies over the upper 250 m of the water column in winter 2020 (Figure D.1.4). Warm anomalies near the surface layers (10 and 50 m) were the strongest during winter and early spring before moderating in the summer of 2020, increasing again with the coastal intersection of the 2020 marine heatwave (see next section), and then turning negative in the fall. Line 67 anomalies at greater depths were mostly neutral or positive for the full year. Generally, the temperature anomalies were larger offshore than nearshore.

Time-depth temperature anomaly profiles were different to the south along Line 90 in the Southern California Bight. The 10-m temperature anomalies were positive for nearly all of 2020 for the full 500-km transect (Figure D.1.5). The anomalies were warmest near the coast and were even negative offshore at certain depths and seasons. Positive anomalies were weaker at the greater depths and transitioned to cool anomalies at points throughout the year.

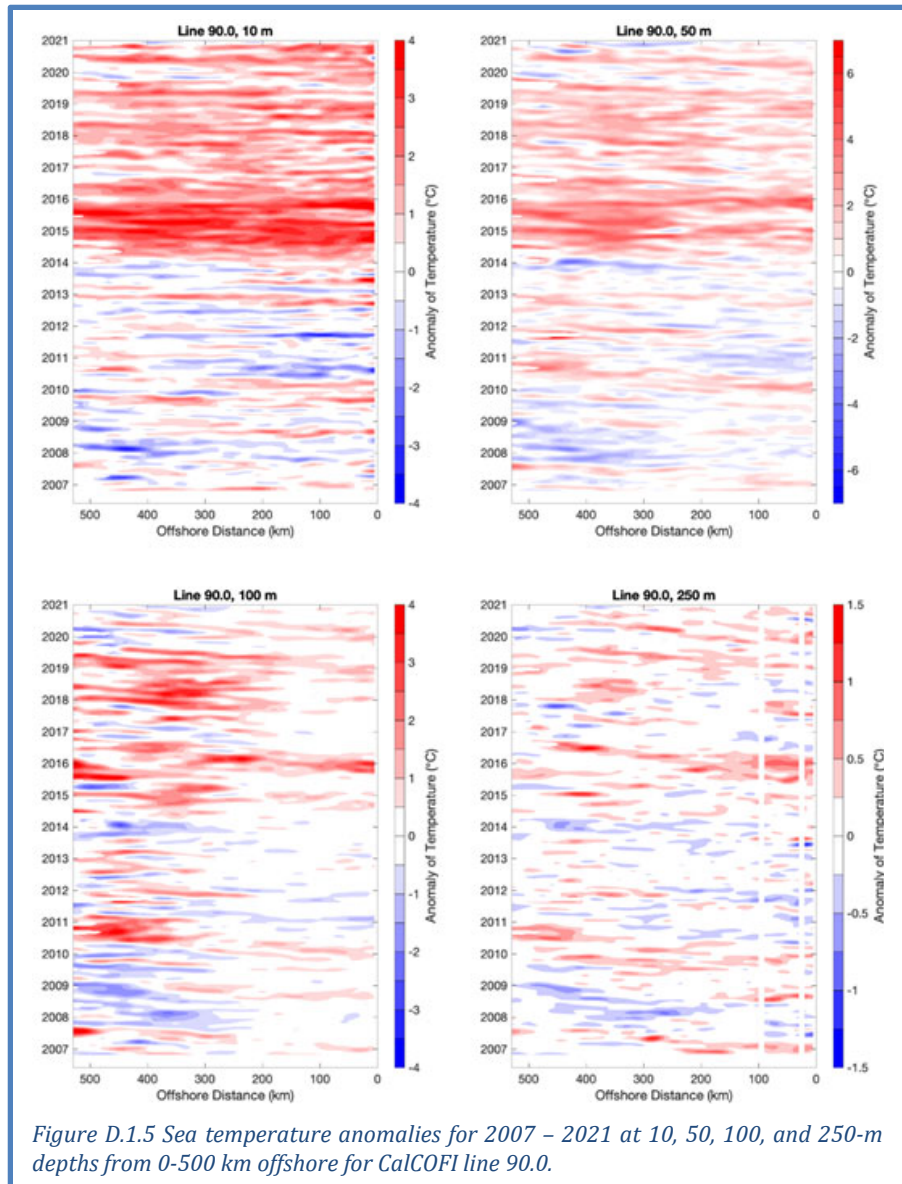


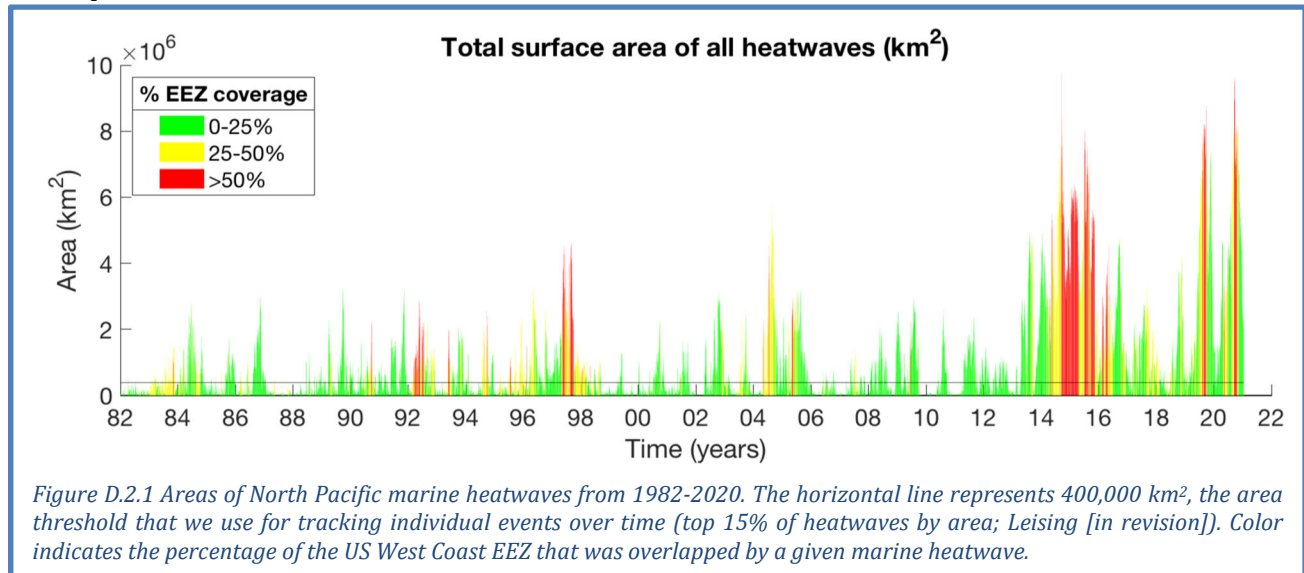
Figure D.1.5 Sea temperature anomalies for 2007 – 2021 at 10, 50, 100, and 250-m depths from 0-500 km offshore for CalCOFI line 90.0.

D.2 ASSESSING MARINE HEATWAVES IN 2020

There is increased recognition that marine heatwaves can have immediate short-term impacts on the ecosystem, as well as an indication of stock displacements that may occur with long-term climate warming (Morgan et al. 2019, Jacox et al. 2020). As discussed in Section 3.1, the North Pacific experienced two large marine heatwaves in 2020. The second heatwave had the second largest total area recorded in the region, behind only the peak of the 2013-2016 marine heatwave known as the “Blob,” and larger than the large heatwave of 2019 (Figure D.2.1). Here we provide details of the heatwaves that occurred in 2020 and relate them to prior North Pacific heatwaves.

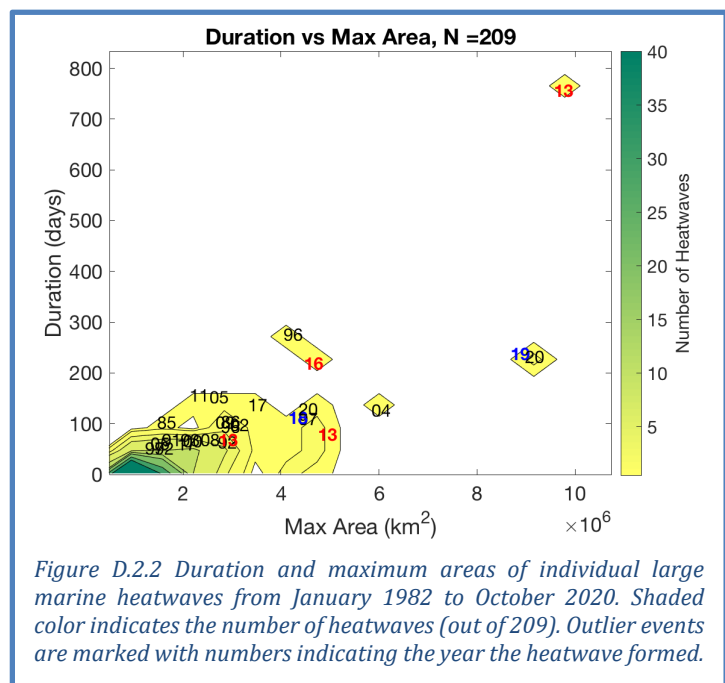
Based on an analysis of sea surface temperature anomalies (SSTa) from 1982–2019, a marine heatwave has the potential to cause impacts in the CCE that are comparable to those from the 2013–2016 event if the anomalous feature: 1) has statistically normalized SSTa >1.29 s.d. (90th percentile) of the long-term

SSTa time series at a location; 2) is $\geq 3.5 \times 10^6$ km² in area; 3) lasts for >5 days; and 4) comes within 500 km of the coast (Hobday et al. 2016; Leising in revision). Events in the North Pacific have regularly met or surpassed these criteria every year since 2013 (Figure D.2.1). In the case of the second 2020 event, because it only encroached on coastal waters from September to November, it is too early to determine the impacts of the event on the CCE.



In mid-January 2020, a North Pacific marine heatwave that had begun in summer 2019 shrunk to an area less than 100,000 km² and receded to a region far offshore in the Gulf of Alaska, with SST in the region mostly falling below the threshold for classification as a heatwave. In February 2020, another marine heatwave began to grow in the same region where the 2019 event faltered. This first marine heatwave of 2020 eventually covered 4.6M km² on April 25th, 2020, before weakening by the end of June. This heatwave remained >1500 km from the coast, and likely had little impact on the CCE. As this heatwave was fading, a second and much larger marine heatwave formed in the same far offshore region in early June. This new heatwave reached its maximum size of ~9.1M km² on September 18, 2020, which made it the second largest marine heatwave on record, only 6.1% smaller in area than the 9.7M km² of the 2013-2016 “Blob” and slightly larger than the peak of the 2019 marine heatwave (Figure D.2.1, Figure D.2.2). During this peak period, the second 2020 heatwave covered over 50% of the CCE (Figure D.2.1), particularly in waters off central and northern California, Oregon, and Washington (Figure 3.1.2). The 2020 event diminished and moved offshore over the course of the fall, and remains far offshore of California as of mid January 2021 (Figure 3.1.2).

Although similar in their spatial and temporal patterns in terms of origination, eventual size, and intensity, there are



several key differences between the second heatwave of 2020 and the 2019 heatwave. Both events reached their maximum size during late September, however the 2019 event intersected the coast of OR and WA earlier in September (Thompson et al. 2019b), whereas the 2020 event remained offshore for most parts of the West Coast until later September, presumably due to the moderate to strong upwelling in summer of 2020 (Figure 3.2.1). Another important difference between the 2019 and 2020 events relates to their spatial pattern during October. The 2019 event shrank and moved from the coast into far offshore waters, whereas the 2020 event cooled in the far offshore region, while retaining a significant amount of warm water in the coastal region ~100 km from shore (Figure D.2.3). The 2020 event lingered in the coastal regions, mostly off WA and OR for approximately 1 month longer (until mid November) than the 2019 event. Lastly, the 2020 event had a significant amount of warming in the offshore regions of southern California and within the Southern California Bight during most of the year, which was similar to the pattern seen during 2014 but not present during the 2019 event (Figure D.2.3).

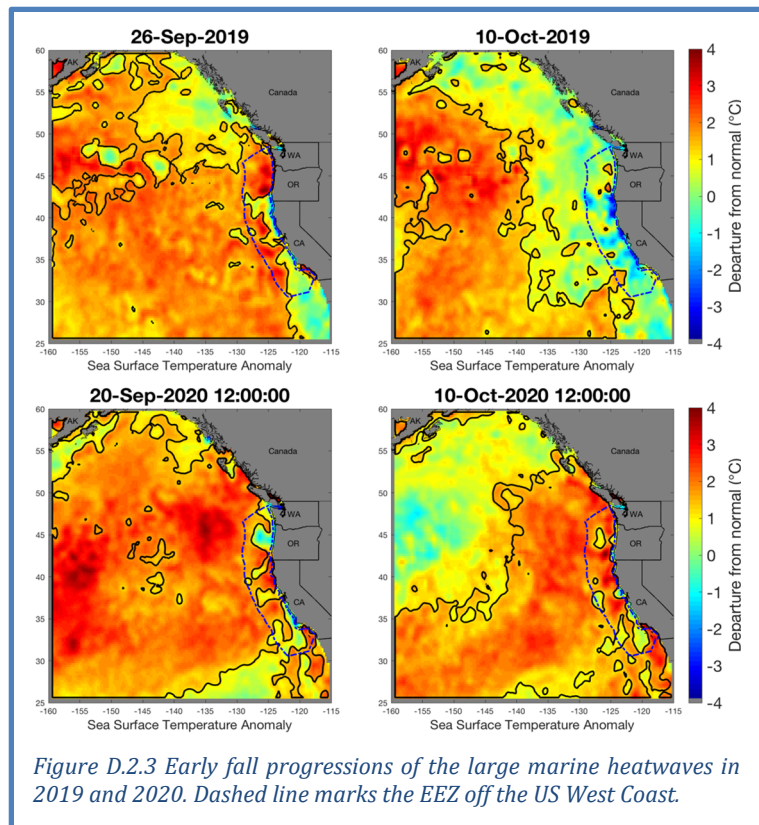


Figure D.2.3 Early fall progressions of the large marine heatwaves in 2019 and 2020. Dashed line marks the EEZ off the US West Coast.

D.3 HABITAT COMPRESSION INDEX

Upwelling creates a band of relatively cool water along the coast during the spring and summer, which is suitable habitat for a diverse and productive portion of the CCE food web. A concern that has emerged in the CCE during the anomalously warm years that began with the 2013–2016 marine heatwave is “habitat compression.” Santora et al. (2020) used this term to denote how offshore warming during the 2013–2016 marine heatwave restricted the relatively cool upwelling habitat to a narrower-than-normal band along the coast in the CCE configuration of the Regional Ocean Modeling System (ROMS) model with data assimilation (Neveu et al. 2016). This compression of the upwelling habitat consequently altered pelagic species composition and distribution, from forage species to top predators, and likely contributed to impacts such as increased rates of whale entanglements in fixed fishing gear.

Santora et al. (2020) developed a Habitat Compression Index (HCI) to track latitudinal changes in the area of cool upwelled surface waters. They defined HCI for a region of central California, and have since expanded it to four biogeographical provinces within the CCE: 43.5°–48°N, 40°–43.5°N, 35.5°–40°N, and 30°–35.5°N. HCI is defined as the area of monthly averaged ROMS model temperatures at a depth of 2 m that fall below a temperature threshold. Each region/month has a unique temperature threshold defined as the spatial average of all 2-m ROMS temperatures from the coast to 75 km offshore in the latitudinal region for a given month over a climatological period of 1980 to 2010. Winter and spring means for central California are shown in the main body of the report (Figure 3.2.2). Winter and spring means for all four regions are shown here, in Figure D.3.1.

The most evident patterns in the seasonal means are short-term positive trends in wintertime HCI in the three northerly regions, and spring 2020 means that are generally close to the long-term means in all regions (Figure D.3.1). The positive winter trends from 2016-2020 reflect the fact that the 2016 HCI was very low, reflecting high compression of cool winter habitat in that year in all but the southernmost

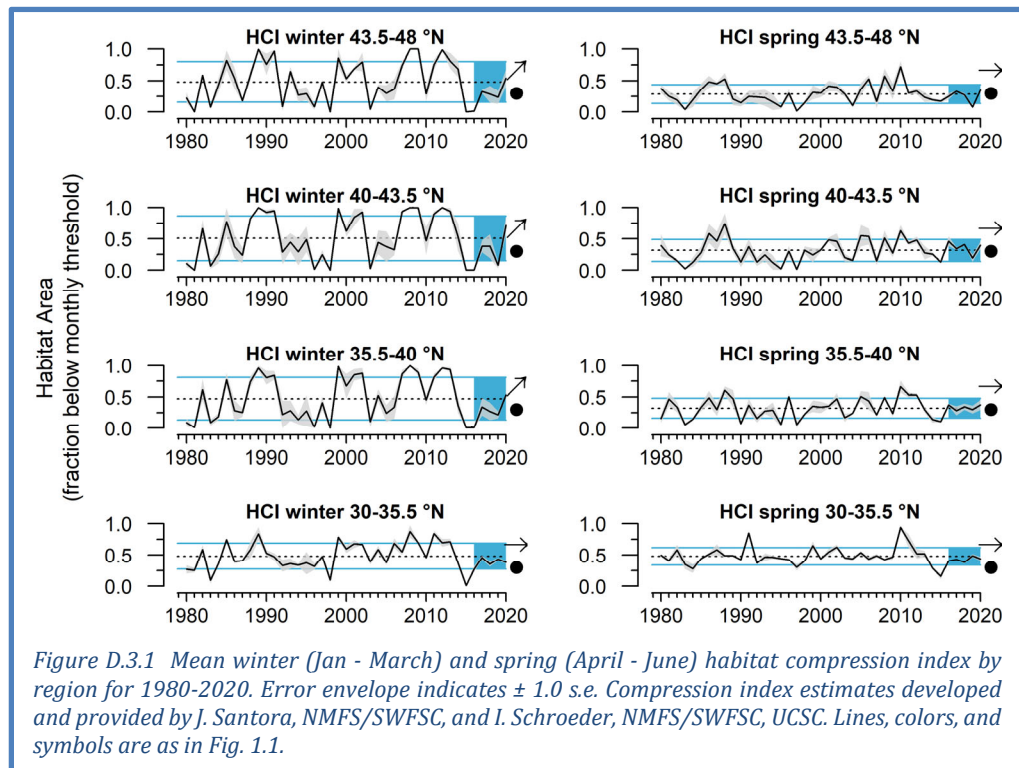


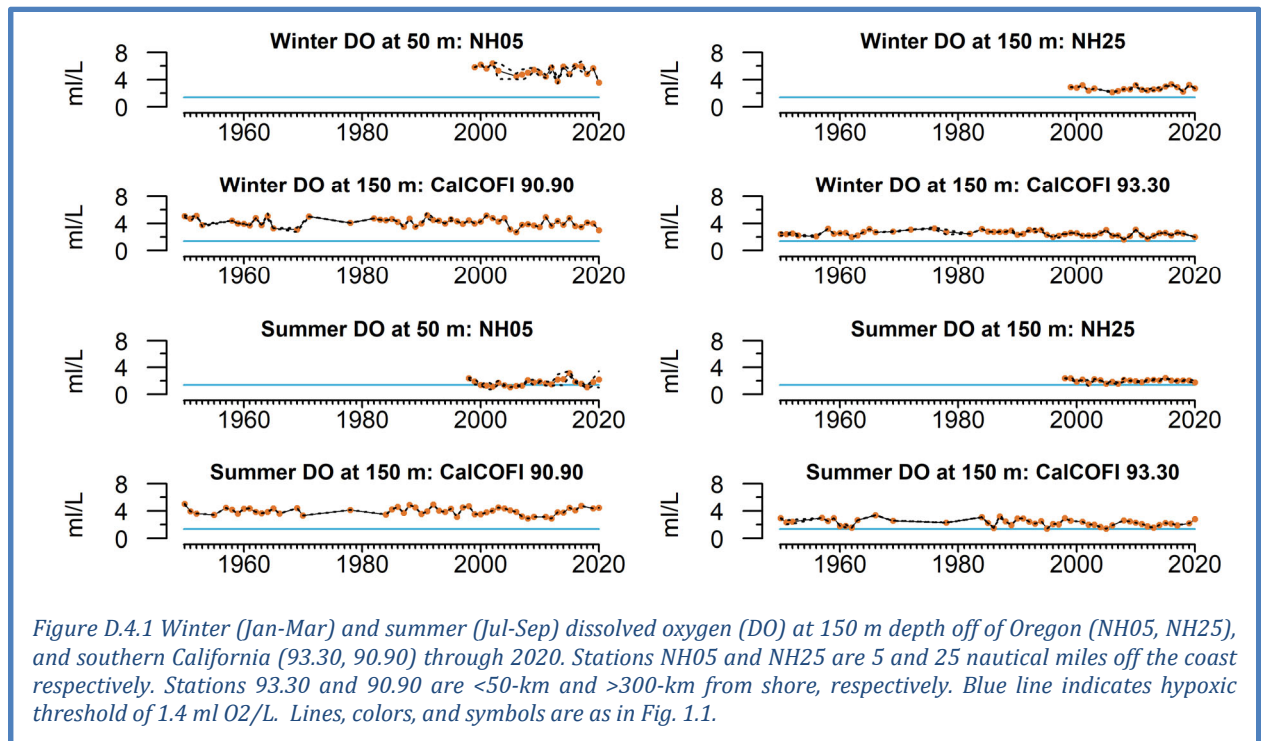
Figure D.3.1 Mean winter (Jan - March) and spring (April - June) habitat compression index by region for 1980-2020. Error envelope indicates ± 1.0 s.e. Compression index estimates developed and provided by J. Santora, NMFS/SWFSC, and I. Schroeder, NMFS/SWFSC, UCSC. Lines, colors, and symbols are as in Fig. 1.1.

region. The 2020 winter means are mostly close to average, so even with the moderate to strong winter upwelling described elsewhere in this report (e.g., Figure 3.2.1), HCIs remain considerably lower (more compressed) than peak values last seen before the 2013-2016 heatwave (Figure D.3.1). Similarly, the springtime means are close to average, which is an improvement over means in 2014-2016 (particularly south of 43.5°N), but remains well below model estimates from before the 2013-2016 heatwave.

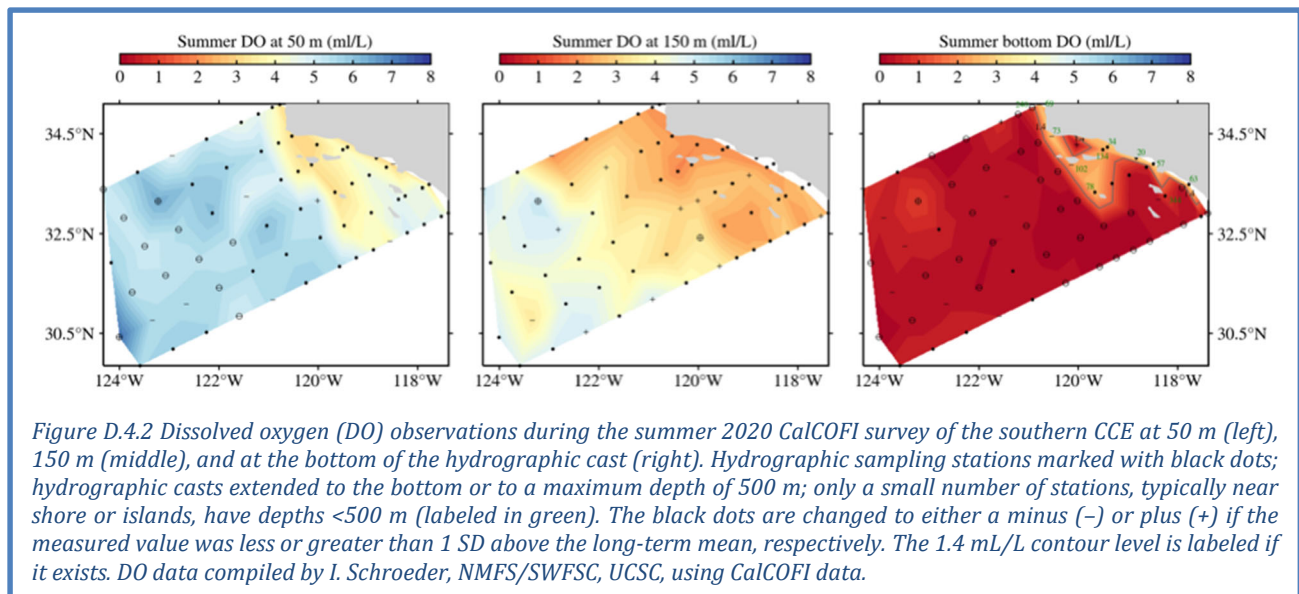
D.4 SEASONAL DISSOLVED OXYGEN AND OCEAN ACIDIFICATION INDICATORS

Nearshore dissolved oxygen (DO) depends on many processes, including currents, upwelling, air-sea exchange, and community-level production and respiration in the water column and benthos. DO is required for organismal respiration; low DO can compress habitat and cause stress or die-offs for sensitive species. Waters with DO levels < 1.4 mL/L (or 2 mg/L) are considered to be hypoxic; such conditions may occur on the shelf following the onset of spring upwelling, and continue into the summer and early fall months until the fall transition vertically mixes shelf waters. Upwelling-driven hypoxia occurs because upwelled water from deeper ocean sources tends to be low in DO, and microbial decomposition of organic matter in the summer and fall increases overall system respiration and oxygen consumption, particularly closer to the seafloor (Chan et al. 2008).

The first series of plots in this section (Figure D.4.1) shows summer and winter averages for dissolved oxygen (DO) data off Newport, OR (stations NH05 and NH25, 5 and 25 nautical miles off the coast respectively) and in the Southern California Bight (stations CalCOFI 90.90 and CalCOFI 93.30). In 2020, winter DO concentrations were consistently above the hypoxia threshold (1.4 ml O₂ per L water) at each of the stations at the depths measured (near bottom at NH05; 150 m at the other stations). These results were typical of the entirety of the winter time series. Winter DO levels in 2020 were lower than in 2019. Summer DO concentrations in 2020 were also above the hypoxia threshold at each station, though the seasonal mean at NH25 was close to the threshold and was at the threshold in July.



Summer DO concentrations over the CalCOFI region have large inshore/offshore and depth gradients, with lower values measured at depth and along the coast and higher values at the surface and farther offshore. The Summer 2020 CalCOFI survey measured DO concentrations above the hypoxic threshold for all stations at depths of 50 m and 150 m (Figure D.4.2, left and center). At 50-m depths, summer DO at stations farthest offshore was well above the hypoxia threshold, although many stations had the lowest observed summer concentrations since the time series began in 1984 (Figure D.4.2,).



Ocean acidification (OA), caused by anthropogenically increased levels of atmospheric CO₂, reduces pH and carbonate ion levels in seawater. A key indicator of OA is aragonite saturation state, a measure of the availability of aragonite (a form of calcium carbonate). Aragonite saturation <1.0 indicates corrosive conditions that have been shown to be stressful for many CCE species, including oysters, crabs, and

pteropods. Upwelling transports hypoxic, acidified waters from offshore onto the continental shelf, where increased community-level metabolic activity can further exacerbate OA (Feely et al. 2008). Aragonite levels thus tend to be lowest during spring and summer upwelling, and highest in winter.

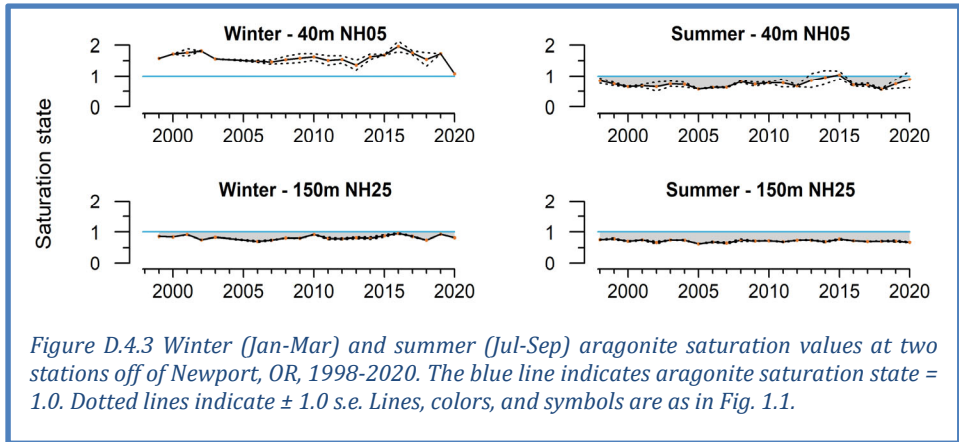


Figure D.4.3 Winter (Jan-Mar) and summer (Jul-Sep) aragonite saturation values at two stations off of Newport, OR, 1998-2020. The blue line indicates aragonite saturation state = 1.0. Dotted lines indicate ± 1.0 s.e. Lines, colors, and symbols are as in Fig. 1.1.

Figure D.4.3 shows time series of winter and summer aragonite saturation from near bottom at stations NH05 and NH25. Winter saturation state was consistently above the threshold of 1.0 at station NH05, but was close to the threshold in 2020 and has been decreasing steadily since 2016. The winter 2020 measure at NH05 was one of the lowest values of the time series. Winter conditions were consistently corrosive in the deeper water of station NH25 for most of the time series, including 2020. Summer aragonite saturation indicated corrosive waters at depth for both stations for most of the time series, including 2020.

More of the water column was undersaturated in 2020 (i.e., aragonite saturation state <1.0) during peak periods of corrosivity than in 2019 (Figure D.4.4). The corrosive water on the shelf at NH05 is largely driven by seasonal upwelling, where upwards of 80% of the water column becomes corrosive each summer, and in 2020 the corrosive water came within ~ 5 m of the surface, which was the shallowest level of this isocline of the entire time series. The brief winter spike in corrosivity in early 2020 can also be seen. While the offshore station over the slope at NH25 is slightly influenced by seasonal upwelling and downwelling, a much larger portion of the water column remains undersaturated throughout the year (Figure D.4.4). As with station NH05, the aragonite saturation horizon reached a shallower depth in 2020 than in 2019, although it was not unusual relative to long-term observations at NH25.

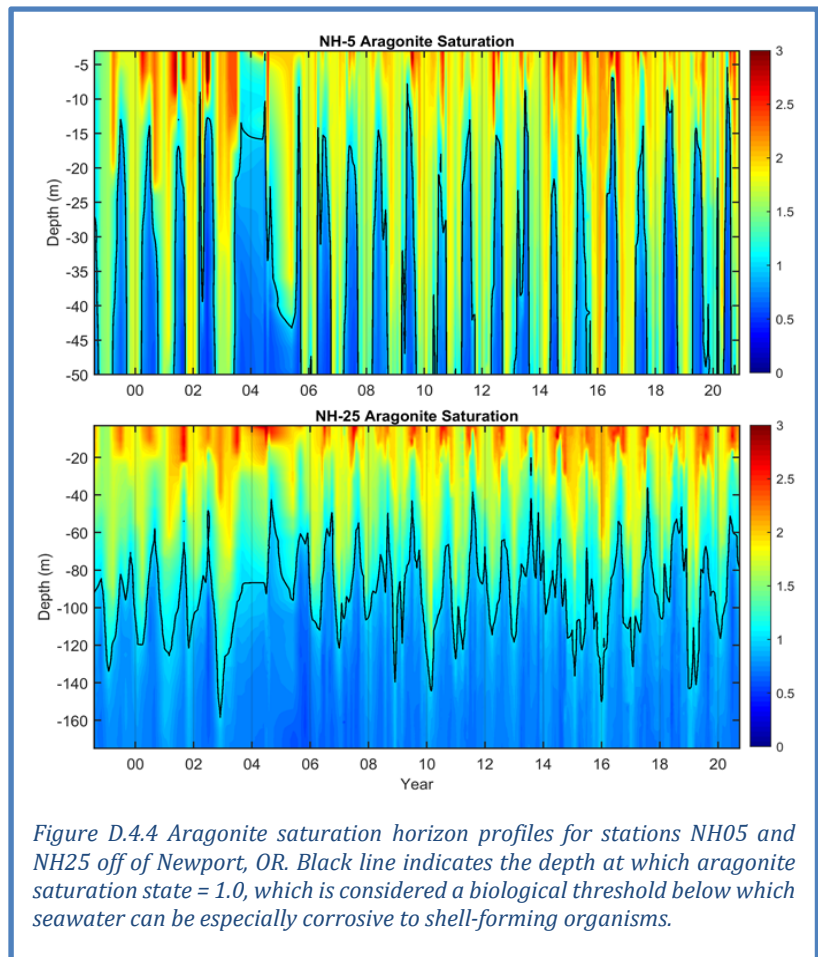


Figure D.4.4 Aragonite saturation horizon profiles for stations NH05 and NH25 off of Newport, OR. Black line indicates the depth at which aragonite saturation state = 1.0, which is considered a biological threshold below which seawater can be especially corrosive to shell-forming organisms.

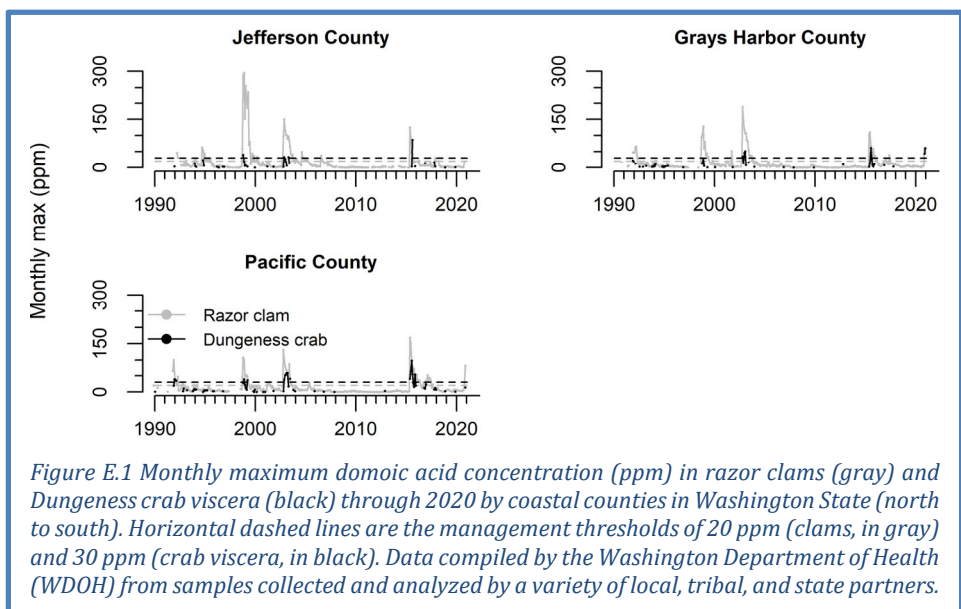
Appendix E HARMFUL ALGAL BLOOMS IN 2020

E.1 DOMOIC ACID

Harmful algal blooms (HABs) of diatoms in the genus *Pseudo-nitzschia* have been of particular concern along the West Coast in recent years. Certain species of *Pseudo-nitzschia* produce the toxin domoic acid that can accumulate in filter feeders and extend through food webs to cause harmful or lethal effects on people, marine mammals, and seabirds (Lefebvre et al. 2002, McCabe et al. 2016). Consumption of seafood with unsafe levels of domoic acid can cause amnesic shellfish poisoning in people. To protect human health, fisheries that target shellfish (including razor clam, Dungeness crab, rock crab, and spiny lobster) are delayed, closed, or operate under a health advisory in the recreational sector when domoic acid concentrations exceed safety thresholds for human consumption. Fishery closures can cause tens of millions of dollars in lost revenue and a range of sociocultural impacts in fishing communities (Dyson and Huppert 2010, NMFS 2016, Ritzman et al. 2018), and can also cause “spillover” of fishing effort into other fisheries.

Extremely toxic HABs of *Pseudo-nitzschia* are influenced by ocean conditions. In the northern CCE, they have been found to coincide with or closely follow El Niño events or positive PDO regimes and track regional anomalies in southern copepod species (McCabe et al. 2016, McKibben et al. 2017). The largest and most toxic HAB of *Pseudo-nitzschia* ever recorded on the West Coast coincided with the 2014-2016 Northeast Pacific marine heatwave and caused extensive closures and delays in the opening of crab fisheries, resulting in the appropriation of over \$25M in federal disaster relief funds (McCabe et al. 2016).

Domoic acid had impacts on Washington shellfish fisheries in 2020, for the first time in several years (Figure E.1). Domoic acid was present at low levels in razor clams for most of 2020, but increased rapidly on beaches of the Long Beach Peninsula (Pacific County) in the fall, leading to the closure of recreational razor clamming in Washington on October 21. Tribal razor clam harvests were halted on October 31 as domoic acid levels increased on beaches further north (Point Chehalis to the Quinault Reservation, Grays Harbor County). Recreational Dungeness crab closures began November 11 in Grays Harbor, and all recreational crabbing was closed south of Destruction Island (except for the Columbia River) by December 28. State and Tribal commercial Dungeness crab fisheries were delayed due to domoic acid in December. The Point Chehalis to Destruction Island Tribal fishery opened December 23, but on December 28, all un-eviscerated product from this fishery was embargoed due to domoic acid, and whole Dungeness crab were recalled. Delay of the 2020-21 commercial Dungeness crab season and closure of state and Tribal razor clam fisheries continue into 2021.



In Oregon, domoic acid in razor exceeded advisory levels at several sites over the course of 2020 (Figure E.2). A statewide closure of the razor clam fishery due to domoic acid that began in late 2019 was lifted first for the north coast on January 22, 2020, followed by the central coast on February 27, 2020, and finally the southern coast on August 7, 2020. It was then reinstated for the remainder of the year beginning first in the central coast on October 22, 2020, the north coast on October 29, 2020, and the southern coast on November 20, 2020. A delay in the opening of the 2020-21 Oregon commercial Dungeness crab fishery due to low meat quality extended until December 16th from Cape Falcon to the Oregon/California border. The area north of Cape Falcon to the Oregon/Washington border was delayed for the entire month of December due to both low meat quality and concerns of high domoic acid levels in southern Washington crab.

In northern California, domoic acid levels were above the threshold in razor clams in 2020 (Figure E.3); the razor clam fishery remained closed throughout 2020, extending a closure that began in 2016. The start of the 2020-21 commercial Dungeness crab fishery in the Central and Northern Management Areas was delayed until December 23, 2020 to avoid marine life

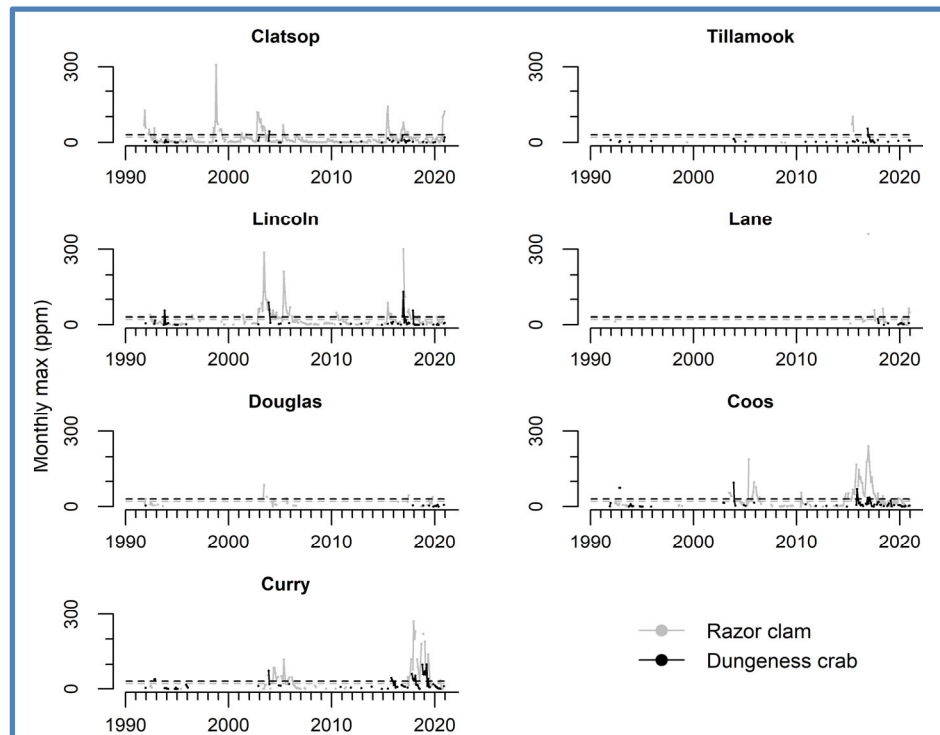


Figure E.2 Monthly maximum domoic acid concentration (ppm) in razor clams (gray) and Dungeness crab viscera (black) through 2020 by coastal counties in Oregon (north to south). Horizontal dashed lines are the management thresholds of 20 ppm (clams, in gray) and 30 ppm (crab viscera, in black). Razor clam tissue sampling is conducted twice monthly at multiple sites across the Oregon coast.

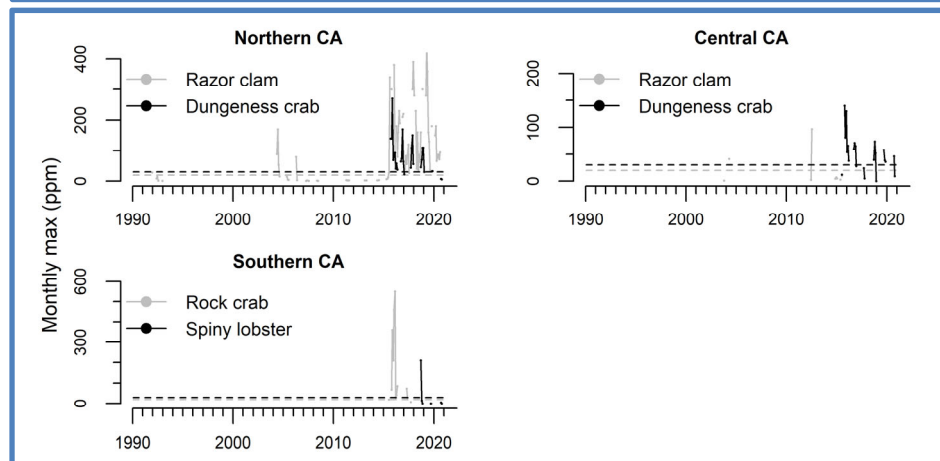


Figure E.3 Monthly maximum domoic acid concentration (ppm) in razor clams (gray) and Dungeness crab viscera (black) through 2020 in northern California (NCA; Del Norte south to Mendocino counties) and central California (CCA; Sonoma south to San Luis Obispo counties). Few to no razor clams or Dungeness crab occur in southern CA (SCA), where rock crab (gray) and spiny lobster (black) are typically monitored for domoic acid. Horizontal dashed lines are the management thresholds of 20 ppm (clams, in gray) and 30 ppm (crab viscera, in black). Data compiled by the California Department of Public Health (CDPH) from samples collected by a variety of local, tribal, and state partners.

extending a closure that began in 2016. The start of the 2020-21 commercial Dungeness crab fishery in the Central and Northern Management Areas was delayed until December 23, 2020 to avoid marine life

entanglements; however, exceedances of domoic acid were also observed in Dungeness crab from one region of California that eventually cleared prior to this delayed start date. Domoic acid can also affect California fisheries that target rock crab and spiny lobster. In Southern California, there were no domoic acid-related closures of spiny lobster or rock crab in 2020 (Figure E.3). However, the northern rock crab fishery has been closed since 2015 in two areas due to domoic acid concerns (data not shown; see <https://wildlife.ca.gov/Fishing/Ocean/Health-Advisories>).

E.2 “RED TIDE” OFF SOUTHERN CALIFORNIA IN 2020

In spring 2020, an incredibly dense and prolonged bloom of the dinoflagellate *Lingulodinium polyedra* extended from Los Angeles to Baja, coloring the water a deep red/brown and produced spectacular night-time bioluminescence. Cell numbers at the Scripps Pier were the highest recorded at 9 million cells/L (the previous maximum was just under 1.5 million cells/L) and chlorophyll was also the highest recorded (1,083 µg/L) since monitoring began in 1983. Conditions thought to have led to the development of the bloom include unusually high precipitation (200-400% above normal) in March-April and low wind that contributed to stratification, and seasonal warming of waters against a backdrop of anomalously warm water temperatures in the region since 2015 promoting growth and further contributing to stratification, which *L. polyedra* is known to prefer.

Occasional blooms of *L. polyedra* lasting one week to one month are not unusual in California and generally do not cause harm. In early May, after a month of sustained cell concentrations above 1 million cells/L, a widespread stranding of fishes (e.g., bass, sardines, rockfish, and rays) and invertebrates (e.g., snails, sea hares, sea dollars, mussels, sea pansy, octopuses, and lobster) occurred on beaches throughout Orange County and San Diego. In addition, anecdotal reports from surfers and beach-goers claimed respiratory irritation from sea spray emerging near “red tide” water. Hypoxia and anoxia were reported at Scripps Pier for several days in early May (J. Smith, preliminary data) and likely contributed to the die-offs. Bacterial degradation of the large amount of organic matter at the end-stage of the bloom depleted oxygen to levels expected to cause lethal effects in marine organisms due to hypoxia and produced hydrogen sulfide. This effect was amplified in semi-enclosed bays and lagoons with little exchange with the ocean and reduced mixing with the atmosphere. However, local research aquaria at SIO/UCSD and SWFSC, which use seawater from Scripps Pier, also experienced a nearly complete loss of all vertebrate and invertebrate specimens, including in tanks with additional aeration systems, suggesting that die offs may have been due to more than hypoxia.

A toxin associated with *L. polyedra*, yessotoxin (YTX), is known to occasionally cause harm in other parts of the world and may also have played a role in the die-offs. Preliminary analysis of particulate, dissolved, and aerosol samples collected during the 2020 bloom detected YTX in particulate and dissolved samples, with the highest concentrations (1.10-1.36 ng/mL) measured near the end of the bloom, after the highest cell abundances of *L. polyedra* (E. Ternon and M. Carter, preliminary data). YTX was also detected in the aerosols at various time points throughout the bloom. Concentrations were low but detectable (≤ 0.40 pg/m³) and particularly high on April 30 (6.34 pg/m³; E. Ternon, preliminary data). This is the first-ever report of YTX in aerosols during a *L. polyedra* bloom, and suggests that up to 6.34 pg of YTX could have been inhaled by an adult within 2 hours (breathing 0.5 m³ per hour). Given the low toxicity of YTX reported so far on human cell lines, it is still not clear whether YTX is responsible, or other compounds are involved, for the reported respiratory symptoms of 25% of 872 respondents to a survey by Surfrider, SCCOOS, and Surfline. While the timing of high in-water YTX coincides with the earliest reports of dead animals on beaches, YTX levels measured thus far are not significant enough to be the culprit for the massive die-offs. A preliminary analysis of aerosol samples showed that sulfur compounds (most likely sulfolipids) are being transferred from the cells to the aerosols. Ongoing isolation and characterization of these compounds should provide more insight on the cytotoxicity. In addition, sulfur gas precursors and the role of bacteria in the degradation and toxicity of the bloom are under investigation.

Appendix F SNOW-WATER EQUIVALENT, STREAMFLOW, AND STREAM TEMPERATURE

Development of habitat indicators in the CCIEA has focused on freshwater habitats. All habitat indicators are reported based on a hierarchical spatial framework. This spatial framework facilitates comparisons of data at the right spatial scale for particular users, whether this be the entire California Current, ecoregions within these units, or smaller spatial units. The framework we use divides the region encompassed by the California Current ecosystem into ecoregions (Figure 2.1b), and ecoregions into smaller physiographic units. Freshwater ecoregions are based on the biogeographic delineations in Abell et al. (2008; see also www.feow.org), who define six ecoregions for watersheds entering the California Current, three of which comprise the two largest watersheds directly entering the California Current (the Columbia and the Sacramento-San Joaquin Rivers). Within ecoregions, we summarized data using evolutionary significant units and 8-field hydrologic unit classifications (HUC-8). Status and trends for all freshwater indicators are estimated using models that account for spatial and temporal autocorrelation (Lindgren and Rue 2015).

Snow-water equivalent (SWE) is measured using two data sources: a California Department of Water Resources snow survey program (data from the California Data Exchange Center <http://cdec.water.ca.gov/>) and The Natural Resources Conservation Service's SNOTEL sites across Washington, Oregon, California and Idaho, <http://www.wcc.nrcs.usda.gov/snow/>). Snow data (Figure F.1) are converted into SWEs based on the weight of samples collected at regular intervals using a standardized protocol. Measurements at April 1 are considered the best indicator of maximum extent of SWE; thereafter snow tends to melt rather than accumulate. Data for each freshwater ecoregion are presented in Section 3.5 of the main report.

The COVID-19 pandemic appears not to have had much effect on SWE data quality: there were ~10% fewer snow measurements collected in 2020, but considering that snow measurements are autocorrelated (i.e., sites in the same ecoregion and year tend to have similar snowpack), losing 10% of the data is unlikely to strongly affect the patterns shown in Figure 3.5.1.

The outlook for snowpack in 2021 is limited to examination of current SWE, an imperfect correlate of SWE in April due to variable atmospheric temperature and precipitation patterns. SWE on January 31, 2021 was above the long-term median in northern Washington, the northernmost Idaho panhandle, and parts of eastern Oregon and southwestern Idaho,

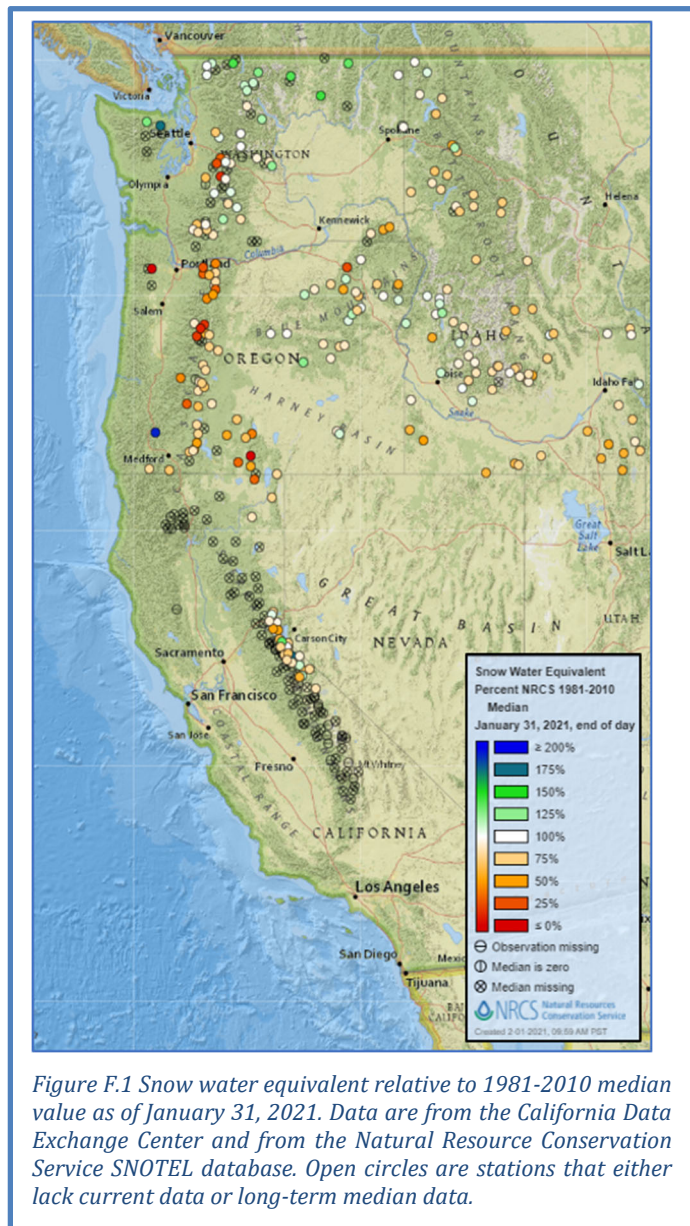


Figure F.1 Snow water equivalent relative to 1981-2010 median value as of January 31, 2021. Data are from the California Data Exchange Center and from the Natural Resource Conservation Service SNOTEL database. Open circles are stations that either lack current data or long-term median data.

but the rest of the system was below the median (Figure F.1). The April 1, 2021 SWE measurements will be presented in next year’s report.

The NOAA seasonal drought outlook as of January 21, 2021 is for persistent drought in nearly all of California and parts of southernmost Oregon and Idaho between now and April. Drought is expected to continue but improve during that time in most of Oregon and parts of central Washington and central Idaho.

Mean maximum temperatures in August were determined from 446 USGS gages with temperature monitoring capability. While these gages did not necessarily operate simultaneously throughout the period of record, at least two gages provided data each year in all ecoregions. Stream temperature records are limited in California, so two ecoregions (Sacramento-San Joaquin and Southern California Bight-Baja) were combined. Maximum temperatures exhibit strong ecoregional differences (for example, the Salish Sea and Washington Coast streams are much cooler on average than California streams). The most recent 5 years have been marked by largely average values region-wide (Figure F.2). One exception is the Salish Sea and Washington Coast, which experienced above-average temperatures for much of period of 2014-2019 before returning close to average in 2020. Another exception is that August temperatures from Oregon southward increased in 2020 compared to 2019, and were comparable to the marine heatwave years of 2014-2015.

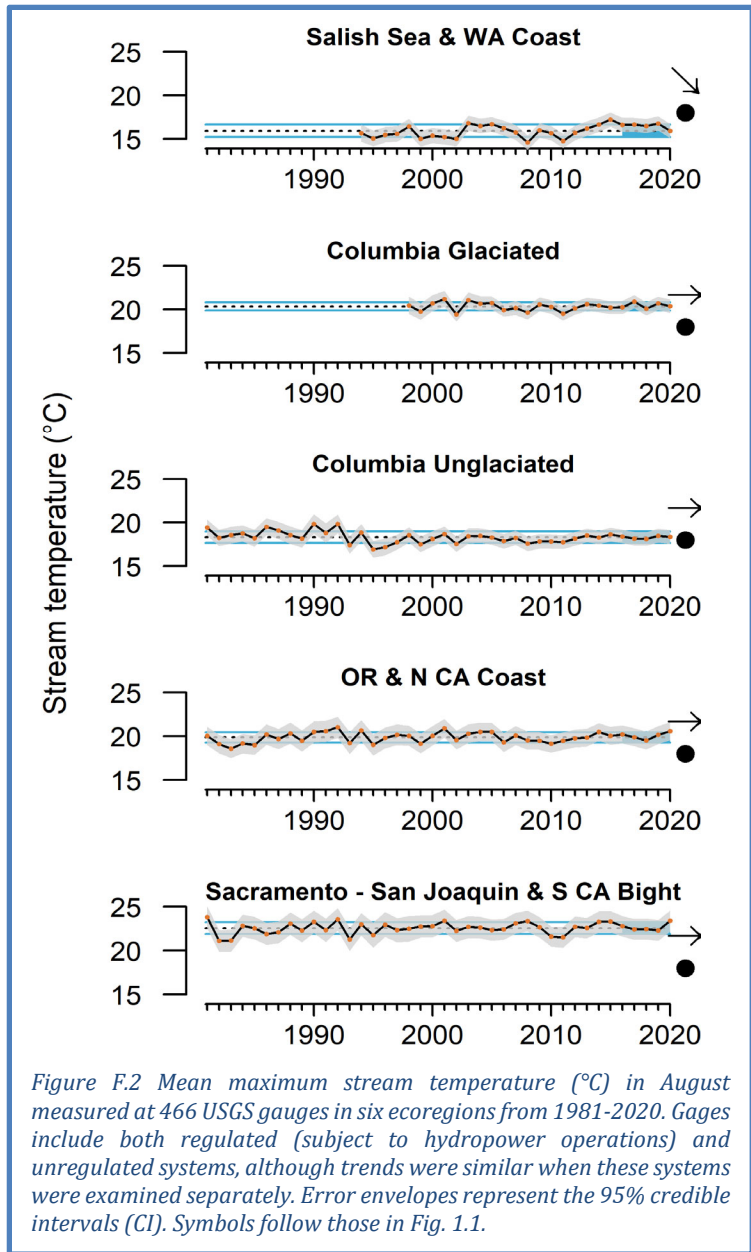
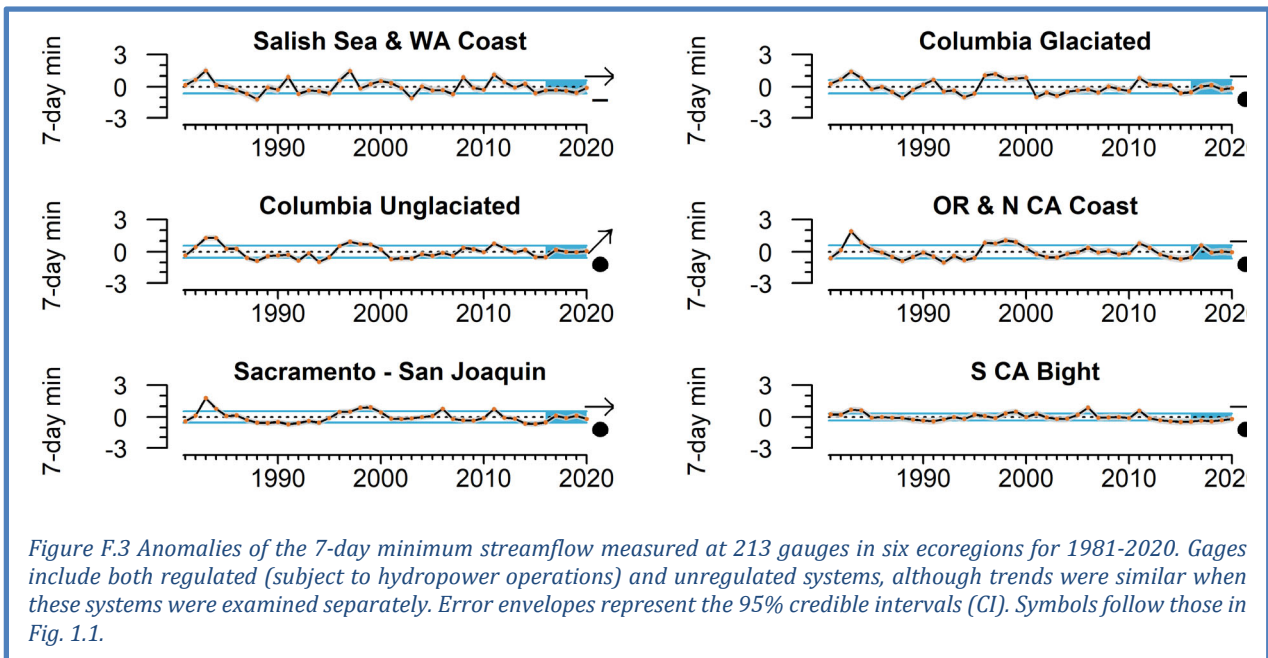


Figure F.2 Mean maximum stream temperature (°C) in August measured at 466 USGS gages in six ecoregions from 1981-2020. Gages include both regulated (subject to hydropower operations) and unregulated systems, although trends were similar when these systems were examined separately. Error envelopes represent the 95% credible intervals (CI). Symbols follow those in Fig. 1.1.

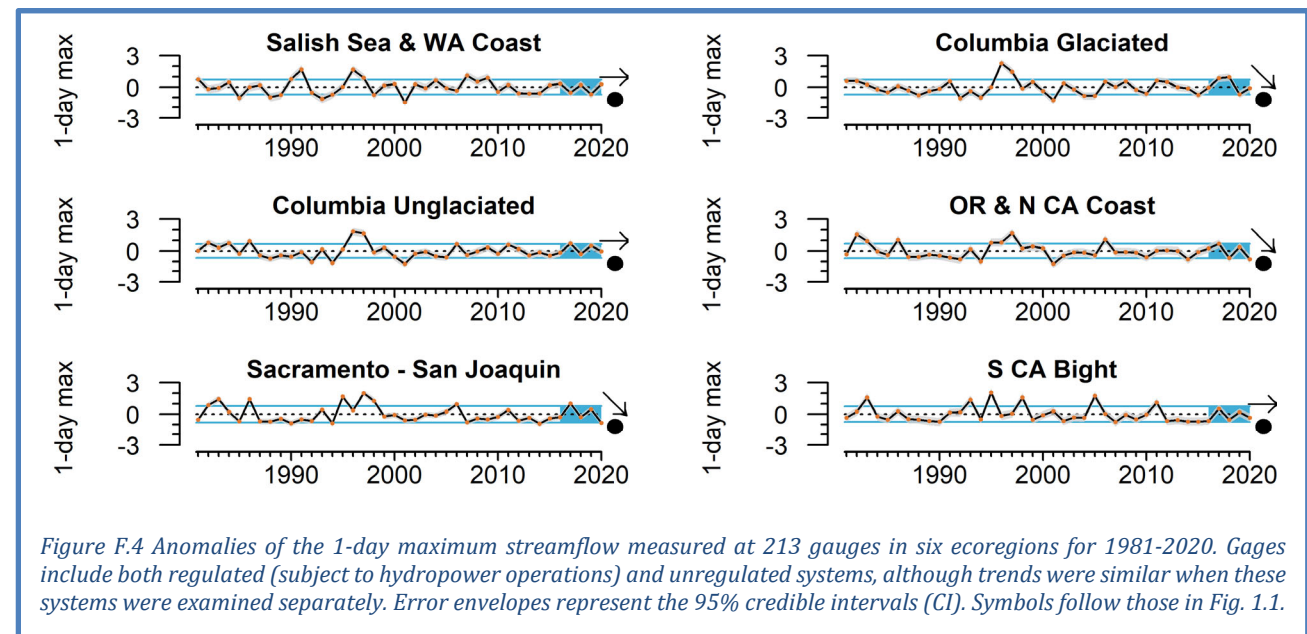
Streamflow is measured using automated USGS gages with records that meet or exceed 30 years in duration. Average daily values from 213 gages were used to calculate both annual 1-day maximum and 7-day minimum flows. These indicators correspond to flow parameters to which salmon populations are most sensitive. We use standardized anomalies of streamflow time series from individual gages.

Across ecoregions of the California Current, both minimum and maximum streamflow anomalies have exhibited some variability in the most recent five years, although generally not outside of historical ranges. Minimum stream flows have exhibited fairly consistent patterns across all ecoregions, and were close to long-term means in 2020 (Figure F.3). The Sacramento-San Joaquin exhibited a slight decline compared to 2019, while the Salish Sea and Washington Coast ecoregion returned close to average in 2020 after several years of below-average minimum flows. Within ecoregions, there is basin-scale

variability in minimum flow patterns; see Figure F.5 for flows by Chinook salmon ESU.



Maximum flows in 2020 declined in several of the California Current’s ecoregions relative to 2019 (Figure F.4). In the Sacramento-San Joaquin, maximum flows were lower even than the marine heatwave year of 2015, and the Oregon / Northern California Coast ecoregion also experienced maximum flows that were well below average; these values are consistent with 2020 SWE patterns shown in Figure 3.5.1. Variability across basins exists within each ecoregion; see Figure F.6 for flows by Chinook salmon ESU.



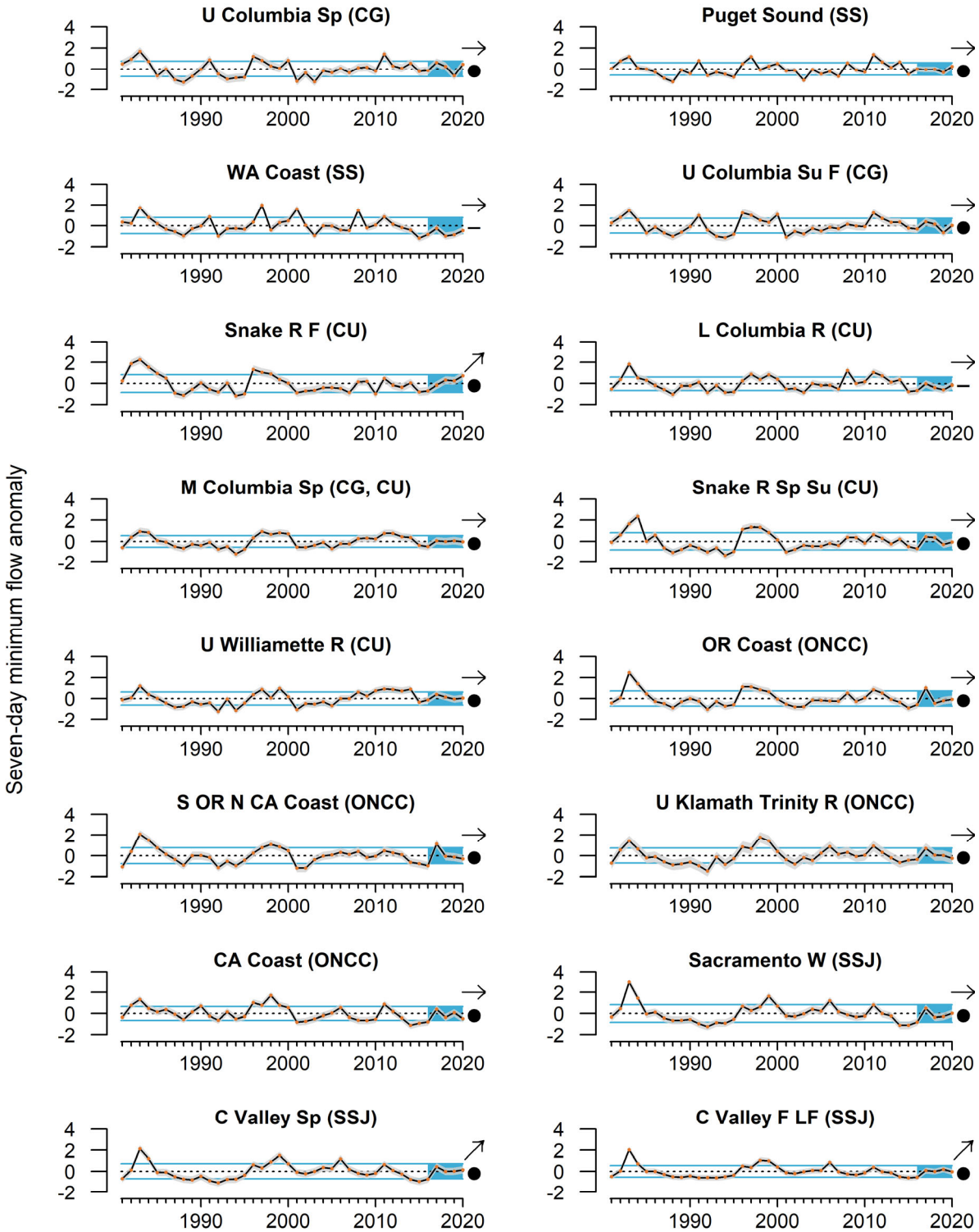


Figure F.5 Anomalies of the 7-day minimum streamflow measured at 213 gauges in 16 Chinook salmon ESUs for 1981-2020. Gages include both regulated (subject to hydropower operations) and unregulated systems, although trends were similar when these systems were examined separately. Error envelopes represent the 95% credible intervals (CI). Symbols follow those in Fig. 1.1.

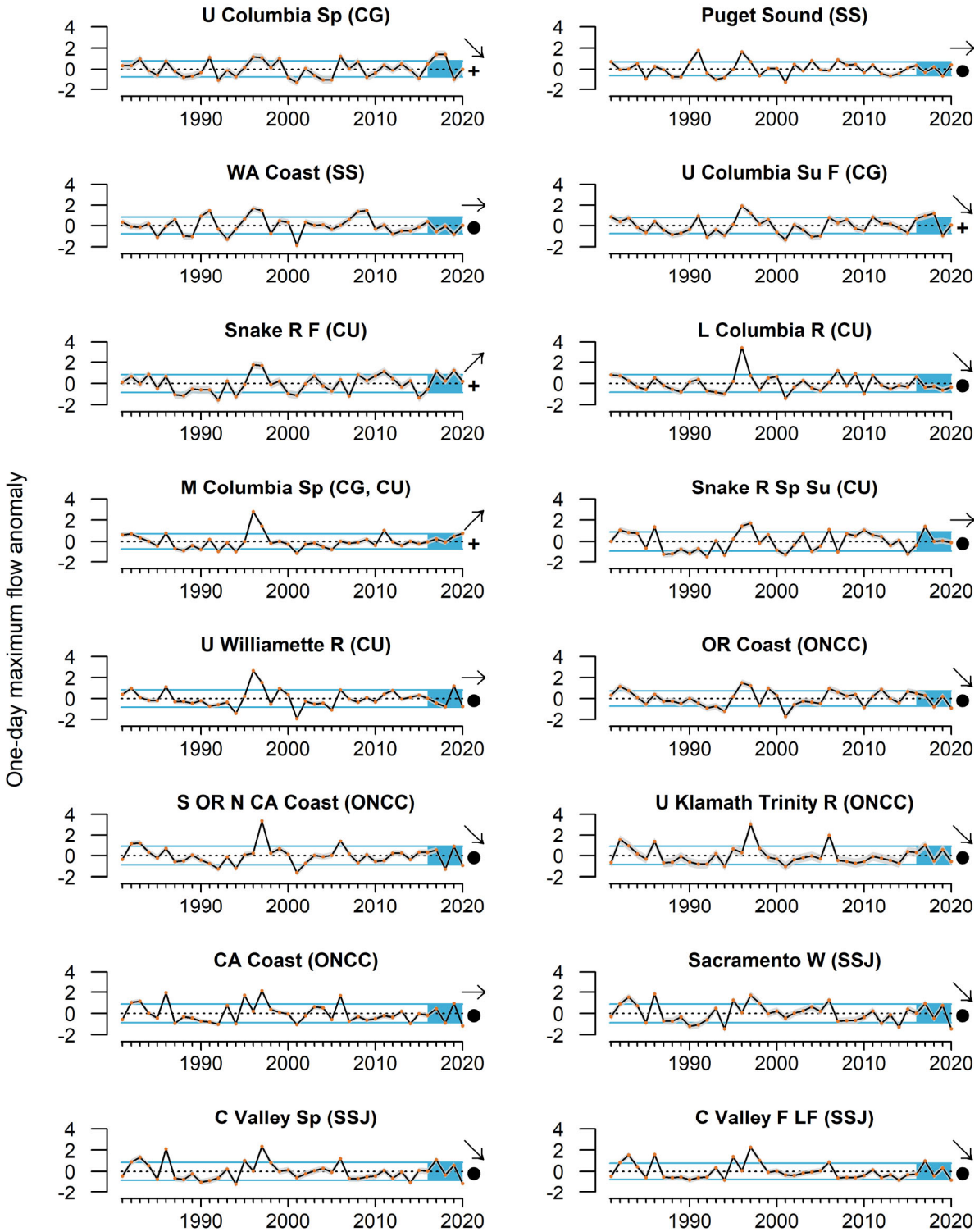


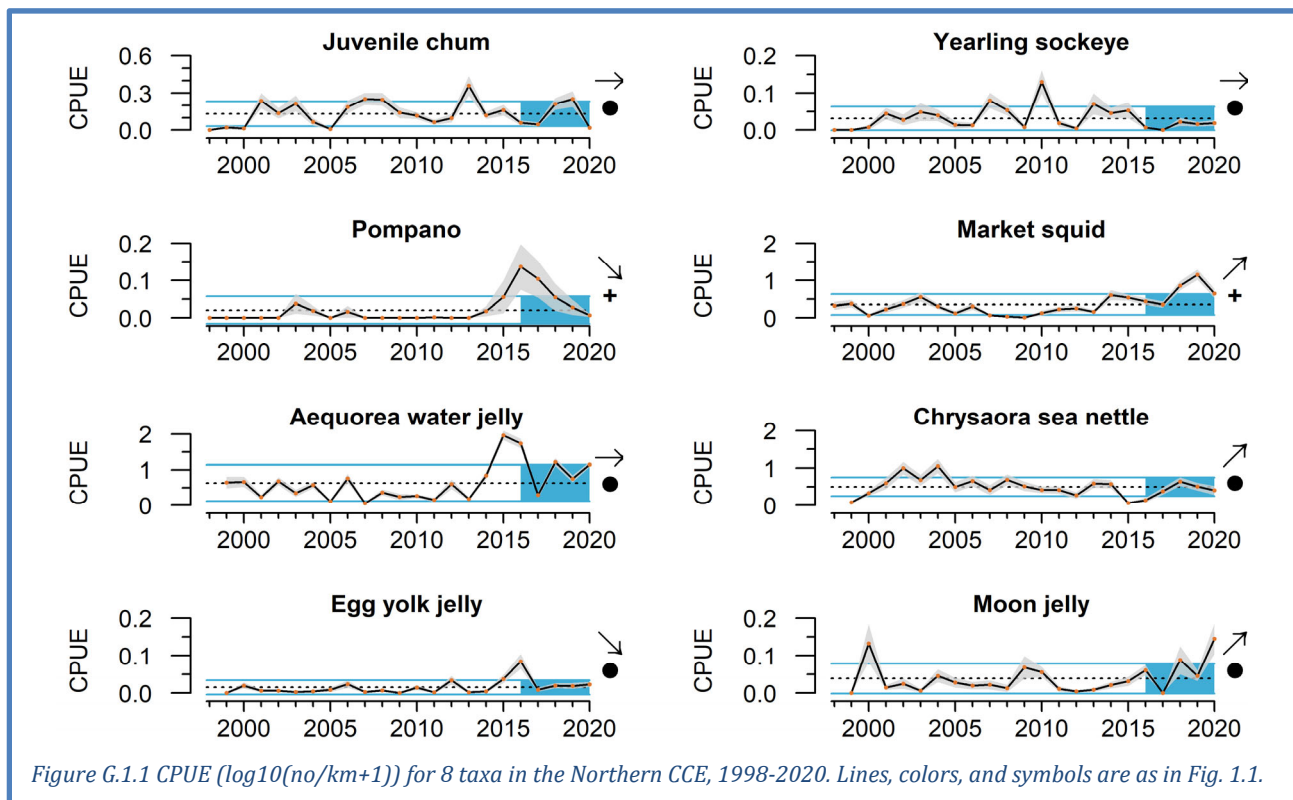
Figure F.6 Anomalies of the 1-day maximum streamflow measured at 213 gauges in 16 Chinook salmon ESUs for 1981-2020. Gages include both regulated (subject to hydropower operations) and unregulated systems, although trends were similar when these systems were examined separately. Error envelopes represent the 95% credible intervals (CI). Symbols follow those in Fig. 1.1.

Appendix G REGIONAL FORAGE AVAILABILITY

G.1 NORTHERN CALIFORNIA CURRENT FORAGE

The Northern CCE survey (known as the “Juvenile Salmon Ocean Ecology Survey”) occurs in June and targets juvenile salmon in surface waters off Oregon and Washington, but also collects adult and juvenile (age 1+) pelagic forage fishes, market squid, and gelatinous zooplankton with regularity. The gear is fished during daylight hours in near-surface waters, which is appropriate for targeting juvenile salmon.

In 2020, catches of juvenile chum salmon catches dropped to >1 s.d. below the long term mean, while juvenile sockeye catches were average; both had non-significant 5-year trends (Figure G.1.1). Catches of market squid in 2020 remained above average, and high catches from 2018 to 2020 have contributed to an increasing trend. Water jelly *Aequorea* were 1 s.d. above the mean in 2020, although they are down from peaks in 2015-2016 associated with the 2013-2016 marine heatwave (the Blob). Catches of *Chrysaora* jellyfish (sea nettles) have increased back to near-average values since the lows in 2015-2016, associated with the marine heatwave. Moon jellies have also shown an increasing trend and were well above long-term averages in 2020. In contrast, catches of pompano (butterfish) and egg yolk jelly, which peaked during the marine heatwave in 2015 and 2016, declined in 2020 to within long-term averages. As noted in Section 4.2, catches of age-0 sablefish were anomalously large in this survey. As noted in Section 4.3, catches of juvenile subyearling Chinook salmon in 2020 were ~1 s.d. above average, juvenile yearling Chinook salmon were ~1 s.d. below average, and juvenile coho salmon were close to average.



G.2 CENTRAL CALIFORNIA CURRENT FORAGE

The Central CCE forage survey (known as the “Rockfish Recruitment and Ecosystem Assessment Survey” or RREAS) samples this region using midwater trawls, which collect young-of-the-year (YOY) rockfish species and a variety of other YOY and adult forage species, market squid, adult krill, and gelatinous zooplankton. Time series presented here are from the “Core Area” of that survey (see Figure 2.1a).

Effort for the RREAS was considerably reduced as a result of the COVID-19 pandemic (15 hauls in 2020 for the core area, relative to a long-term average of >60 per year from 1990 to 2019). Because the survey was conducted on a chartered fishing vessel rather than a survey vessel, the timing and spatial distribution of effort was also anomalous, with more trawls conducted in shelf habitat relative to offshore habitat, and all hauls conducted later than usual (mid- to late June rather than a broader May-mid-June time period). As initial evaluations using average log-transformed catch rates indicated substantial bias for many taxa (particularly those with strong inshore or offshore habitat associations), abundance indices were instead developed using a delta-generalized linear model to explicitly account for spatial and temporal sampling covariates, consistent with the approach typically used to develop pre-recruit indices of rockfish and other groundfish for stock assessments (e.g., Ralston et al., 2013). The best candidate models (including error distributions) were determined based on Akaike’s Information Criteria, and uncertainty was estimated by running the model in a Bayesian framework with vague priors and computing 95% credible intervals using the package ‘rstanarm’ in R. The resulting indices were log (x+1) transformed, and standardized anomalies (z-scores, with transformed uncertainty estimates) are presented in this report, consistent with how these indicators have been reported in prior years. Comparisons with past indices indicated that the previous methods of reporting (average of log-transformed indices) yielded highly comparable and unbiased results relative to the model-based approach for the historical time series, but that approach would have led to substantial bias if applied to the sparse 2020 data. Although uncertainty was considerably greater for most taxa (particularly less-abundant taxa) due to the small number of trawls conducted in 2020, comparisons of catch rates with seabird diets indicated comparable relative abundance levels for several key forage species (YOY rockfish and northern anchovy), as has been reported previously in the literature for this region.

As shown in Figure 4.2.2, catches of adult anchovy were above average in this region in 2020, for the third straight year, and have increased over the past 5 years, while juvenile rockfish catches continued a recent decline and were 1 s.d. below average. Among other species, all groups shown in Figure G.2.1 had average to below-average catches in 2020, although many estimates had greater uncertainty than in previous years, especially myctophids, YOY hake, and octopus. YOY Pacific hake, YOY sanddabs, YOY rockfish, octopus, and krill all had decreasing trends over the past 5 years. Pyrosomes were also highly prevalent, occurring in abundance in almost every tow, but trends have not yet been quantified due to likely sampling biases associated with survey conditions in 2020.

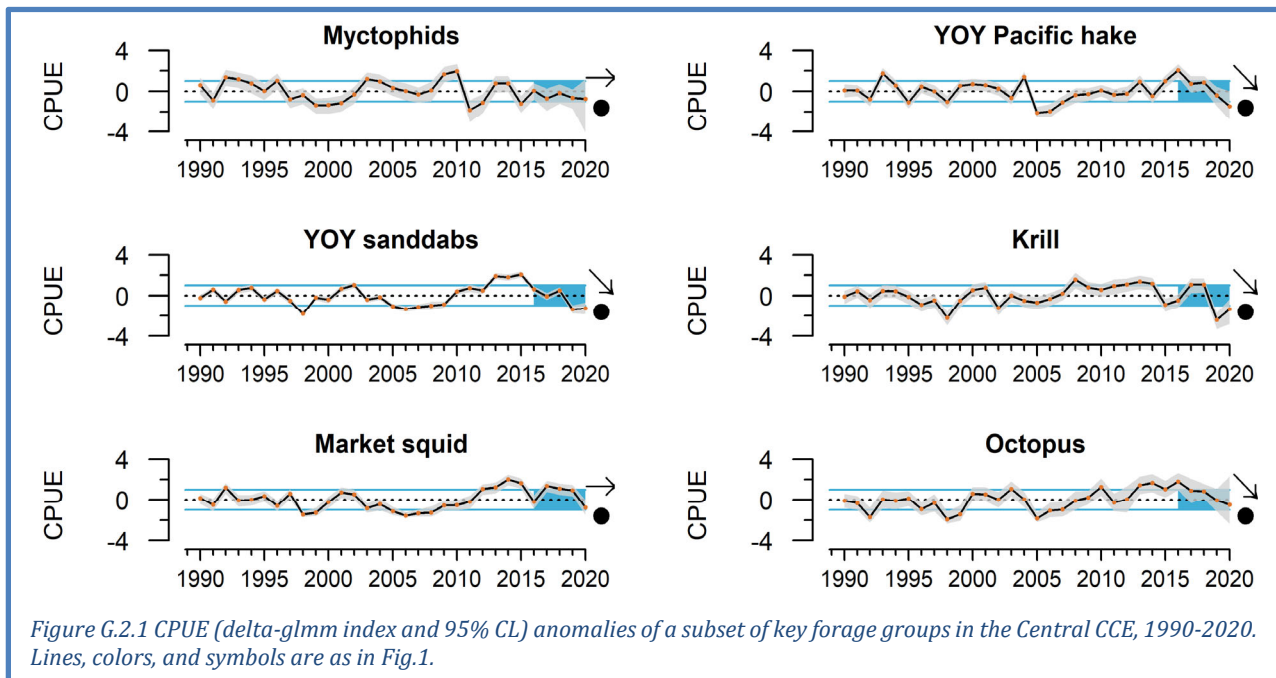


Figure G.2.1 CPUE (delta-glm index and 95% CL) anomalies of a subset of key forage groups in the Central CCE, 1990-2020. Lines, colors, and symbols are as in Fig.1.

G.3 SOUTHERN CALIFORNIA CURRENT FORAGE

Abundance indicators for forage in the Southern CCE usually come from fish and squid larvae collected in the spring (May-June) across all core stations of the CalCOFI survey. Larval data are indicators of the relative regional abundances of adult forage fish, such as sardines and anchovy, and other species, including certain groundfish, market squid, and mesopelagic fishes. In 2020, the spring larval survey was cancelled due to COVID-19. For this year's report, we instead show data from the winter (January-February) CalCOFI larval cruise, because that is the seasonal cruise with the greatest similarity in larval community composition to the spring cruise, although some key species, including anchovy, likely have peak spawning somewhat later in the year and may be underrepresented in the winter data. The survey samples a variety of fish and invertebrate larvae (<5 d old) from several taxonomic and functional groups, collected via oblique vertical tows of fine mesh Bongo nets to 212 m depth.

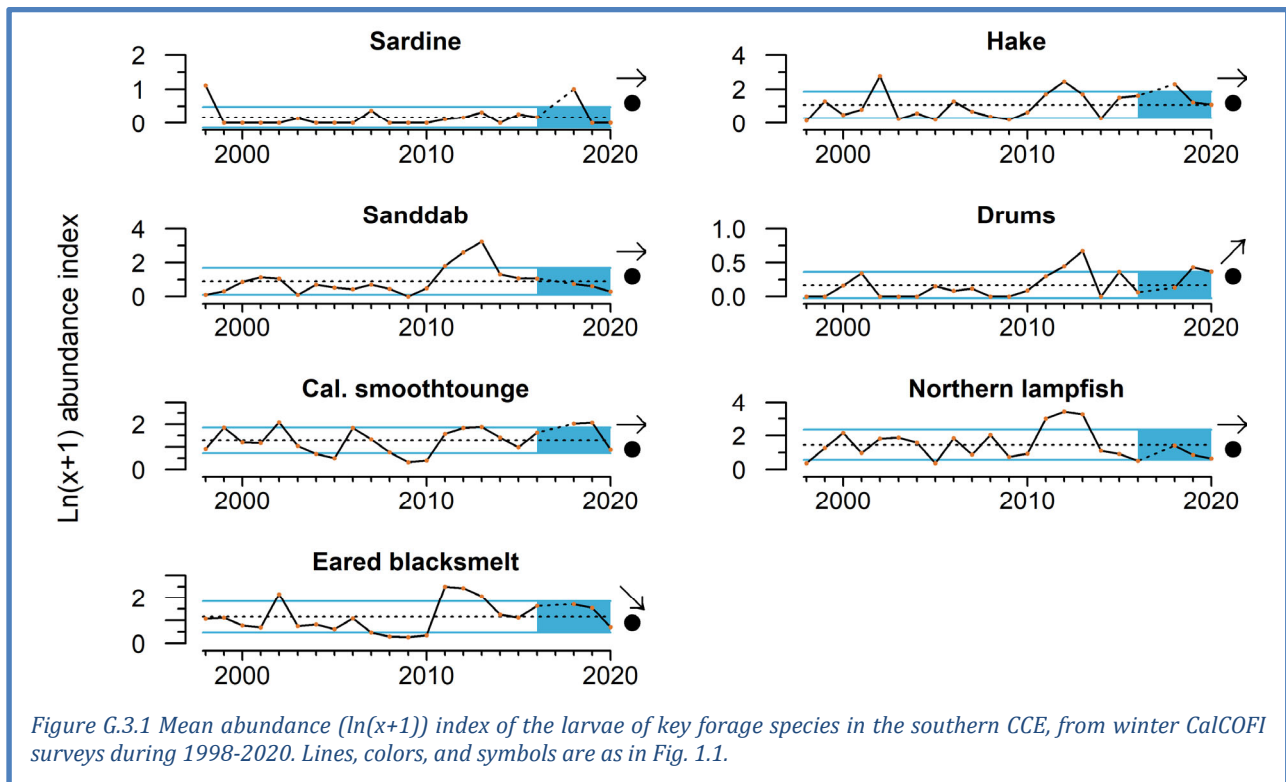


Figure G.3.1 Mean abundance ($\ln(x+1)$) index of the larvae of key forage species in the southern CCE, from winter CalCOFI surveys during 1998-2020. Lines, colors, and symbols are as in Fig. 1.1.

Besides the species described in the body of the report (Figure 4.2.3), noteworthy observations from 2020 winter survey include the continued low abundance of Northern lampfish, a mesopelagic species common north of southern California, which has been scarce since 2013 (Figure G.3.1). Another mesopelagic, eared blacksmelt, and drums showed declining abundance trends over the past 5 years.

In past years, we have used multivariate cluster analysis methods (described in Thompson et al. 2019a) to discern if forage communities within each region have undergone considerable changes in composition over time, and if the timing of major changes is synchronized across regions of the CCE and linked to major events. The Southern CCE winter forage community is the only time series we have analyzed with this approach with 2020 data as of this report, and the analysis indicates that there was a significant shift from 2019 to 2020 (data not shown), mostly driven by the decreases in southern mesopelagic larvae and larval anchovy that were shown in Figure 4.2.3. It is important to note again that anchovy larval abundances in 2020 remained above average, and that the winter survey may have occurred before peak anchovy spawning and thus not fully represent anchovy reproductive output.

Appendix H SALMON ESCAPEMENT INDICATORS

Salmon escapement data are indicators of relative abundance and reproductive potential of naturally spawning stocks. Escapement information for several Chinook and coho salmon ESUs is provided in Section 4.3 of this report. Figure 4.3.1 uses a quad plot to summarize recent escapement status and trends relative to full time series. These plots are useful for summarizing large amounts of data, but they hide informative short-term variability in these dynamic species. The full time series for all ESUs are therefore presented here. We note again that these are escapement numbers, not run-size estimates, which take many years to develop. Status and trends are estimated for the most recent 10 years of data (unlike 5 years for all other time series in this Report) in order to account for the spatial segregation of successive year classes of salmon.

H.1 CALIFORNIA CHINOOK SALMON ESCAPEMENTS

The Chinook salmon escapement time series from California include data from as recent as 2018 extending back over 20 years, with records for some populations stretching back to the 1970s. No population showed short-term trends over the past 10 years of available data (Figure H.1.1), but escapement estimates in 2018 for two populations (Central Valley Spring, Central Valley Late) were 1 s.d. below the long-term mean for their respective time series, and several others were close to 1 s.d. below the mean. On the other hand, Klamath Fall Chinook were close to the time series average escapement in 2018. Many populations have experienced decreasing escapements from 2013-2018 after some increases in the preceding years. California Coast ESU data have not been updated since 2015, so Figure H.1.1 is likely not representative of recent California Coast ESU escapement levels.

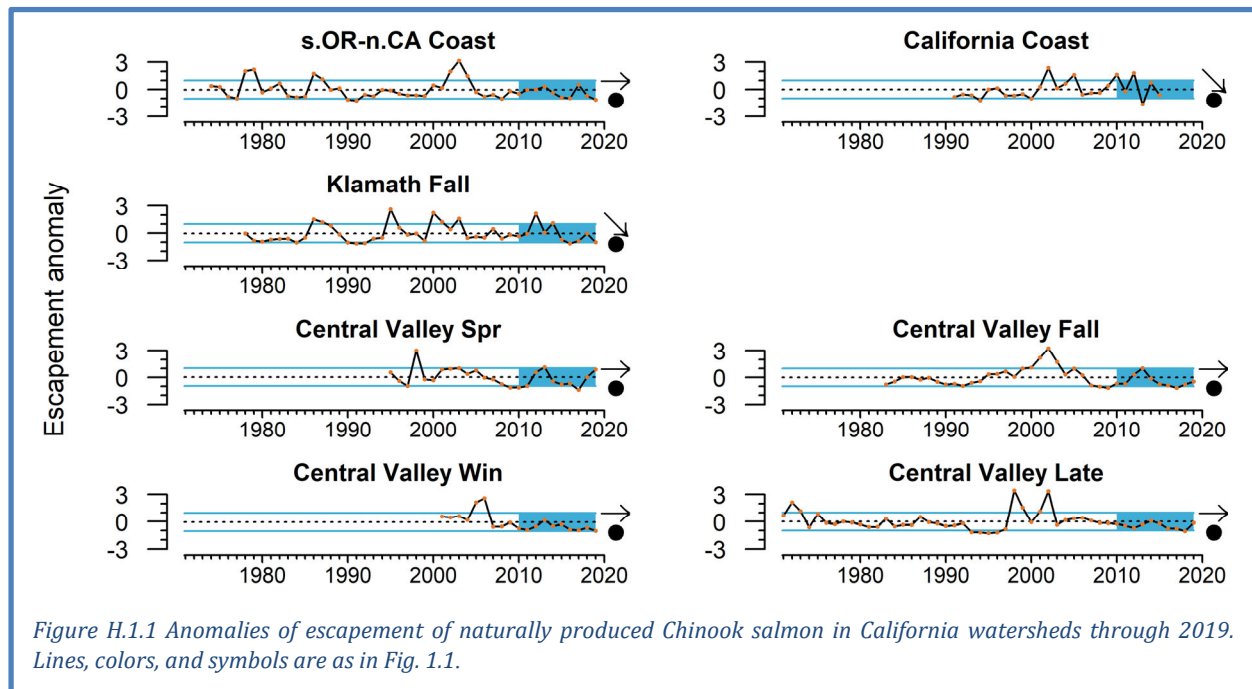
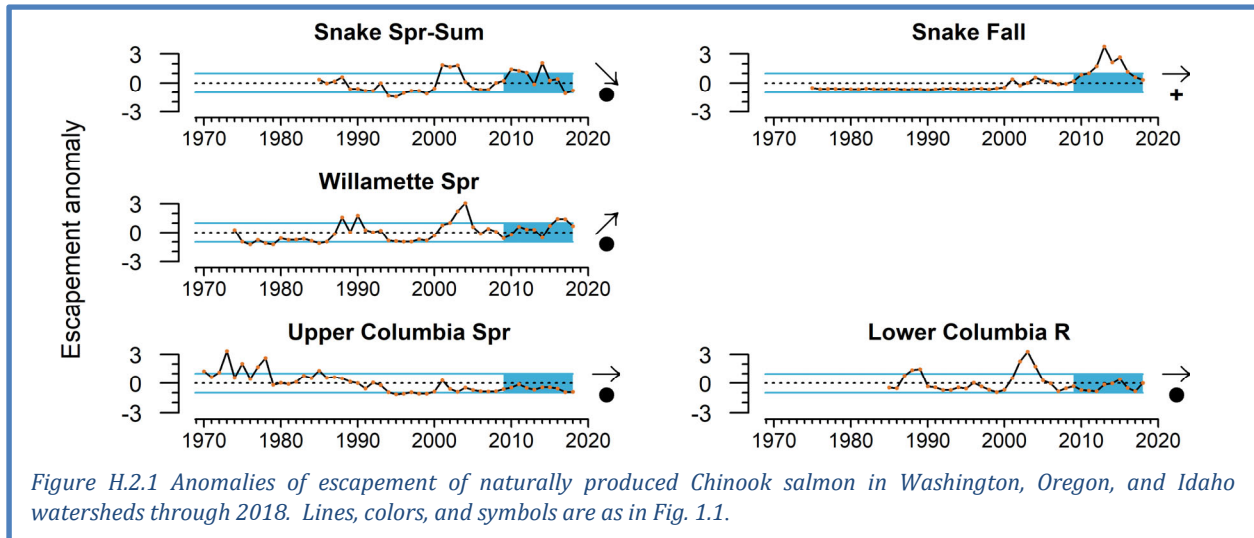


Figure H.1.1 Anomalies of escapement of naturally produced Chinook salmon in California watersheds through 2019. Lines, colors, and symbols are as in Fig. 1.1.

H.2 WASHINGTON/OREGON/IDAHO CHINOOK SALMON ESCAPEMENTS

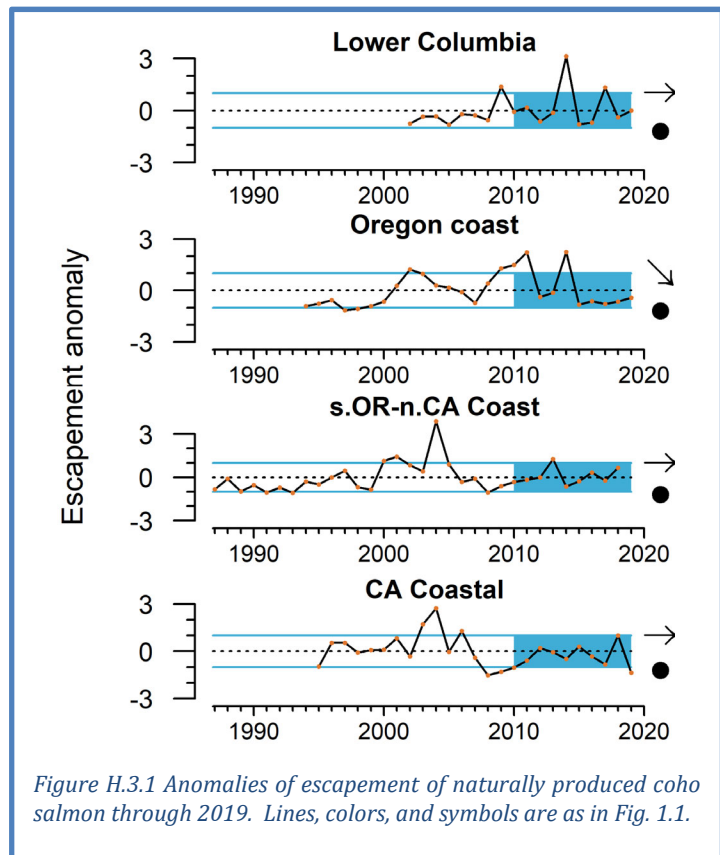
The escapement time series used for Chinook salmon populations from Washington, Idaho, and Oregon extend back for up to 40+ years, and the most recent data currently available are through 2018 (Figure H.2.1). Stocks are often co-managed and surveyed by a variety of state and tribal agencies. Patterns over the past 10 years were mixed: Snake River Spring-Summer Chinook escapement had a negative trend after declining from peaks earlier in the decade, while Willamette River Spring



Chinook had an increasing trend. Snake River Fall Chinook escapement in 2018 was near the long-term mean and have declined over the past few years, but several years of relatively high escapements in the middle of the decade resulted in a 10-year average that is >1 s.d. greater than the long-term mean. Upper Columbia Spring Chinook escapement has been below average for most of the last decade, while Lower Columbia Chinook escapement has been average to below average; both populations' recent averages are within 1 s.d. of the long-term mean, and have neutral escapement trends in the last ten years.

H.3 COHO SALMON ESCAPEMENTS

Available escapement data for naturally produced coho salmon ESUs are current through 2019 (2018 for southern Oregon/northern California coastal) (Figure H.3.1). Ten-year means for these four ESUs are within 1 s.d. of the time series averages. Recent observations range from slightly above the time series average (southern OR / northern CA coastal coho in 2018) to well below average (CA coastal coho in 2019). The trend over the most recent ten years of data was negative for Oregon Coast coho, following declines from relative peaks in 2010, 2011 and 2014; other ESUs shown had non-significant trends but general interannual variability.



H.4 ECOSYSTEM INDICATOR-BASED OUTLOOKS FOR CHINOOK SALMON ESCAPEMENT IN THE COLUMBIA BASIN

The main body of the report features a “stoplight” table (Table 4.3.1) that provides a qualitative, ecosystem-based outlook of returns of Columbia Basin Chinook salmon in 2021, based on indicators of conditions affecting marine growth and survival in the years that returning salmon went to sea as smolts. A related quantitative analysis uses an expanded set of ocean indicators plus principal components analysis and dynamic linear modeling to estimate outlooks for salmon returns for the same region. The principal components analysis essentially is used for weighted averaging of the ocean indicators from the stoplight table, reducing the total number of indicators while retaining the bulk of the information from them. The dynamic linear modeling technique relates salmon returns to the principal components of the indicator data, and the approach used here also incorporates dynamic information from sibling regression modeling. The model fits well to data for Spring Chinook and Fall Chinook at the broad scale of returns to Bonneville Dam (Figure H.4.1). Model outputs with 95% confidence intervals estimate 2021 Bonneville counts of Spring Chinook salmon that are similar to the poor counts in 2019 and 2020 (Figure H.4.1, top), while the outlook is for a decrease in Fall Chinook at Bonneville in 2021 relative to 2020 (Figure H.4.1, bottom).

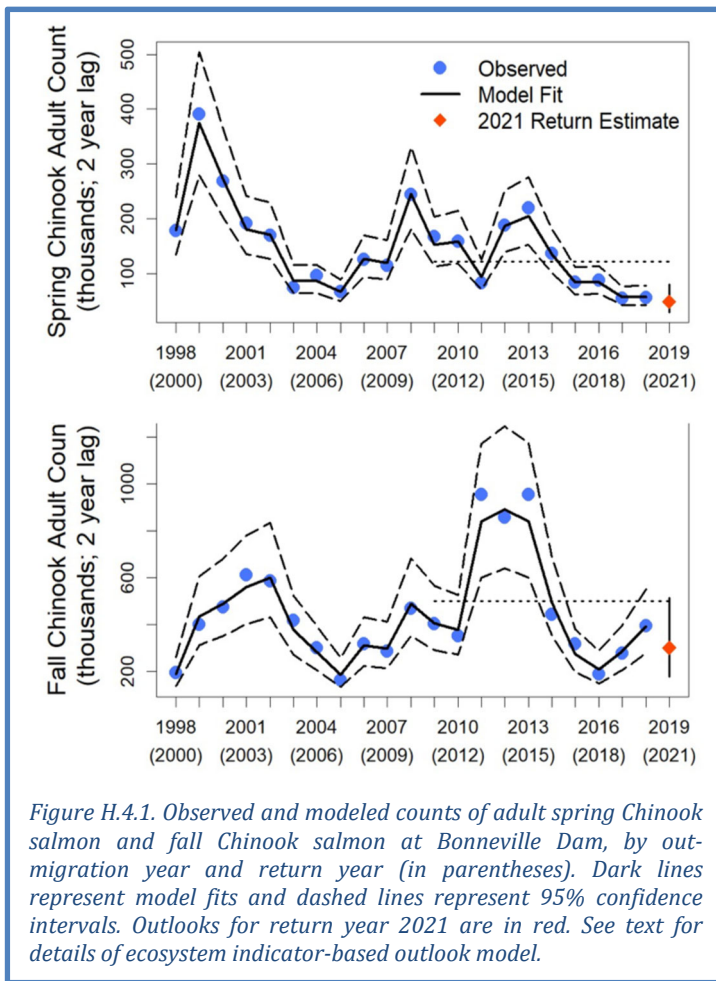


Figure H.4.1. Observed and modeled counts of adult spring Chinook salmon and fall Chinook salmon at Bonneville Dam, by out-migration year and return year (in parentheses). Dark lines represent model fits and dashed lines represent 95% confidence intervals. Outlooks for return year 2021 are in red. See text for details of ecosystem indicator-based outlook model.

(In past years, a similar model was run for coho salmon returns to the Oregon coast, but that model has proven unreliable and will not be included in the report until further study is done to improve it.)

Although these analyses represent a general description of ocean conditions related to multiple populations, we must acknowledge that the importance of any particular indicator will vary among salmon species and runs. NOAA scientists and partners are working towards stock-specific salmon projections by using methods that can optimally weight the indicators for each response variable in which we are interested (Burke et al. 2013). We will continue to work with the Council and advisory bodies to identify data sets for Council-relevant Pacific Northwest stocks for which analyses like these could be possible.

H.5 ECOSYSTEM CONDITIONS FOR FALL CHINOOK SALMON IN CALIFORNIA

Central Valley Fall Chinook stoplight table: In last year’s report, we introduced a relatively simple “stoplight” table of ecosystem indicators that were shown by Friedman et al. (2019) to be correlated with returns of naturally produced Central Valley Fall Chinook salmon. An updated stoplight chart for adult Fall Chinook salmon returning to the Central Valley in 2021 is in Table 4.3.1. The focal

ecosystem indicators are: spawning escapement of parent generations; egg incubation temperature between October and December at Red Bluff Diversion Dam (Sacramento River); median flow in the Sacramento River in the February after fry emergence; and a marine predation index based on the abundance of common murrelets at Southeast Farallon Island and the proportion of juvenile salmon in their diets. Reflecting discussions with the SSC-Ecosystem Subcommittee in September 2020, we emphasize that the stoplight chart in Table 4.3.1 is strictly qualitative and contextual decision-support information. The qualitative categories (e.g., terms like “poor” or “very poor” in color in the table cells) are based on expert opinion of how a given environmental indicator value relates to quantitative functions describing the relationship between the indicator and estimated life-stage specific survival (from Figure 5 in Friedman et al. 2019), or of how escapement of a parent generation relates to the natural area escapement goal of 120,000 fish. For example, in Table 4.3.1, February flows rated “very low” were near the low end of the range of observed values reported by Friedman et al. (2019) from 1982-2016, and are consistent with ~25% outmigrant survival, while the flows rated “high” or “very high” were consistent with ~50% to ~90% outmigrant survival (see Friedman et al. 2019, Figure 5). Egg incubation temperatures in Table 4.3.1 were consistent with egg-to-fry survival ranging from ~50% (which we rated as “suboptimal”) to ~33% (“poor”). The CCIEA team will refine these qualitative categories for next year’s report so that their basis is more explicit.

The qualitative nature of this stoplight table is in part due to the fact that some of the parameters used by Friedman et al. (2019) were estimated using information from both natural-origin and hatchery-origin fish, and while it is reasonable to assume that true parameter values would be similar, given correlations between natural and hatchery escapements, additional data specific to natural-origin fish are likely necessary in order to improve model fits, evaluate other potential covariates, and support adequate testing of model predictive skill.

Stoplight tables for Sacramento and Klamath Fall Chinook salmon: The recent determination of overfishing in four Pacific salmon stocks prompted evaluations of potential non-fishing related issues, including environmental drivers and habitat changes, that may have influenced poor stock performance. Many potential habitat issues were highlighted for Sacramento and Klamath Fall Chinook salmon runs in rebuilding plans, and the Council’s Habitat Committee advocated an indicators approach to address this challenge. The goals for this new summary were to 1) illustrate multiple habitat factors in years that triggered the rebuilding plan, 2) document how habitat impacts will remain in years after rebuilding plan, 3) identify potential cumulative effects of multiple habitat stressors, and 4) identify potential avenues for Council engagement related to management actions that influence indicators.

After review by multiple scientists and members of various advisory bodies, members of the HC developed a suite of 22 indicators for Sacramento River Fall Chinook and 18 indicators for Klamath River Fall Chinook (Table H.5.1). Many of the indicators are already included in this Ecosystem Status Report. The indicators have been shown in previous studies or were proposed in rebuilding plans to be strongly related with life-stage specific Chinook salmon productivity, and these studies helped determine expected directionality of indicators with stock productivity (Table H.5.1).

Four of the five categories of indicators in the stoplight charts align with the simpler stoplight chart for Central Valley Fall Chinook presented in the main body of this report (Table 4.3.2): Adult Spawners, Incubation conditions, Freshwater/Estuarine Residence conditions, and Marine Residence conditions (for the first year of marine residence). The fifth category of indicators in these more complex stoplight tables is Hatchery Releases, which expands the scope relative to the simple stoplight chart (Table 4.3.2) that focuses only on naturally produced fish. These stoplight charts also share qualities with the stoplight chart developed for Columbia Basin Chinook salmon and Oregon coast coho salmon (Table 4.3.1) by including regional and basin-scale oceanographic indicators, as part of the Marine Residence conditions.

Table H.5.1 Habitat indicators, definitions, and key references. Months is the months for which indicators were summarized, Effect is the predicted direction of the indicator's effect on productivity, and Stock indicates whether indicators were summarized for (S)acramento or (K)lamath runs.

Life stage-specific indicator	Abbreviation	Months	Effect	Reference	Stock
Adult spawners					
Fall run spawners	Spawners		+	Friedman et al. 2019	S, K
Fall closures of Delta Cross Channel	CChannel.F	Sep-Oct	+	Rebuilding plan	S
Fall low flows	Flows.F	Sep-Oct	+	Strange et al. 2012	S, K
Fall temperatures in mainstem	Temp.F	Sep-Oct	-	Fitzgerald et al. 2020	S, K
Incubation and emergence					
Fall-winter low flows in tributaries	Flows.W	Oct-Dec	+	Jager et al. 1997	S, K
Egg-fry temperatures	Temp.W	Oct-Dec	-	Friedman et al. 2019	S, K
Egg-fry productivity	FW.surv		+	Hall et al. 2018	S, K
Freshwater/delta residence					
Winter-spring flows	Flows.S	Dec-May	+	Friedman et al. 2019	S, K
Delta outflow index	Delta	Apr-Jul	+	Reis et al. 2019	S
7-day flow variation (SD)	SDFlow.S	Dec-May	-	Munsch et al. 2020	S, K
Maximum flushing flows	Max.flow	Nov-Mar	+	Jordan et al. 2012	K
Total annual precipitation	Precip	Annual	+	Munsch et al. 2019	S, K
Spring temperatures	Temp.S	Apr-Jul	-	Munsch et al. 2019	S, K
Spring closures of Delta Cross Channel	CChannel.S	Feb-Jul	+	Perry et al. 2013	S
Days Yolo bypass was accessible	Yolo	Dec-May	+	Limm & Marchetti 2009	S
Hatchery releases					
Release number	Releases		+	Sturrock et al. 2019	S, K
Prop net pen releases	Net.pen		+	Sturrock et al. 2019	S, K
Release timing rel. to peak spring flow	FW.Timing	Jan-Aug	+	Sykes et al. 2009	S, K
Release timing rel. to spring transition	Mar.Timing	Jan-Aug	+	Satterthwaite et al. 2014	S, K
Marine residence					
Coastal sea surface temperature	SSTarc	Mar-May	-	Wells et al. 2008	S, K
North Pacific High	NPH	Mar-May	-	Wells et al. 2008	S, K
North Pacific Gyre Oscillation	NPGO	Mar-May	+	Wells et al. 2008	S, K
Marine predation index	Predation		-	Friedman et al. 2019	S

The Sacramento River Fall Chinook habitat stoplight chart is shown in Table H.5.2 for brood years 1983-2019; the brood years defined by the rebuilding plan were 2012-2014. Indicators were standardized and tabulated using a similar approach to Peterson et al. (2014), whereby red (the bottom 33% of scores) represents relatively poor conditions, yellow represents average conditions, and green (the top 33% of scores) represents beneficial conditions. Separate stoplight charts were developed for the Sacramento and Klamath Fall Chinook populations. Overall, the suite of indicators has been highly variable, with signs of declining conditions for stock productivity since the mid-1990s. While both marine and freshwater conditions have shown signs of decline, they often have done so in opposition (e.g., short periods of poor freshwater conditions coinciding with periods of good marine conditions), but that is not always the case.

We next focus on conditions during the brood years defined by the rebuilding plan (2012-2014) and since then (Table H.5.2, bottom). The four habitat indicators for Adult Spawners were mixed during the brood years defined by the rebuilding plan. In years since, these indicators have generally worsened, though they were mixed for the 2020 outmigration year (i.e., fish from brood year 2019). For Incubation conditions, the three habitat indicators declined over the three brood years defined by the rebuilding plan. In years since, habitat indicators of Incubation conditions have generally improved, and conditions were mixed for the 2020 outmigration year. For the Freshwater/ Estuarine Residence, habitat conditions were generally poor over the three brood years defined by the

Table H.5.2 Stoplight table of freshwater and marine conditions for naturally produced Sacramento River Fall Chinook salmon. Values are standardized values for the given indicator time series. Green cells represent values ranked in the upper third of all years ("good"), yellow cells rank in the middle third of all years ("average"), and red cells rank in the bottom third of all years ("poor") for a given indicator. The rebuilding plan period (brood years 2012-2014) is outlined.

Brood year	Freshwater Conditions															Marine Conditions						
	Adult Spawners				Incubation			Freshwater/Estuarine Residence					Hatchery Releases			Marine Residence						
	Spawners	Cchannel.F	Flows.F	Temp.F	Flows.W	Temp.W	FW.surv	Flows.S	Delta	SDFlow.S	Precip	Temp.S	Cchannel.S	Yolo	Releases	Net.pen	FW.timing	Mar.timing	SSTarc	NPH	NPGO	Predation
1983	-0.54	-0.48	2.96	0.82	1.92	2.68	NA	0.56	-0.47	0.91	2.10	0.05	0.06	0.60	-1.30	-0.58	0.61	-0.39	-0.31	0.99	0.95	0.11
1984	-0.20	-0.48	3.44	-0.32	2.31	1.50	NA	-0.60	-0.82	-0.94	0.24	-0.97	-0.82	-0.74	0.49	-0.81	0.58	1.35	0.35	-0.57	0.24	2.91
1985	0.50	-0.09	0.74	NA	0.88	0.89	NA	0.48	1.18	1.54	-0.74	0.33	-0.35	0.58	0.34	-1.16	1.02	1.52	-0.39	-0.13	-0.65	0.42
1986	0.55	1.07	-0.53	0.15	-0.76	-0.28	NA	-0.73	-0.73	-1.09	0.91	-0.57	-1.04	-0.74	-0.05	-1.06	0.53	-0.17	-0.28	0.19	0.34	2.91
1987	0.28	0.23	0.33	0.15	0.49	0.17	NA	-0.65	-0.86	-0.85	-1.33	0.11	-2.46	-0.74	-0.27	-0.98	-0.11	0.17	0.06	0.75	1.44	0.41
1988	0.45	-0.48	-0.86	1.58	-1.40	0.01	NA	-0.68	-0.50	-0.66	-0.83	-0.01	-2.19	-0.55	-1.88	-1.29	1.12	1.72	-0.06	-0.33	0.76	2.91
1989	-0.12	-0.48	-0.64	-1.75	-0.93	0.05	NA	-1.04	-0.89	-1.42	-0.14	0.05	-2.86	-0.74	-0.12	0.18	-1.39	-0.59	-0.04	0.64	0.26	-0.42
1990	-0.66	-0.48	0.79	1.58	-1.03	-0.58	NA	-1.06	-0.75	-1.06	-0.92	1.52	-2.39	-0.74	0.37	-0.14	-0.32	0.79	0.11	0.74	-0.36	-0.23
1991	-0.52	-0.48	-1.07	-0.32	-1.33	-1.76	NA	-0.84	-0.84	-0.40	-0.96	-0.97	-1.05	-0.74	0.82	-1.28	-0.34	-0.64	-0.49	-0.64	-1.35	0.40
1992	-1.07	-0.48	-1.04	-1.27	-0.96	-1.03	NA	0.57	0.23	0.96	-0.88	1.35	0.04	0.38	-1.34	-1.26	0.32	-0.37	-0.45	1.74	-1.20	0.27
1993	-0.28	-0.23	-1.47	-1.75	-1.74	-0.44	NA	-1.00	-0.80	-1.37	0.95	-0.12	-0.17	-0.74	-0.64	-1.06	1.25	-1.77	-0.36	0.96	-1.20	0.16
1994	-0.05	-0.48	0.20	-0.80	0.04	0.36	NA	1.74	2.71	1.43	-1.09	1.86	0.22	2.28	-0.25	-1.07	1.02	0.52	-0.18	0.05	-1.79	-0.40
1995	0.74	-0.20	-0.76	-0.32	-1.11	-1.33	NA	0.58	0.65	0.38	2.03	-0.18	0.53	1.02	0.41	-1.11	-3.52	-2.60	-0.66	1.00	-0.95	-0.68
1996	0.81	-0.48	0.25	0.15	-0.14	-1.19	NA	0.65	-0.48	1.33	0.59	-0.29	0.52	1.12	-1.15	-1.20	1.09	0.07	-0.52	0.94	-0.67	-0.17
1997	0.87	0.36	0.47	2.05	0.32	-0.60	NA	2.04	1.45	1.19	0.60	2.26	0.75	1.70	1.01	-0.58	0.20	0.61	-0.27	0.84	0.56	-0.38
1998	0.28	4.72	0.28	0.15	-0.43	0.09	NA	0.87	0.16	0.45	1.92	1.35	0.68	0.67	-0.84	-1.17	0.07	-0.39	0.90	-0.46	1.74	0.37
1999	1.17	-0.48	1.14	1.10	1.33	0.36	NA	0.53	0.27	0.88	-0.15	-0.12	-0.05	0.31	-1.07	-1.19	-0.01	-1.25	0.23	-1.04	2.25	-0.11
2000	1.21	1.60	0.57	0.15	0.73	-0.09	NA	-0.74	-0.62	-0.67	0.05	-0.40	-0.25	-0.74	-0.06	0.00	-0.19	-0.71	0.33	0.09	2.18	0.08
2001	1.69	-0.10	0.09	0.63	0.53	-0.30	NA	-0.26	-0.65	-0.09	-1.03	-0.46	0.58	-0.58	-0.90	-0.71	-0.24	-0.76	0.34	-0.37	1.30	-0.10
2002	1.99	-0.19	-0.60	-0.80	0.26	-0.07	NA	0.92	-0.29	0.74	0.42	0.28	0.55	-0.29	1.12	0.57	-1.06	1.20	0.34	0.00	1.17	-0.29
2003	1.36	-0.48	-0.34	0.63	0.22	0.17	-0.83	0.63	-0.18	0.95	0.30	-0.52	0.68	0.09	0.29	0.21	-0.11	-1.15	-0.40	0.13	0.24	-0.61
2004	0.48	-0.48	0.04	2.29	0.42	-0.49	-0.40	0.09	0.09	0.14	-0.28	0.90	0.63	-0.61	0.92	0.89	-1.44	-0.02	-0.64	0.12	-1.32	-1.31
2005	0.53	-0.48	0.17	0.63	-0.49	-0.39	-0.38	2.21	2.55	1.10	0.37	0.86	0.70	2.44	1.32	0.75	-0.73	-0.56	0.17	0.49	-0.47	-1.26
2006	0.42	-0.48	0.39	0.15	0.78	0.62	-0.68	-0.82	-0.73	-1.14	1.32	-0.46	0.34	-0.74	1.23	0.99	0.02	-1.72	0.49	0.27	0.13	-0.95
2007	-0.88	-0.48	0.17	-0.04	0.54	-0.41	-0.06	-0.71	-0.77	-0.64	-1.07	-0.01	0.35	-0.74	1.32	1.20	0.30	1.01	0.78	-0.41	1.50	-0.81
2008	-1.37	-0.48	-0.34	-0.51	0.44	-1.01	-0.45	-0.83	-0.60	-0.49	-0.92	-0.35	0.28	-0.74	0.80	0.98	0.53	1.08	0.67	-0.98	0.43	-0.59
2009	-2.17	-0.10	-0.93	-0.51	-1.27	-0.23	1.13	-0.32	-0.46	-0.10	-0.61	1.75	0.39	-0.61	0.87	0.84	0.73	-0.10	0.18	-0.09	1.57	-0.51
2010	-0.55	-0.29	-0.64	-0.42	-1.00	0.44	1.21	0.57	1.22	0.72	-0.01	2.14	0.75	0.48	1.17	0.90	0.22	0.07	0.25	-0.45	1.06	-0.65
2011	-0.74	0.49	0.09	-0.04	0.27	1.14	-0.31	-0.87	-0.48	-1.13	0.76	0.33	0.67	-0.74	1.18	0.53	0.30	1.45	0.58	-0.88	1.56	-0.39
2012	0.21	-0.48	0.57	NA	2.11	0.49	-0.01	-0.54	-0.75	-0.27	-0.79	-1.20	0.66	-0.39	0.32	0.13	-2.83	-0.02	0.21	-0.33	0.66	0.02
2013	0.97	0.80	-0.20	-0.42	0.69	0.38	0.13	-1.22	-0.82	-1.26	-0.51	-1.48	0.48	-0.74	0.31	1.51	0.53	1.30	-0.81	-0.23	-0.28	0.49
2014	0.23	-0.29	-0.85	-1.37	-1.25	-2.82	-1.38	-0.78	-0.88	-0.03	-1.26	-1.14	0.52	-0.71	-0.21	0.68	0.48	-0.44	-1.32	0.32	-1.16	0.87
2015	-0.80	-0.39	-1.18	-0.61	-0.34	-0.58	0.26	-0.16	-0.12	0.58	-0.72	-0.97	0.44	-0.32	0.69	0.40	0.20	0.34	-1.12	0.09	-0.20	-0.51
2016	-1.15	-0.48	-1.37	-1.56	-0.84	0.86	2.82	2.21	1.80	1.47	0.14	-0.91	0.75	2.70	-0.92	-0.01	0.58	-0.47	-0.50	0.23	-0.49	NA
2017	-2.59	2.00	0.21	-0.51	0.25	0.86	-0.65	-1.01	-0.27	-1.10	1.92	-1.03	0.67	-0.61	-0.26	1.10	-0.14	-0.49	-0.62	-0.10	-2.01	NA
2018	-0.85	-0.48	0.23	0.25	0.61	0.98	-0.41	1.17	1.41	1.54	-0.66	-0.35	0.75	0.64	-0.78	0.90	0.68	0.79	-0.84	0.29	-2.09	NA
2019	-0.20	-0.19	-0.36	-0.51	-0.62	1.55	NA	-0.97	1.05	-1.59	1.08	-0.91	0.64	-0.74	-2.92	2.62	0.04	0.61	-0.39	0.33	-1.57	NA

rebuilding plan; they have generally improved since then, although they were poorer for the 2020 outmigration year than in 2019, due to poor flows and high temperatures. Hatchery Release indicators were mixed in the three rebuilding plan brood years, and have remained mixed since then. Marine Residence indicators were generally below average for the brood years in the rebuilding plan, although they improved somewhat in the 2014 brood year. Since then, these indicators have generally worsened. Habitat conditions for the 2020 outmigration year showed some improvement compared to the previous four years, but were nonetheless mixed.

The Klamath River Fall Chinook habitat stoplight chart is in Table H.5.3. As with the Sacramento River chart, the indicator suite as a whole has been highly variable, but there is less clear evidence of any sustained long-term trends in habitat conditions during the 1983-2019 brood years. In the brood years defined by the rebuilding plan (2012-2014) and since then (Table H.5.3, bottom), conditions for Adult Spawners were mixed during the three brood years of the rebuilding plan (2012-2014) and worsened in the brood years since. For Incubation conditions, the three indicators generally declined over the three brood years defined by the rebuilding plan. In years since, habitat indicators have generally improved, though conditions for the 2020 outmigration year were mixed. Freshwater Residence conditions were mixed for the three brood years defined by the rebuilding plan, and have remained mixed since then. Hatchery Release indicators were mixed in the three rebuilding plan brood years, but have been relatively poor since then (though data are unavailable for the 2020

outmigration year). Marine Residence indicators were generally below average for brood years in the rebuilding plan, although they improved somewhat for the 2014 brood year. Since then, these indicators have generally worsened, although they showed some improvement for the 2020 outmigration year (brood year 2019).

Table H.5.3 Stoplight table for naturally produced Klamath River Fall Chinook salmon. Values are standardized values for the given indicator time series. Green cells represent values ranked in the upper third of all years ("good"), yellow cells rank in the middle third of all years ("average"), and red cells rank in the bottom third of all years ("poor") for a given indicator. The rebuilding plan period (brood years 2012-2014) is outlined.

Brood year	Freshwater Conditions											Marine Conditions					
	Adult Spawners			Incubation			Freshwater Residence					Hatchery Releases			Marine Residence		
	Spawners	Flows.F	Temp.F	Flows.W	Temp.W	FW.surv	Flows.S	SDFlow.S	Precip	Temp.S	Max.flows	Releases	FW.timing	Mar.timing	SSTarc	NPH	NPGO
1983	-0.66	1.23	NA	2.87	NA	NA	1.6	1.02	-1.24	-0.66	0.99	-0.31	2.11	0.66	-0.31	0.99	0.95
1984	-0.95	1.94	NA	1.89	NA	NA	0.0	-0.08	-1.04	0.23	0.42	-1.27	0.49	1.72	0.35	-0.57	0.24
1985	-0.49	1.18	NA	-0.38	NA	NA	0.9	2.41	-0.55	0.24	0.35	2.93	1.49	1.72	-0.39	-0.13	-0.65
1986	1.16	1.12	NA	0.23	NA	NA	-0.5	-0.58	0.69	0.83	1.62	2.50	1.51	0.39	-0.28	0.19	0.34
1987	1.26	1.13	NA	0.52	NA	NA	-0.7	-0.57	1.22	1.12	-0.73	-0.59	-1.03	0.24	0.06	0.75	1.44
1988	1.13	-0.24	NA	-0.07	NA	NA	0.2	0.25	-0.36	-0.35	-0.84	2.58	0.49	0.87	-0.06	-0.33	0.76
1989	0.49	1.17	NA	-0.60	NA	NA	-0.7	-0.62	0.46	1.32	0.82	0.21	-0.69	-0.08	-0.04	0.64	0.26
1990	-1.36	-0.24	NA	0.40	NA	NA	-1.1	-1.01	-0.93	0.71	-0.73	-0.73	1.23	1.53	0.11	0.74	-0.36
1991	-1.50	-1.65	NA	-0.67	NA	NA	-1.2	-0.98	2.49	1.37	-0.95	-0.39	0.86	1.03	-0.49	-0.64	-1.35
1992	-1.80	-3.12	NA	-0.96	NA	NA	0.7	0.45	-1.02	-0.50	-1.30	-0.43	1.32	0.05	-0.45	1.74	-1.20
1993	-0.67	1.22	NA	-0.44	NA	NA	-1.2	-1.16	1.00	1.73	1.06	-0.98	0.49	-2.89	-0.36	0.96	-1.20
1994	-0.50	-0.85	NA	-0.35	NA	NA	1.6	2.07	-0.44	-0.20	-1.20	0.12	1.03	0.31	-0.18	0.05	-1.79
1995	1.35	1.22	NA	-0.55	NA	NA	-1.7	-1.76	0.76	-1.37	0.57	0.15	-0.18	-0.24	-0.66	1.00	-0.95
1996	1.00	0.50	NA	0.41	NA	NA	NA	NA	-0.18	-2.24	1.35	0.31	-0.21	-0.06	-0.52	0.94	-0.67
1997	-0.10	-0.23	NA	0.30	NA	NA	2.0	1.69	-0.89	-1.22	2.91	-0.08	-0.30	-0.14	-0.27	0.84	0.56
1998	0.02	1.40	NA	0.51	NA	NA	1.4	0.70	-1.91	-1.01	0.56	-0.24	0.66	-0.19	0.90	-0.46	1.74
1999	-0.84	1.13	NA	0.82	NA	NA	0.2	0.05	-0.15	-0.37	0.65	0.12	0.92	-0.69	0.23	-1.04	2.25
2000	1.32	0.04	NA	0.64	NA	NA	-1.2	-1.34	-0.36	1.66	-0.31	0.10	-0.27	-0.58	0.33	0.09	2.18
2001	1.10	-0.27	NA	0.00	NA	-1.00	-0.1	-0.07	0.38	0.42	-1.02	0.12	-0.67	-0.51	0.34	-0.37	1.30
2002	0.87	-1.53	NA	-0.23	NA	-1.69	0.4	0.37	0.22	-1.19	-0.79	0.26	0.27	1.35	-0.34	0.00	1.17
2003	1.13	0.50	NA	-0.59	0.82	-1.60	0.00	0.06	0.52	0.09	-0.53	0.13	0.32	-1.03	-0.40	0.13	0.24
2004	-0.19	-0.79	0.26	-0.10	-0.27	-1.03	-0.29	-0.45	-0.42	-0.18	-0.54	0.25	-1.63	-0.32	-0.64	0.12	-1.32
2005	-0.47	0.44	-0.44	-0.19	0.12	2.18	1.86	1.96	-0.18	-1.78	1.14	0.61	-0.95	-0.32	0.17	0.49	-0.47
2006	-0.56	-0.46	-1.11	-0.36	-0.83	-0.79	-0.29	-0.36	-0.41	-0.10	1.14	0.29	-0.04	-1.80	0.49	0.27	0.13
2007	0.58	-0.24	-0.75	0.11	-0.48	1.19	-0.22	-0.70	-0.79	0.43	-0.57	0.24	-1.74	0.98	0.78	-0.41	1.50
2008	-0.36	-0.29	0.08	0.31	-0.21	-0.02	-0.64	-0.61	0.04	0.88	-0.73	-0.30	0.15	0.87	0.67	-0.98	0.43
2009	0.17	-0.42	0.63	-0.50	-0.34	0.00	-0.13	-0.55	-1.50	0.26	-1.10	-0.12	-2.73	-1.09	0.18	-0.09	1.57
2010	0.02	-0.27	-0.05	-0.45	0.21	0.31	0.70	-0.04	-1.39	-0.69	-1.07	-0.28	0.04	-0.58	0.25	-0.45	1.06
2011	0.19	-0.29	1.22	0.16	-1.20	-0.46	-0.12	0.12	-0.21	0.04	-0.18	0.07	-0.21	1.19	0.58	-0.88	1.56
2012	1.77	-0.33	0.91	-0.14	0.00	0.75	-0.61	-0.49	0.00	-0.46	-0.58	-0.31	-0.89	-0.29	0.21	-0.33	0.66
2013	0.91	-0.39	-1.33	-0.35	-2.00	0.39	-1.14	-0.74	0.93	0.59	-0.95	0.00	-0.13	0.61	-0.81	-0.23	-0.28
2014	0.87	-0.39	1.50	-0.70	2.66	-0.21	-0.70	-0.13	2.50	0.71	-1.08	-0.58	-0.47	-0.98	-1.32	0.32	-1.16
2015	-0.21	-0.51	1.88	-0.46	1.18	0.96	0.49	0.74	1.65	-0.40	-0.76	-0.45	0.24	0.16	-1.12	0.09	-0.20
2016	-1.92	-0.52	-1.14	-0.45	-0.26	NA	2.01	1.61	0.00	-1.55	0.78	-2.50	0.13	-0.64	-0.50	0.23	-0.49
2017	-1.47	-0.31	-1.08	0.39	0.10	0.53	-0.66	-0.69	0.42	1.36	0.90	-0.15	-0.78	-1.35	-0.62	-0.10	-2.01
2018	0.02	-0.42	-0.33	-0.09	0.36	0.65	0.20	0.37	-0.07	-0.82	-0.05	-1.28	-0.84	0.13	-0.84	0.29	-2.09
2019	-1.30	-0.46	-0.24	-0.48	0.14	-0.16	-1.1	-0.96	0.76	1.11	0.76	NA	NA	NA	-0.39	0.33	-1.57

The Council has a long history of engaging with other agencies to advocate for improved habitat conditions for the Sacramento and Klamath Fall Chinook salmon runs. While many possible management "dials" exist for improving habitat, few can easily be tracked annually. For both stocks, river flow is highly managed through hydropower, and flows at particular stages can influence water temperature. These indicators have shown evidence for long-term change as well as recent variability during brood years highlighted by the rebuilding plan and years thereafter. In particular, temperature conditions for the Sacramento (during spawning, spring rearing), and flow conditions for the Klamath (all types except maximum flushing flows) continue to remain at relatively low status, suggesting that improved flow management can have positive improvements for populations (Munsch et al 2020). The IEA team will work with the HC, the STT, and the SSC as necessary to continue to present and refine these indicators for these two important stocks.

Appendix I AVAILABILITY OF GROUNDFISH TO PORTS

Methodology for calculating the relative availability of groundfish biomass to individual ports follows that of Selden et al. (2020). In brief, we used data from the Northwest Fisheries Science Center's West Coast Groundfish Bottom Trawl Survey (WCGBTS, 2003-2019) and vector autoregressive spatio-temporal (VAST) modeling (Thorson 2019) to estimate spatial distribution of species-specific biomass (Location Biomass), and the Center of Gravity (CoG) of the Location Biomass. We then calculate the Availability Index for each port by summing the Location Biomass within a radius from that port based on the 75th quantile of the distance travelled from port to harvest any of the five species in Selden et al (2020), weighted by catch, as measured by trawl logbooks 1981-2015 (Figure I.1). We analyzed species that make up a large component of landings for vessels using bottom trawl gear along the West Coast, or that have broader management interest (e.g., shortbelly rockfish).

The present analysis differs from Selden et al. (2020) in three ways. First, here we use the Location Biomass directly instead of scaling it by spawning stock biomass from the assessment. Thus the Availability Index is a relative biomass index and not actual available biomass. Second, we use only the WCGBTS, and do not combine the Triennial survey (1980-2004) with the WCGBTS (2003-2019). This approach shortens the analysis period but allows us to expand the depth range to 55-1250 m. Finally, we updated the VAST to match the base settings used in West Coast groundfish stock assessments.

The Availability Index for most of the selected species was highest for the northern ports, particularly Astoria (Figure I.2). This pattern is due in part to distribution of stock biomass. In addition, vessels from Astoria utilize a larger area on average than those from most other ports, plus the shelf and upper slope are wider near Astoria than in regions adjacent to other ports (Figure I.1).

Availability for big skate, petrale sole, and sablefish increased from approximately 2010 onwards for Astoria, doubling in availability for big skate and sablefish and increasing 6-fold for petrale sole, before dropping back to earlier levels (Figure I.2). Availability of lingcod increased rapidly for Bellingham and Astoria from 2009 to 2013 but then declined steeply from 2014 to 2019. In contrast, availability of canary and yellowtail rockfishes and shortspine thornyhead to northern ports also increased since approximately 2010, but did not decrease in availability later in the time series. Overall, individual species tended to show some synchrony in availability coastwide, although variation at southern ports was generally muted compared to the two northern ports (shortbelly rockfish being the exception). However, for some species, there were within-region differences. For example, availability of arrowtooth flounder spiked sharply for Bellingham in 2016, but not for other northerly ports. Similarly, darkblotched rockfish availability spiked off Coos Bay in 2013, but not off other northerly ports. Further research is needed to discern if these represent actual changes in availability or statistical artifacts.

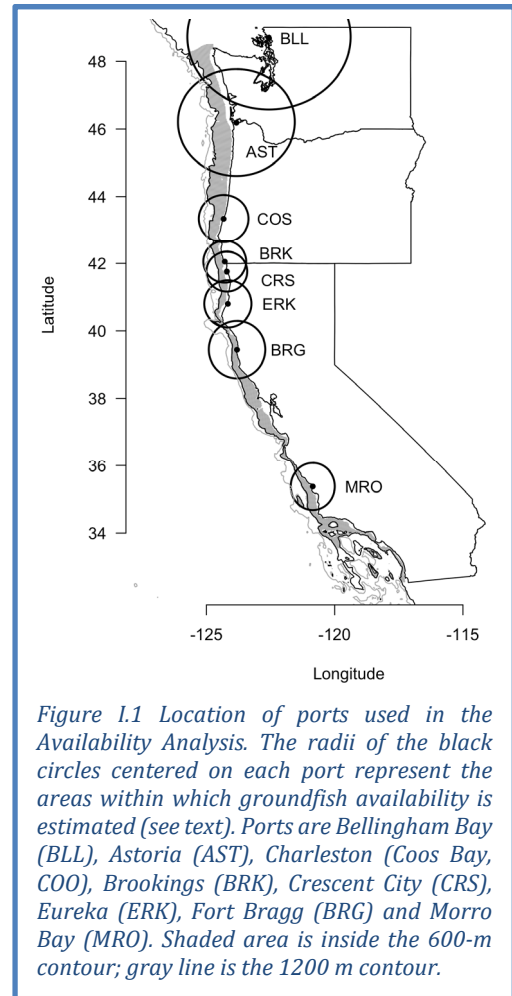
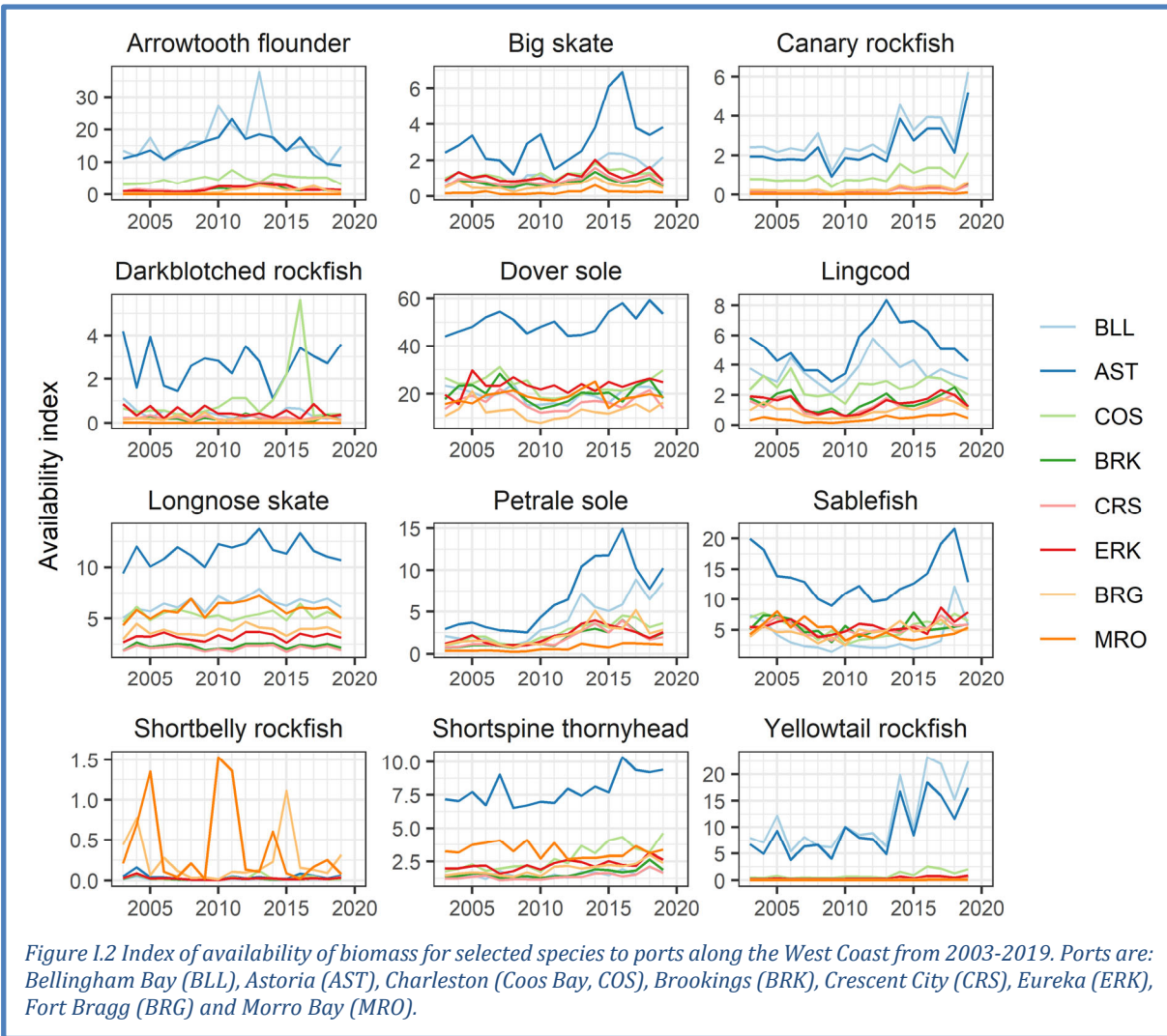
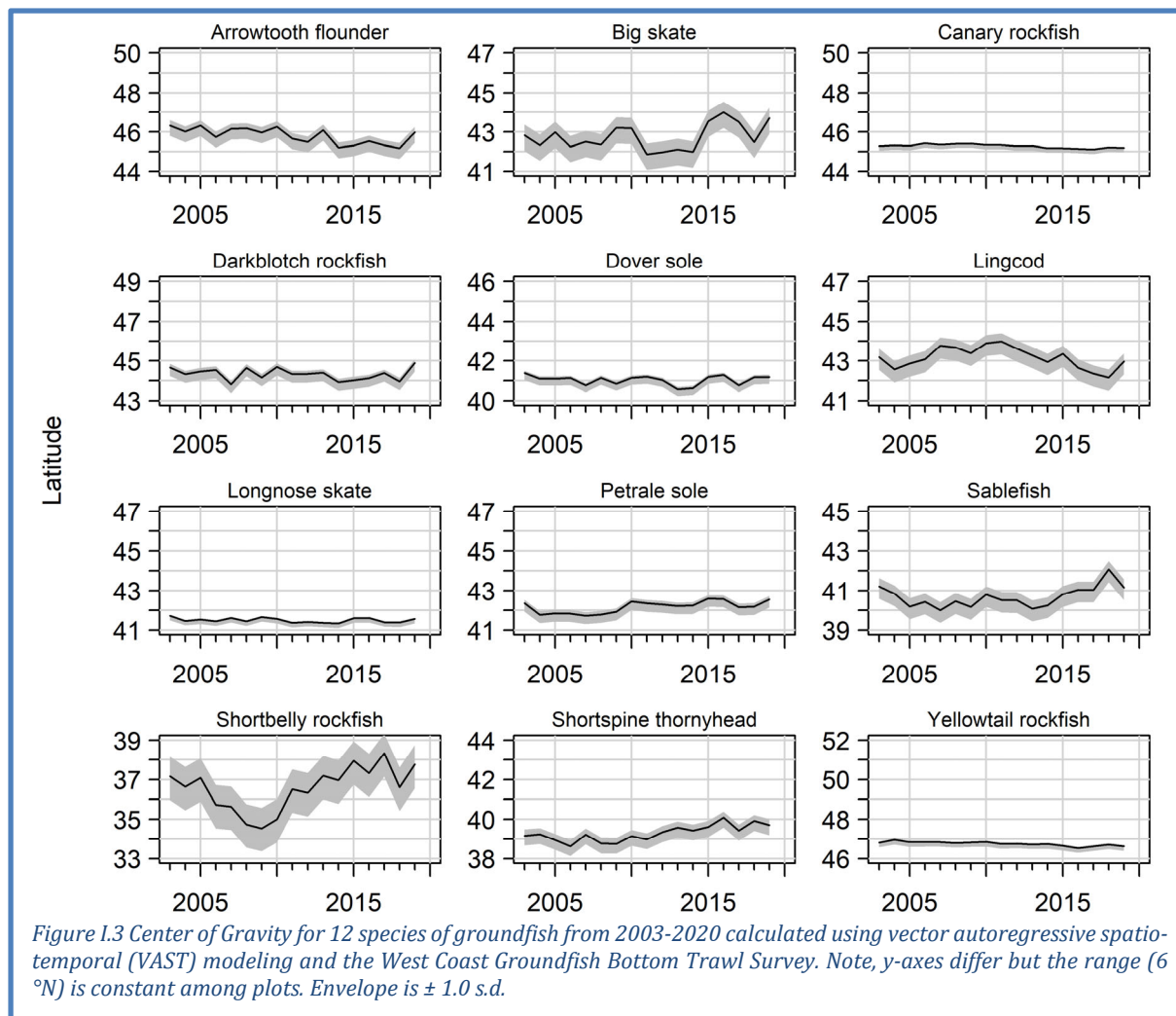


Figure I.1 Location of ports used in the Availability Analysis. The radii of the black circles centered on each port represent the areas within which groundfish availability is estimated (see text). Ports are Bellingham Bay (BLL), Astoria (AST), Charleston (Coos Bay, COO), Brookings (BRK), Crescent City (CRS), Eureka (ERK), Fort Bragg (BRG) and Morro Bay (MRO). Shaded area is inside the 600-m contour; gray line is the 1200 m contour.



Variation in Center of Gravity (CoG) (Figure I.3) was only directional for short periods of 5-10 years. However, shifts in the CoG could be considerable, up to 2-3° of latitude. CoG variability was highest for big skate, lingcod, sablefish, and shortbelly rockfish. Sablefish CoG initially shifted south and remained stable for several years. Sablefish CoG then shifted north until 2018, and then returned to ~41°N where it was in 2003. Lingcod, shortbelly, and big skate showed similar patterns. Even arrowtooth flounder, which showed a slight long-term southward shift in CoG, shifted back north to a similar latitude in 2019 as in 2003. Thus there is as yet no evidence of unidirectional latitudinal or longitudinal shifts of groundfish during this time series, e.g., the types of climate-driven unidirectional shifts that have been observed or predicted for groundfish in other systems (e.g., Nye et al. 2009, Morley et al. 2018), but analysis of longer time periods or larger spatial extents (e.g., from the West Coast to the Gulf of Alaska) might be informative.

We will continue to track these changes in distribution and abundance as potential indicators of environmentally driven changes in groundfish stocks, as indicators of fishing opportunities for ports, and to inform decisions regarding allocation of fishing effort and catch. Future work to understand the relative roles of climate, recruitment, stock size, fisheries removal, and other factors will help us to clarify observed variability in centers of gravity of key groundfish stocks.

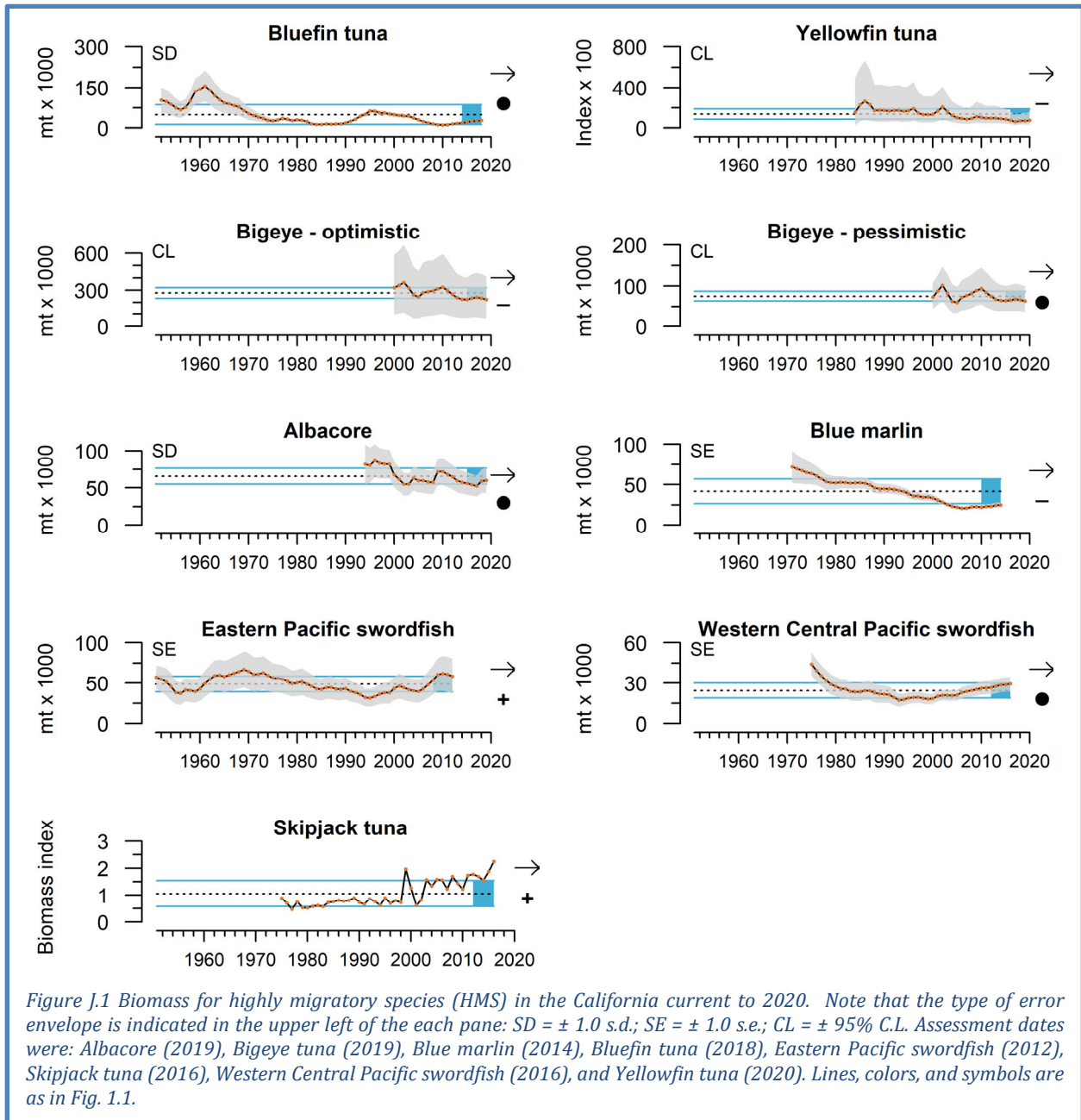


Appendix J HIGHLY MIGRATORY SPECIES

Highly migratory species are discussed in Section 4.5 of the main document. Time series for spawning stock biomass (Figure J.1) and recruitment (Figure J.2) are plotted here, and include information from the most up-to-date assessments for these seven stocks. Below, we also provide general descriptive summaries of spawning stock biomass, recruitment, and implications for each stock.

Pacific bluefin tuna: Pacific bluefin are considered to be one stock throughout the Pacific Ocean, and are fished throughout their range by many countries and fishing gears. At present, most are caught by purse seine. The spawning stock biomass and recruitment indexes for Pacific bluefin come from the latest (2020) stock assessment, completed through the International Scientific Committee for Tuna and Tuna-like Species in the North Pacific Ocean (ISC). Their population dynamics are assessed using a fully integrated age-structured model (Stock Synthesis v3). Since the previous benchmark assessment in 2016, the stock assessment model was thoroughly reviewed and improved. Fleet definitions were refined to better capture the difference in the nature of fisheries, and model parameterization was further fine-tuned to better describe the population dynamics. Annual recruitment is primarily indexed by catches from troll fisheries on age-0 juvenile fish near Japan. The full assessment is available from http://isc.fra.go.jp/reports/stock_assessments.html, and indices were provided by Hui-Hua Lee (NOAA Fisheries, SWFSC). The next assessment is expected in 2022.

Spawning stock biomass has increased slowly since 2011 (Figure J.1), and is estimated at ~4.5% of unfished biomass. The abundance of young (<2 year old) fish appears to have increased since 2016, which may accelerate the recovery of the species. Estimated recruitment has fluctuated since 1950 without any apparent trend (Figure J.2). Fishing mortalities on ages 0-2 in 2016-2018 declined relative to previous years. While no reference points have been agreed upon, an evaluation of stock status against some common reference points shows that the stock is overfished relative to biomass-based limit reference points adopted for other species in managed through the WCPFC. The impact of eastern Pacific fisheries on the stock was high before the mid-1980s, but since the early 1990s the western Pacific purse seine fishery group targeting small fish (ages 0-1) has had a greater impact.



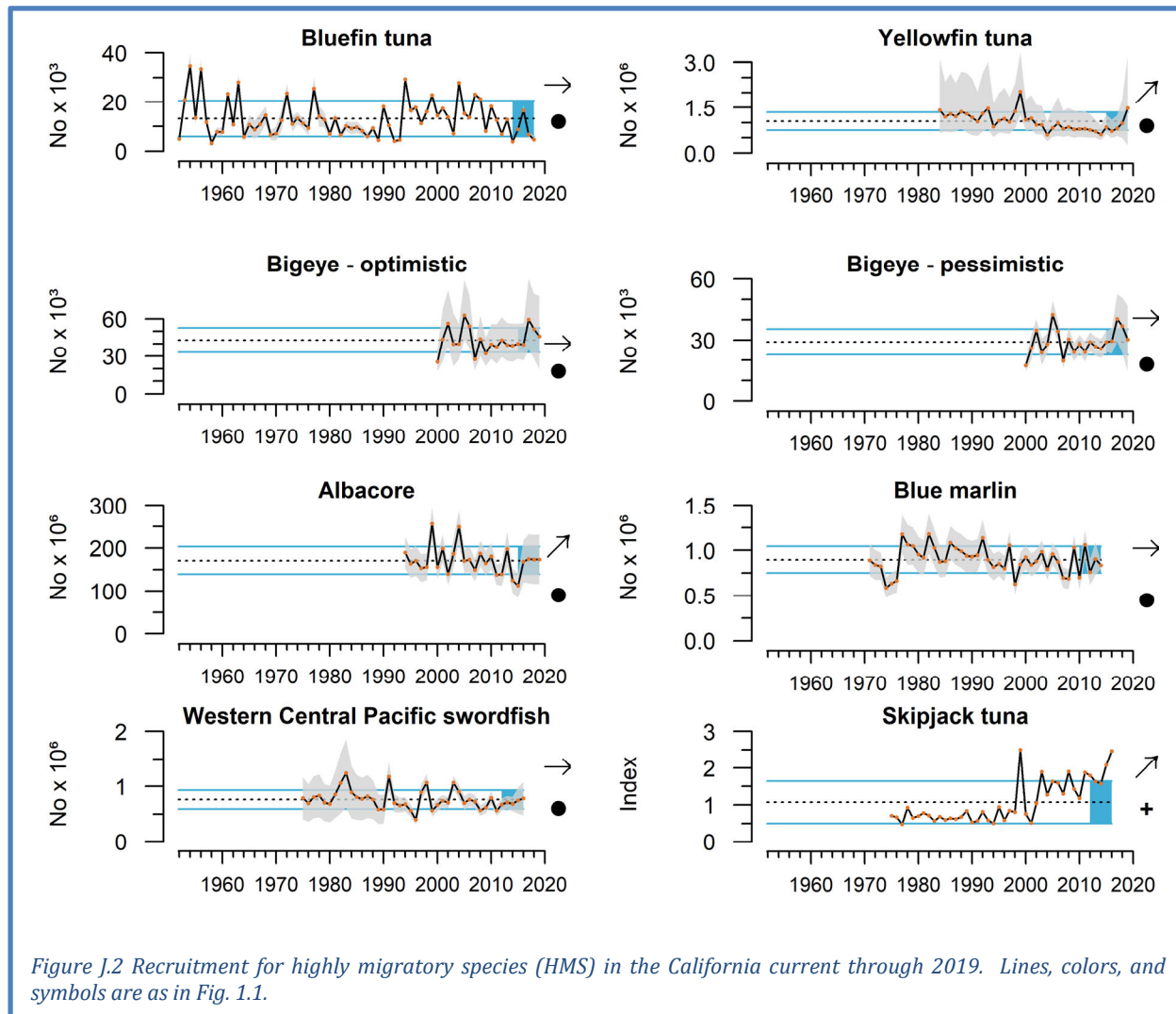


Figure J.2 Recruitment for highly migratory species (HMS) in the California current through 2019. Lines, colors, and symbols are as in Fig. 1.1.

North Pacific albacore: North Pacific albacore are considered one stock throughout the North Pacific Ocean. They are fished throughout their range by many countries, mostly with surface gear (troll, pole & line), as well as pelagic longlines and other gears. Spawning potential biomass and recruitment estimates come from the latest (2020) stock assessment, completed through the ISC using Stock Synthesis v3. The assessment model used was similar to that in the 2017 benchmark assessment, with improvements to the handling of size composition data, and splitting of fleets by season. The assessment is available at http://isc.fra.go.jp/reports/stock_assessments.html, and indices were provided by Steve Teo (NOAA Fisheries, SWFSC). The next assessment is expected in 2023.

Spawning stock biomass has been relatively stable since 2000 (Figure J.1). The stock is not considered likely to be overfished, and although no fishing mortality-based reference points have been adopted, it is not likely that overfishing is currently occurring. Recent recruitment estimates suggest historic low recruitment in 2014 and 2015 (Figure J.2). It is currently unclear whether recruitment improved after 2015 because recruitment estimates during the terminal years of the assessment (2016–2018) have large uncertainties.

Swordfish: Swordfish are considered to comprise two stocks in the North Pacific. The western and central Pacific stock is located throughout most of the North Pacific, while the eastern Pacific stock is found off Baja California and central and south America. However, recent electronic tagging of

swordfish off southern California suggests that there may be more mixing of fish between northern and southern regions than previously thought. The highest catches in the North Pacific are from pelagic longline gears. The spawning biomass and recruitment indexes for the western central Pacific swordfish stocks come from the latest (2018) stock assessment report, completed through the ISC and available from http://isc.fra.go.jp/reports/stock_assessments.html. The next benchmark assessment is expected in 2022. The assessment for the eastern stock has not been updated recently.

Estimates of stock biomass show relatively stable populations for both stocks, with a slight decline until the mid-1990s, followed by a slight increase from 2000-2016 (Figure J.1). The base case model indicated that the western stock is not likely overfished and not likely experiencing overfishing relative to MSY-based or 20% of unfished spawning biomass-based reference points. No long term trend in recruitment is apparent, and recent recruitment estimates are around average (Figure J.2).

Blue marlin: Blue marlin are considered one stock throughout the Pacific Ocean, and the majority are caught by pelagic longlines. Their spawning stock biomass and recruitment estimates are from the latest (2016) stock assessment report, completed through the ISC using Stock Synthesis v3. The assessment is available at http://isc.fra.go.jp/reports/stock_assessments.html. The next benchmark assessment is expected in 2021.

Spawning stock biomass has been largely stable in the past 5 years (Figure J.1), at historically low levels (around 21% of unfished biomass). Despite this, the stock is currently considered to be not overfished, and overfishing is not likely to be occurring. However, the stock is near fully exploited. In recent years, recruitment has been variable around historical mean levels (Figure J.2).

Yellowfin tuna: The 2020 benchmark stock assessment for yellowfin tuna was composed of 48 models (SAC-11-07 [https://www.iattc.org/Meetings/Meetings2020/SAC-11/Docs/English/SAC-11-07-MTG Yellowfin%20tuna%20benchmark%20assessment%202019.pdf](https://www.iattc.org/Meetings/Meetings2020/SAC-11/Docs/English/SAC-11-07-MTG%20Yellowfin%20tuna%20benchmark%20assessment%202019.pdf)). All models were used to produce management advice by combining them using relative weights determined based on several criteria, including performance on model diagnostics. The multimodel inference was based on the weighted average of the estimates and the 95% confidence intervals were computed using a normal approximation for each model, combined in a mixture of normal distributions with the mixing ratios equal to the model weights and finding the values for each year where the cumulative distribution function was equal to 0.025 and 0.975 for the lower and upper boundaries of the confidence interval. The spawning stock biomass index represents total fecundity, and estimates of recruitment were also derived from the suite of assessment models. A key uncertainty that will be addressed in the future is the spatial structure of the stock of yellowfin tuna in the Eastern Pacific Ocean. This information was provided by Carolina Minte-Vera (IATTC) via IATTC-95-05.

Spawning stock biomass has declined since the early 2000s (Figure J.1). Based on estimates from the suite of models, there is a low probability that yellowfin tuna are overfished, or experiencing overfishing. Recruitment was mostly average or below average until 2014, before increasing in the last several years (Figure J.2). However, these recent estimates are highly uncertain.

Bigeye tuna: These indices show modeled spawning stock biomass and recruitment of bigeye tuna from the 2020 stock assessment report, which was completed through the Inter-American Tropical Tuna Commission (IATTC), using Stock Synthesis V3. The assessment assumes that there is one stock of bigeye in the eastern Pacific. The reference models for the 2020 benchmark assessment of bigeye were built based on three overarching hypotheses. The first deals with the cause of an apparent recruitment shift which coincides with the expansion of the floating-object fishery, and whether this shift is real, or an artefact of model misspecification. The second hypothesis examines the causes of the recruitment shift, assuming it is due to model misspecification. The third hypothesis deals with the steepness of the Beverton-Holt stock-recruitment relationship. In total, 44 reference models were retained in the benchmark assessment. These reference models on which the management advice is

based were combined using relative weights determined by several criteria, including performance on model diagnostics. These models fell into two groups: one representing a more optimistic situation, and one a more pessimistic situation. Estimates from the two groups of models are included here. The 95% confidence intervals were computed using a normal approximation for each model, combined in a mixture of normal distributions with the mixing ratios equal to the model weights and finding the values for each year where the cumulative distribution function was equal to 0.025 and 0.975 for the lower and upper boundaries of the confidence interval. This information was provided by Haikun Xu and Carolina Minte-Vera (IATTC) via IATTC-95-05.

The results from the 44 reference models for bigeye show that the recruitment shift is apparent in some but not all models (Figure J.2). All models show a decreasing trend in spawning biomass (Figure J.1) but the scale of the decrease varies dramatically among models. The results from the 44 reference models were combined in a risk analysis framework to provide management advice. The combined risk curves show that (1) probabilities of fishing mortality during 2017-2019 being higher than the target and limit reference levels are 50% and 5%, respectively; and (2) the probabilities of spawning biomass at the beginning of 2020 being lower than the target and limit reference levels are 53% and 6%, respectively. The models fell into two groups: one more pessimistic, and one more optimistic. This bimodality complicates the evaluation of the status of the bigeye stock and of the potential outcomes of management actions, and needs to be addressed to improve management advice.

Skipjack tuna: Skipjack tuna are assumed to be one stock in the Pacific Ocean. In the eastern Pacific, they are fished with purse seine gear, primarily in the tropics. Skipjack are difficult to assess with standard stock assessment methods, due to high and variable productivity, and uncertainties in natural mortality and growth. They are thus assessed using a simple model that generates indicators of biomass, recruitment and exploitation rate, and compares these to historically observed values (Maunder and Deriso 2007). The stock assessment is completed by IATTC. The relative biomass index shown is from the 2017 update assessment. Indices were provided by Mark Maunder (IATTC).

Biomass and recruitment indices have been increasing since the mid-2000s, and appear to have been above average in the most recent assessed years (Figure J.1, Figure J.2). While no traditional reference points are available for skipjack in the North Pacific, results suggest that the stock is likely not overfished, and overfishing is likely not occurring. The skipjack fishery in the eastern Pacific is constrained by effort restrictions implemented for the conservation of bigeye tuna. Biological data suggest that abundance of larval skipjack tends to increase with water temperature, at least up to ~29°C. However, catches of adults by surface gears tend to be reduced during warmer periods (such as El Niño), as fish spend less time near the surface, possibly due to deepening thermoclines. Environmental variability may therefore influence stock productivity and availability to fisheries.

Appendix K CALIFORNIA SEA LION PUP INDICATORS

California sea lion pup counts and pup growth rates are sensitive indicators of prey availability and composition in the central and southern CCE (Section 4.6). In September 2020, the SSC Ecosystem Subcommittee (SSC-ES) made three requests: (1) that we more precisely describe what we feel these indicators represent about prey community dynamics and foraging conditions; (2) that we provide text in the Supplement that demonstrates that California sea lion population size and carrying capacity are not affecting the value of these metrics as indicators of foraging conditions; and (3) a model-based estimate of total pups. Below, we address the first two requests. Due to time constraints, we have not addressed the third request but will do so in future reports.

Pup count and pup growth as indicators of foraging conditions: The San Miguel Island California sea lion indicators of pup births, pup condition, pup growth and nursing female diet are linked to the availability (a combination of abundance and distribution) and composition of the coastal pelagic

forage community to nursing California sea lions foraging in the CCE from the northern California Channel Islands to Monterey Bay throughout the year. Nursing California sea lions are central place foragers for 11 months of the year, traveling to and from the breeding colonies in the Channel Islands, where their pups reside, to foraging areas within 200 km of the colonies. Consequently, they are sampling the coastal pelagic forage community throughout the year and their diet and resultant reproductive success measured by pup metrics depends on the availability of that forage community.

Nursing California sea lions consume a variety of fish and cephalopods but have a core diet of only seven taxa: Pacific hake, Pacific sardine, northern anchovy, rockfish, jack mackerel, Pacific mackerel, and market squid (Melin et al. 2008, Melin et al. 2012a). These taxa vary annually and seasonally in the diet. The nursing female diet index is based on the frequency of occurrence of these seven core taxa in scats collected at the San Miguel colony during the early lactation period (June-September). This index provides a relative measure of the availability of each prey taxa to nursing females within their foraging range because California sea lions consume prey relative to its abundance in the environment (Thompson et al. 2019a) but not necessarily proportionally. For example, an increase in the frequency of occurrence of anchovy from 5% in 1995 diets to 90% in 1996 diets means that almost no females consumed anchovy in 1995 because it was not available to them but almost all females consumed it in 1996; it does not necessarily mean that the biomass of anchovy increased nearly 20-fold in the CCE, just that the availability increased in the foraging range of nursing females. Nonetheless, it indicates that a change in the forage community occurred between the two years. A weakness of this index is that it only indicates presence or absence of a taxa in the diet; when sardine occurs in high frequency, it could be that sea lions are exploiting a small population of fish or it could be that sardine are ubiquitous in the environment. It also is a retrospective rather than forecasting index. It is thus important to view this as part of a suite of indicators about the prey community, along with ship-based catch or acoustic estimates of forage fish biomass. Strengths of the sea lion diet index are that it is easy to update annually and the core taxa comprise the core diet of many other top predators in the CCE that are difficult to sample or observe. Consequently, the annual variability and trends in the California sea lion diet can inform us on unusual patterns in the coastal pelagic forage community that may affect other top predators in the CCE.

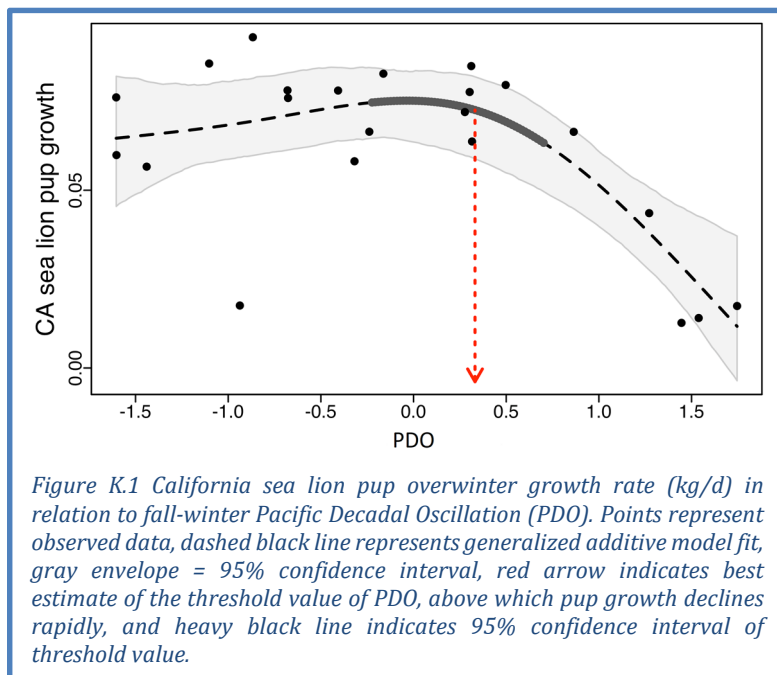
Each of the pup indices in the report represents a different aspect of reproductive success that relies on successful foraging by reproductive females. As such, they are indirect qualitative measures of the forage available to reproductive females and do not provide specific forage community information. The annual number of pup births is an index of successful pregnancies, which are dependent on the nutritional condition of the female, which in turn, is dependent on the quality and quantity of prey available during the gestation period. Higher numbers of pup births indicates that females consumed a diet that provided sufficient quantity and nutrition to support the energetic cost of gestation. Pup condition and growth are dependent on milk intake. The more milk consumed the greater the better condition and growth rate. The amount of food consumed by a female on a foraging trip determines the amount of milk she has to deliver to the pup when she returns. Better pup condition and higher growth rates indicate abundant prey for nursing females during the lactation period.

Declines in pup births and pup growth have been associated with environmental events that reduced marine productivity at all trophic levels in the CCE for prolonged periods supporting the link between these indices and the status of the forage community (DeLong et al. 1991, Iverson et al. 1991, Melin et al. 2010, Melin et al. 2012b, DeLong et al. 2017). Other factors such as diseases (e.g., hookworm, Lyons et al. 2005), immune suppression from pollution (DeLong et al. 1973, Gilmartin et al. 1976) and natural environmental toxins (Goldstein et al. 2009) may affect pup growth or births, but these factors are likely to have less of a population level effect than large-scale food supply issues that accompany anomalous oceanographic conditions.

The influence of population abundance and carrying capacity on these indicators: In discussions

related to past reports, some Council advisory bodies expressed concerns that sea lion pup counts and growth may become less effective indicators when the population is close to carrying capacity, which it was in the 2010s: according to population modeling work by Laake et al. (2018), the San Miguel colony at that time had an estimated carrying capacity of ~275,000 animals (including pups), and annual population estimates between 2006 and 2014 ranged from 242,000 to 306,000 animals. Advisory bodies were concerned that changes in pup count or growth could be due to density dependent mechanisms within the sea lion population, rather than to changes in the prey community.

A linear mixed effects model of California sea lion pup growth that includes environmental variables, sea lion abundance, fish abundance and nursing female diet revealed that the abundance of California sea lions was not a significant factor in annual variability of pup growth rates (Melin et al. in preparation). The model also did not detect a declining trend in pup growth as the population size increased, which might occur if competition among nursing females for limited forage was affecting the ability of females to support the energetic demands of their pups. Elevated SST explained the greatest amount of variability for pup growth rates in the models: a 1°C increase in SST resulted in a 7% decline in the population growth rate, even when the population was much smaller (<100,000 animals) in the 1980s (Laake et al. 2018). The reverse effect was not apparent when SST decreased by 1°C. These analyses indicate that pup count and pup growth are not compromised as indicators by population size, but rather reflect the dynamic relationship between environmental conditions and California sea lion reproduction. We believe the key underlying mechanism is that elevated SST affects the distribution and abundance of the sea lion prey community thereby reducing access to food for nursing females, such that they cannot support the energetic demands of pregnancy, resulting in fewer births, or lactation, resulting in slower pup growth.



A related statistical analysis adds further weight to this conclusion. We are using a model selection approach (from Samhoury et al. 2017) to identify the presence of nonlinear and threshold dynamics in pressure-response relationships in the CCE, with a focus on the response of key species and processes to basin- and regional-scale climate variables. We used a generalized additive model (GAM) to assess California sea lion pup growth as a function of PDO, which is an index of SST in the Northeast Pacific. Pup growth was greatest when the PDO index was negative, indicative of cold phase, while growth estimates quickly declined as the PDO index became positive

(indicative of warm phase) and increased beyond a threshold value of ~0.4 (Figure K.1). The same approach also found a negative relationship between pup growth and coastal SST in the southern and central regions of the CCE. The PDO from August 2020 to early winter of 2021 has been negative (i.e., well to the left of the threshold PDO value in Figure K.1), which is consistent with average or potentially above-average growth conditions for the 2020 cohort of pups at San Miguel Island.

Appendix L SEABIRD PRODUCTIVITY, MORTALITY, AND DIET

L.1 SEABIRD PRODUCTIVITY

Seabird population productivity, as measured through variables related to reproductive success, tracks marine environmental conditions and often reflects forage production near breeding colonies. We monitor and report on standardized anomalies of fledgling production per pair of breeding adults for five focal species on Southeast Farallon Island (SEFI) in the central region of the CCE, and three species at Yaquina Head, Oregon in the northern CCE. Collectively, the six focal species span a range of feeding habits and ways of provisioning their chicks:

- Brandt’s cormorants forage primarily on pelagic and benthic fishes in waters over the shelf, generally within 20 km of breeding colonies, returning to the colony during the day to deliver regurgitated fish to their chicks.
- Cassin’s auklets forage primarily on zooplankton over the shelf break, generally within 30 km of colonies; they forage by day and night and return to the colony at night to feed chicks.
- Common murres forage primarily on pelagic fishes in deeper waters over the shelf and near the shelf break, generally within 80 km of colonies, returning to the colony during daylight hours to deliver single whole fish to their chicks.
- Pelagic cormorants forage primarily on pelagic and benthic fishes in waters over the shelf, generally within 20 km of breeding colonies, returning to the colony during the day to deliver regurgitated fish to their chicks.
- Pigeon guillemots forage primarily on small benthic and pelagic fishes over the shelf, generally within 10 km of colonies, returning to the colony during the day to deliver single fish to chicks.
- Rhinoceros auklets forage primarily on pelagic fishes in shallow waters over the continental shelf, generally within 50 km of colonies, returning to the colony after dusk to deliver multiple whole fish to their chicks.

Data and interpretation for fledgling production of the five species at SEFI are in the main body of the report in Section 4.7. In brief, production at SEFI was mixed in 2020, with above-average production for Brandt’s cormorants and Cassin’s auklets, near-average production for pigeon guillemots and rhinoceros auklets, and below-average production for common murres.

At Yaquina Head, Fledgling production in 2020 was mixed for the three monitored seabirds (Figure L.1.1). Brandt’s cormorant production was above average, but disturbances from bald eagles were observed during incubation, which was new for this species at this location and may have brought chick production down from the higher values of the last two years. Common murres experienced extremely low productivity in 2020, following two years of relatively high production. This was due primarily to bald eagle predation on adult

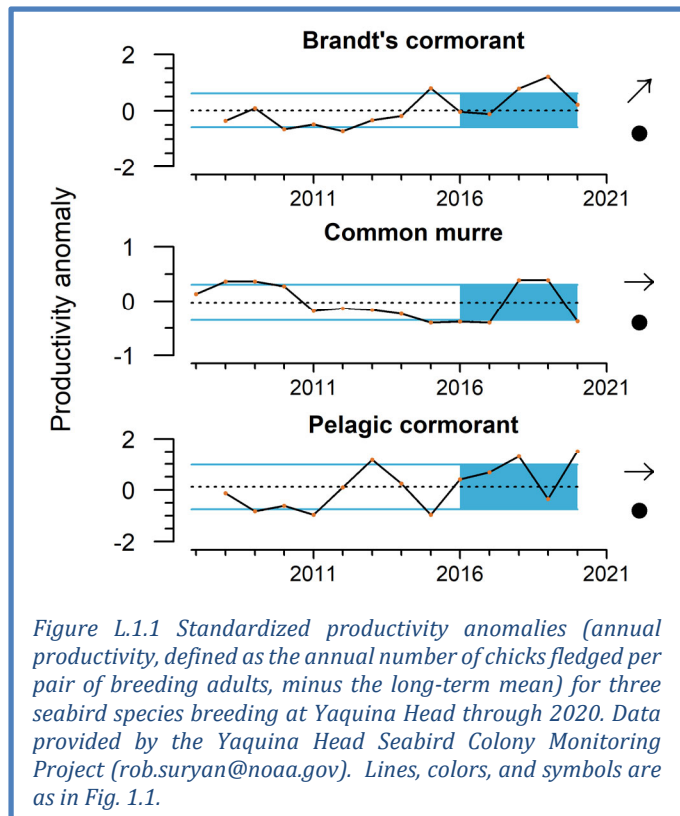


Figure L.1.1 Standardized productivity anomalies (annual productivity, defined as the annual number of chicks fledged per pair of breeding adults, minus the long-term mean) for three seabird species breeding at Yaquina Head through 2020. Data provided by the Yaquina Head Seabird Colony Monitoring Project (rob.suryan@noaa.gov). Lines, colors, and symbols are as in Fig. 1.1.

murre, high levels of colony disturbance, and the greatest egg depredation rates observed at this site. In 2020, 15 eagles were observed simultaneously at Yaquina Head, the largest aggregation of eagles documented over the disturbance study period. Pelagic cormorant production at Yaquina Head in 2020 was the highest recorded at this site.

L.2 SEABIRD AT-SEA DENSITIES

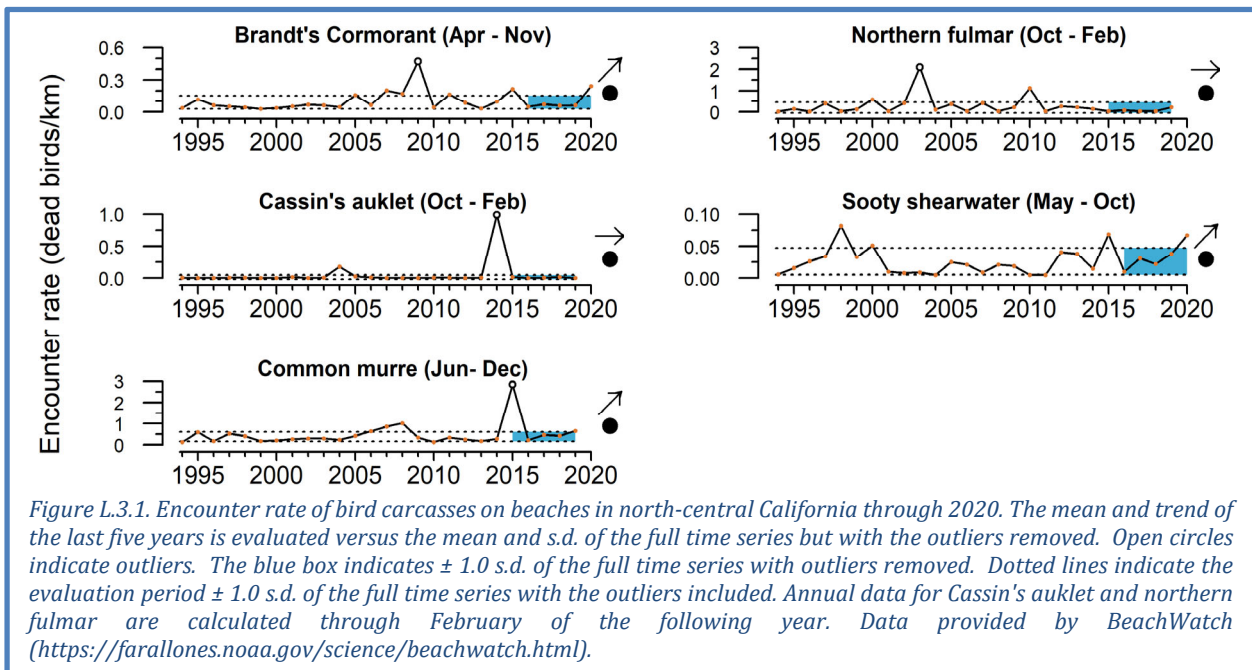
Seabird densities on the water during the breeding season can track marine environmental conditions and may reflect regional production and availability of forage. Data from this indicator type can establish habitat use and may be used to detect and track seabird population movements or increases/declines as they relate to ecosystem change. Due to COVID-19-related impacts on spring surveys, these data were not collected in 2020, and no plots are shown here.

L.3 SEABIRD MORTALITY

Monitoring of dead beached birds provides information on the health of seabird populations, ecosystem health, and unusual mortality events. CCIEA reports from the anomalously warm and unproductive years of 2014–2016 noted major seabird mortality events in each year. In 2020, seabird mortality monitoring effort by citizen scientists was greatly decreased due to the COVID-19 pandemic (details below). Despite this, we feel some confidence in the qualitative patterns described below, because these citizen science networks tend to be aware of and responsive to unusual mortality events, and we have reason to believe that major wrecks would have been detected and that accounts would have been circulated via social or traditional media.

In past reports we have included seabird mortality observations from the University of Washington-led Coastal Observation And Seabird Survey Team (COASST), which documents beach counts in the northern CCE (Washington to northern California). We do not have COASST data to present this year, but according to information provided on their website (<https://coasst.org/>), there were no observations of unusual mortality events among our focal species in 2020.

In the Central CCE (Bodega Bay, California, to Point Año Nuevo, California), the BeachWatch program observed no unusual mortality events among our focal species in 2020 (Figure L.3.1). The Brandt's



cormorant encounter rate was >1 s.d. above average in 2020, but not high enough to be regarded as an unusual event. The Cassin’s auklet encounter rate continued at low baseline levels in the 2018–19 winter (the most available data). The common murre encounter rate was above average in 2019, which continues an increasing recent trend; however, common murre encounter rates remain well below the peak from the wreck in 2015. The northern fulmar encounter rate was average in the 2018–19 winter (the most recent available data). The sooty shearwater encounter rate was >1 s.d. above average in 2020 and has a positive short-term trend, but the encounter rates in 2020 did not constitute a wreck. Due to COVID-19 effects, survey effort in 2020 was roughly 30% of a typical year.

The BeachCOMBERS program conducts surveys of beached seabirds on south-central California beaches from Point Año Nuevo to Malibu, and we have previously reported on two survey regions: North (Point Año Nuevo to Lopez Point, California) and Central (Lopez Point to Rocky Point, California). BeachCOMBERS data have not been made available since our report last year, and are not shown here. After a program transition, data from 2020 will be available; however, due to COVID-19 restrictions, data collection was curtailed from April through August of 2020.

L.4 SEABIRD DIETS

Seabird diet composition during the breeding season tracks marine environmental conditions and often reflects production and availability of forage within regions. Here, we present some seabird diet data that may shed light on foraging conditions along the west coast in 2020. We are working with partner research organizations to better integrate this information into our reporting.

In the northern CCE, seabird diet observations were collected at Yaquina Head, Oregon, despite bald eagle disturbances and low common murre productivity. The proportion of osmerids (smelts) in the diet of common murre provisioning chicks at Yaquina Head was average in

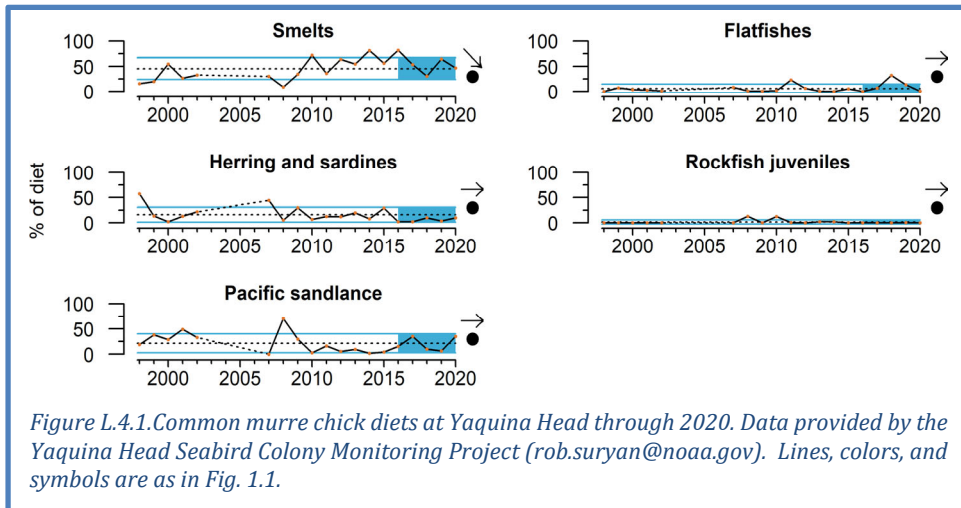


Figure L.4.1. Common murre chick diets at Yaquina Head through 2020. Data provided by the Yaquina Head Seabird Colony Monitoring Project (rob.suryan@noaa.gov). Lines, colors, and symbols are as in Fig. 1.1.

2020, down from 2019, and is showing a short-term decline (Figure L.4.1). The proportion of herring and sardine remained below average, as it has been since 2015. The proportion of Pacific sand lance was above average in 2020, second only to smelts. The proportion of flatfishes was below average, down from a peak in 2018, and the proportion of rockfishes was below average in 2020 for the sixth straight year, and has been close to zero since 2011. The other monitored colony in the northern CCE, the rhinoceros auklet colony on Destruction Island, WA, was not sampled in 2020 due to COVID-19.

At colonies off central California, there are diet trends available for seabirds from Southeast Farallon Island (SEFI), close to the region of the most intense upwelling in the CCE and thus a valuable source of information about ecosystem productivity and prey availability to higher trophic levels. Among piscivores, there has been increasing reliance on anchovy and decreasing reliance on juvenile rockfish over the past five years. The proportions of anchovy in the diets of Brandt’s cormorants and rhinoceros auklets provisioning chicks on SEFI were above average in 2020 and showed significant positive short-term trends, while the proportions of juvenile rockfish in these species’ diets have

shown significant negative short-term trends, although the presence of rockfish was close to average for rhinoceros auklets in 2020 (Figure L.4.2). The anchovy proportion was the highest ever recorded for Brandt's cormorants and the fourth highest recorded for rhinoceros auklets at this location. For common murres, the proportions of anchovy were above average and proportions of rockfish and Pacific salmon were below average in 2020. Pigeon guillemots in 2020 had a below-average amount of rockfish in the diet. Juvenile rockfish did increase in diets of rhinoceros auklets, common murres and pigeon guillemots in 2020 relative to 2019 (Figure L.4.2, right). For Cassin's auklets, which feed heavily on krill, the proportion of the krill species *Euphausia pacifica* in the diet was below average in 2020, while the proportion of the krill species *Thysanoessa spinifera* in the diet was just above average and showed a sharp increase from 2019 (Figure L.4.2, bottom).

At Año Nuevo Island, the size of anchovy returned to rhinoceros auklet chicks in 2020 was slightly above the long-term average and has increased since 2014-2016 (Figure L.4.3). Researchers again expressed concern that, despite anchovy being abundant in the region, individual anchovy may be too large to be ingested by rhinoceros auklet chicks, which may have contributed to the below-average fledging production of these and other birds in central California in 2020 (e.g., Figure 4.7.1). This may speak to the benefit of a more diverse diet that includes prey of different sizes.

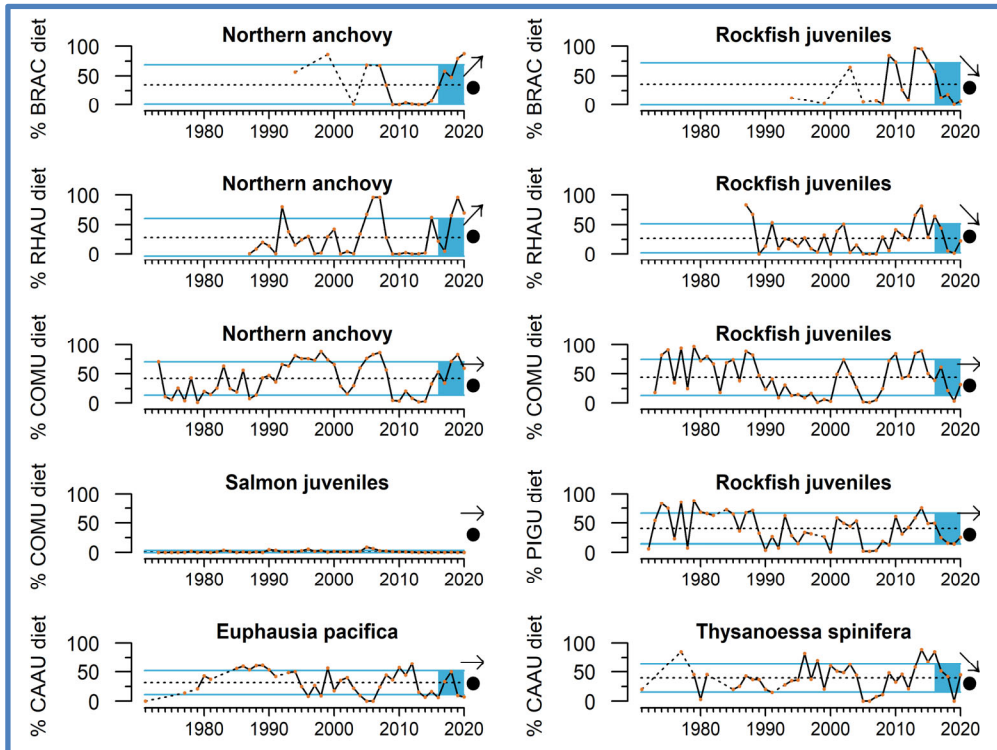


Figure L.4.2. Southeast Farallon Island seabird diets through 2020. BRAC = Brandt's cormorant; CAAU = Cassin's auklet; COMU = common murre; PIGU = pigeon guillemot; RHAU = rhinoceros auklet. Data provided by Point Blue Conservation Science (jjahncke@pointblue.org). Lines, colors, and symbols are as in Fig. 1.1.

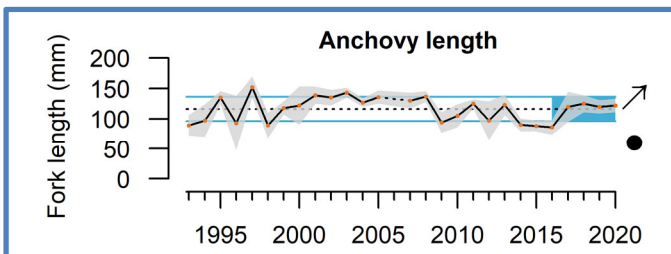


Figure L.4.3. Fork length of anchovy brought to rhinoceros auklet chicks at Año Nuevo from 1993-2020. Error envelope shows ± 1.0 s.d. Data provided by Oikonos/Point Blue (ryan@oikonos.org). Lines, colors, and symbols are as in Fig. 1.1.

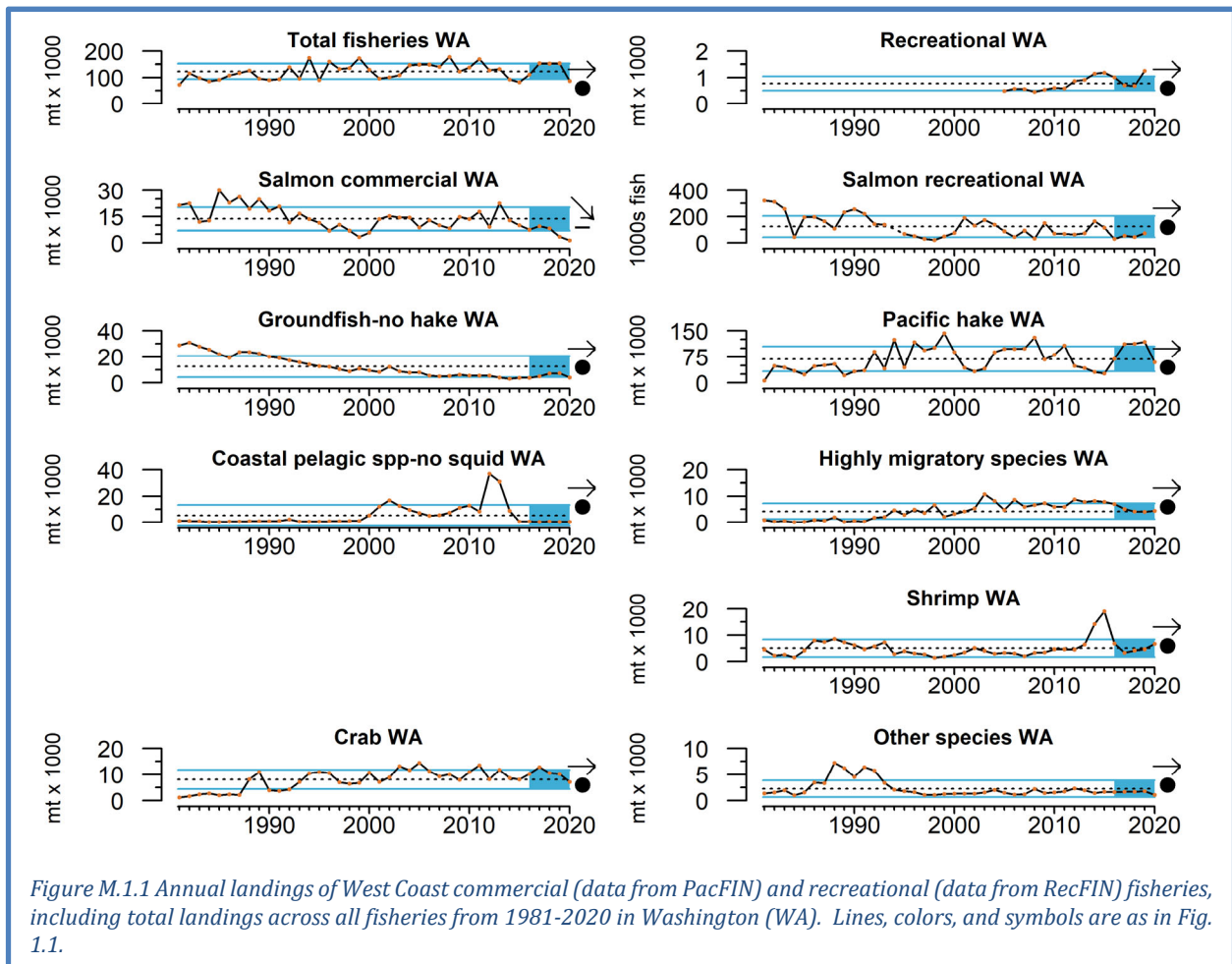
Appendix M STATE-BY-STATE FISHERY LANDINGS AND REVENUES

The Council and the EWG have requested information on state-by-state landings and revenues from fisheries; these values are presented here. Data for landings and revenue were nearly complete for all states through 2020 at the March 2021 Briefing Book deadline. Fishery landings and revenue data are best summarized by the Pacific Fisheries Information Network (PacFIN, <http://pacfin.psmfc.org>) for commercial landings and by the Recreational Fisheries Information Network (RecFIN, <http://www.recfin.org>) for recreational landings. Landings provide the best long-term indicator of fisheries removals. Revenue was calculated based on consumer price indices for 2020.

M.1 STATE-BY-STATE LANDINGS

Commercial fisheries landings in Washington are >90% complete through the end of 2020. Total landings varied by ~1 s.d. around the long-term average from 2016 to 2020, with particularly low landings in 2020 (Figure M.1.1). These patterns were driven primarily by changes in Pacific hake landings over the last five years: for example, 86% of the decrease in total landings in 2020 was due to decreases in Pacific hake landings. Outbreaks of COVID-19 on some Pacific hake vessels may have made it difficult to harvest the available quota (NMFS 2021). Commercial landings of all other individual fisheries showed no trends and were within ± 1 s.d. of long-term averages from 2016 to 2020, with the exception of commercial salmon landings, which decreased and were >1 s.d. below the long-term average over the last five years.

Total landings of recreational catch (excluding salmon and halibut) in Washington state were average



to above-average from 2016 to 2019 (Figure M.1.1). Recreational landings data for Washington in 2020 are only complete through October 2020, and lack HMS data. Available data show average decreases of 44% in 2020 compared to 2019 for the top ten recreational species. Disruptions to recreational charter boat activity and access to boat launches due to COVID-19 restrictions were likely responsible for some of the decrease in 2020. Although HMS landings data for WA were not complete at the time of this report, the assumption of a decrease is consistent with several lines of evidence. First, total recreational landings in Washington and Oregon are highly correlated over time ($R^2=0.70$), and total recreational landings in OR decreased by 45% in 2020. Second, HMS landings make up 33% and 40% of total recreational landings in OR and WA, respectively, and HMS landings, particularly albacore, decreased by 95% in Oregon in 2020. Ocean conditions off Oregon in 2020 were such that most albacore were too far offshore (>100 miles) and limitations on overnight trips due to COVID restrictions limited access to albacore for most recreational anglers in Oregon; these conditions may also have existed for Washington recreational anglers. Recreational landings of salmon (Chinook and coho) were within ± 1 s.d. of the long-term average from 2016 to 2019 (2020 data were not available at time of this report).

Total fisheries landings in Oregon were consistently >1 s.d. above long-term time series averages from 2016 to 2020 (Figure M.1.2; 2020 commercial data >90% complete through the end of 2020). These patterns were primarily driven by landings of Pacific hake, which were consistently >1 s.d. above the long-term average for the last five years, including 2020. Commercial landings of all other individual fisheries showed no trends and were within ± 1 s.d. of long-term averages from 2016 to 2020, with the exception of market squid, which have increased ~270% over the last five years.

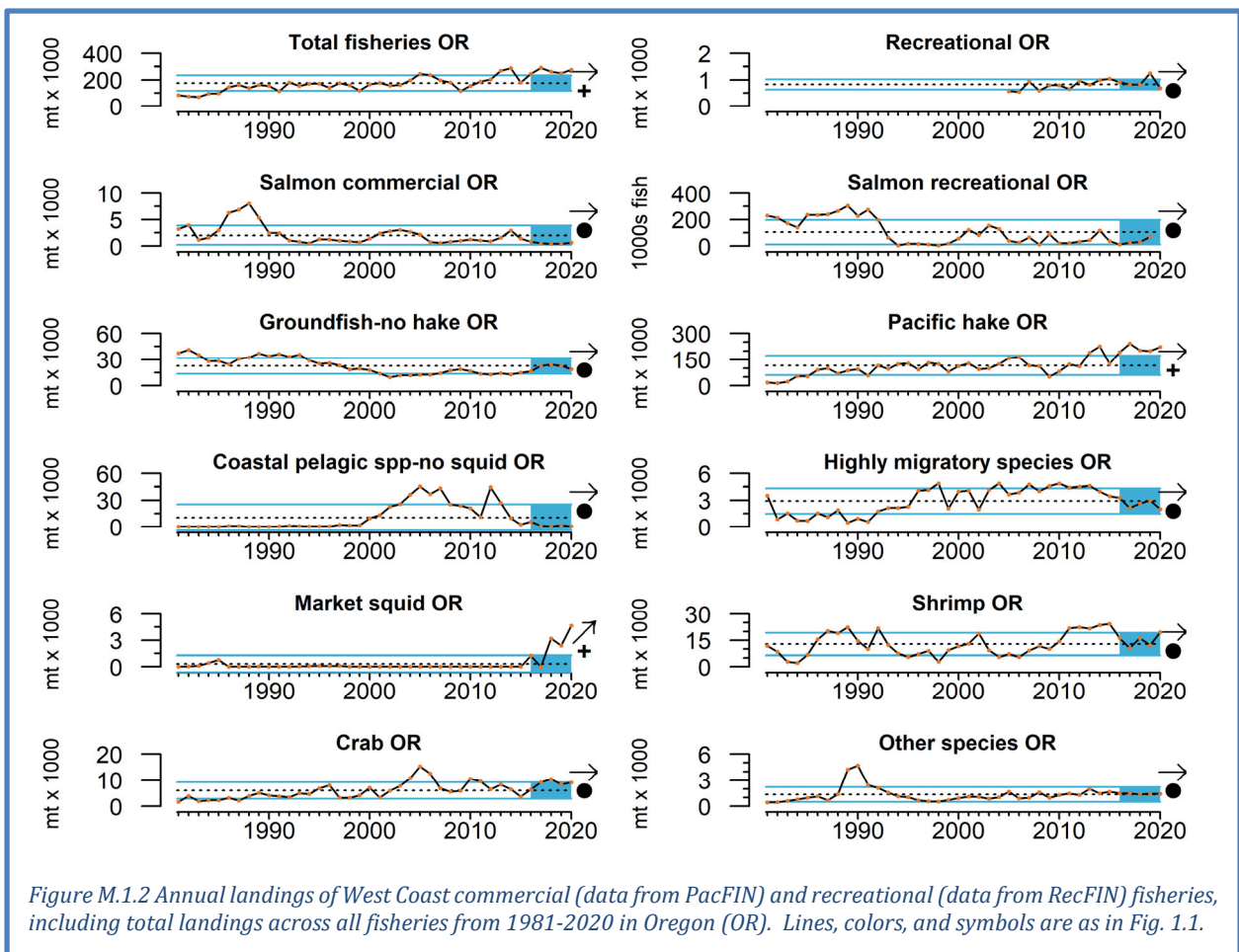


Figure M.1.2 Annual landings of West Coast commercial (data from PacFIN) and recreational (data from RecFIN) fisheries, including total landings across all fisheries from 1981-2020 in Oregon (OR). Lines, colors, and symbols are as in Fig. 1.1.

Recreational fisheries landings (excluding salmon and Pacific halibut) in Oregon for 2020 are >90% complete through November. Landings have been within ± 1 s.d. of time series long-term averages from 2016 to 2020 (Figure M.1.2). However, recreational landings decreased 45% in 2020 relative to 2019, driven primarily by changes in albacore landings. In 2019, Oregon logged the largest catches and most angler trips on record for albacore. In 2020, recreational anglers in Oregon had reduced access to albacore due to COVID-related limitations on overnight trips, as well as ocean conditions, which kept most albacore far offshore (>100 miles). Salmon recreational landings (Chinook and coho) showed no recent trends and were within ± 1 s.d. of the time series long-term average since 2016 (2020 data were not available at time of report).

Total fisheries landings in California were relatively unchanged, but were >1 s.d. below the long-term time series average from 2016 to 2020, primarily due to low levels of CPS finfish landings and recent decreases in landings of crab, market squid and other species (Figure M.1.3; commercial data >90% complete through the end of 2020). There were no significant trends observed for any individual fishery, but commercial landings of CPS finfish and other species were >1 s.d. below long-term averages, while landings of groundfish (excluding hake) and HMS over the last five years were near the lowest recorded levels of their time series.

Recreational landings (excluding salmon and Pacific halibut) and salmon recreational landings in California were near long-term averages from 2015-2019 (Figure M.1.3). Data for 2020 recreational landings in California are not reported because recreational HMS and salmon landings data were not available at the time this report was compiled.

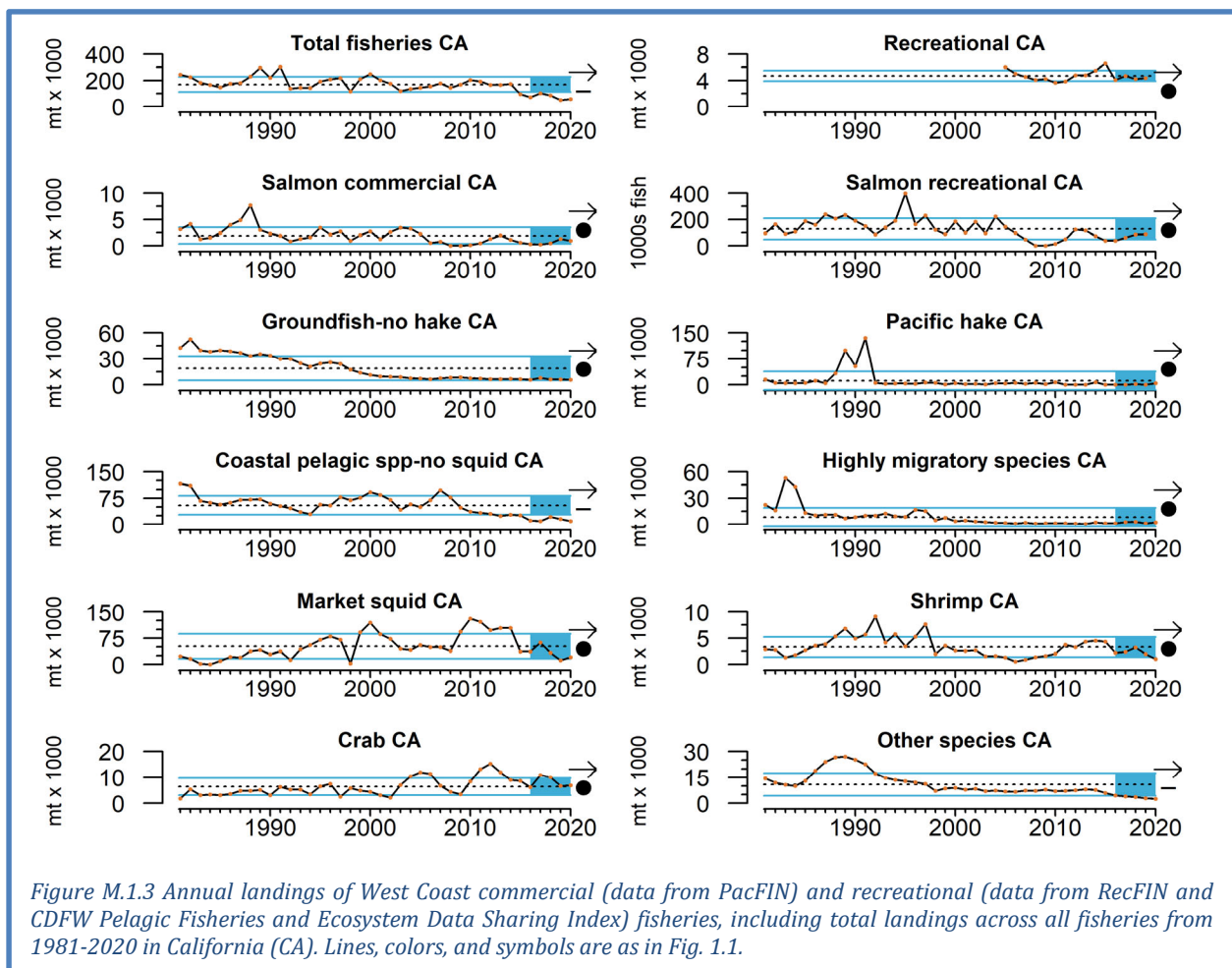
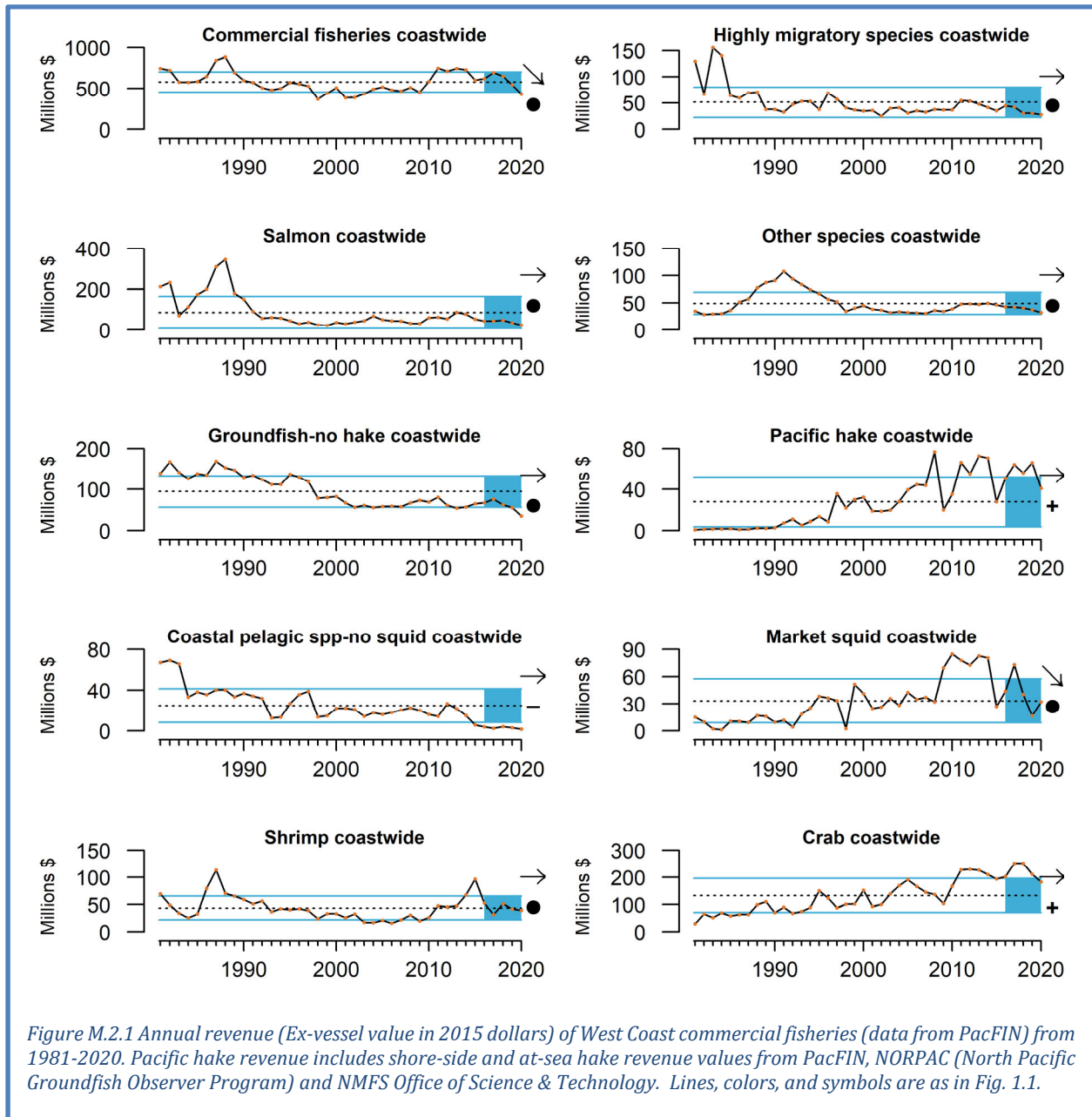


Figure M.1.3 Annual landings of West Coast commercial (data from PacFIN) and recreational (data from RecFIN and CDFW Pelagic Fisheries and Ecosystem Data Sharing Index) fisheries, including total landings across all fisheries from 1981-2020 in California (CA). Lines, colors, and symbols are as in Fig. 1.1.

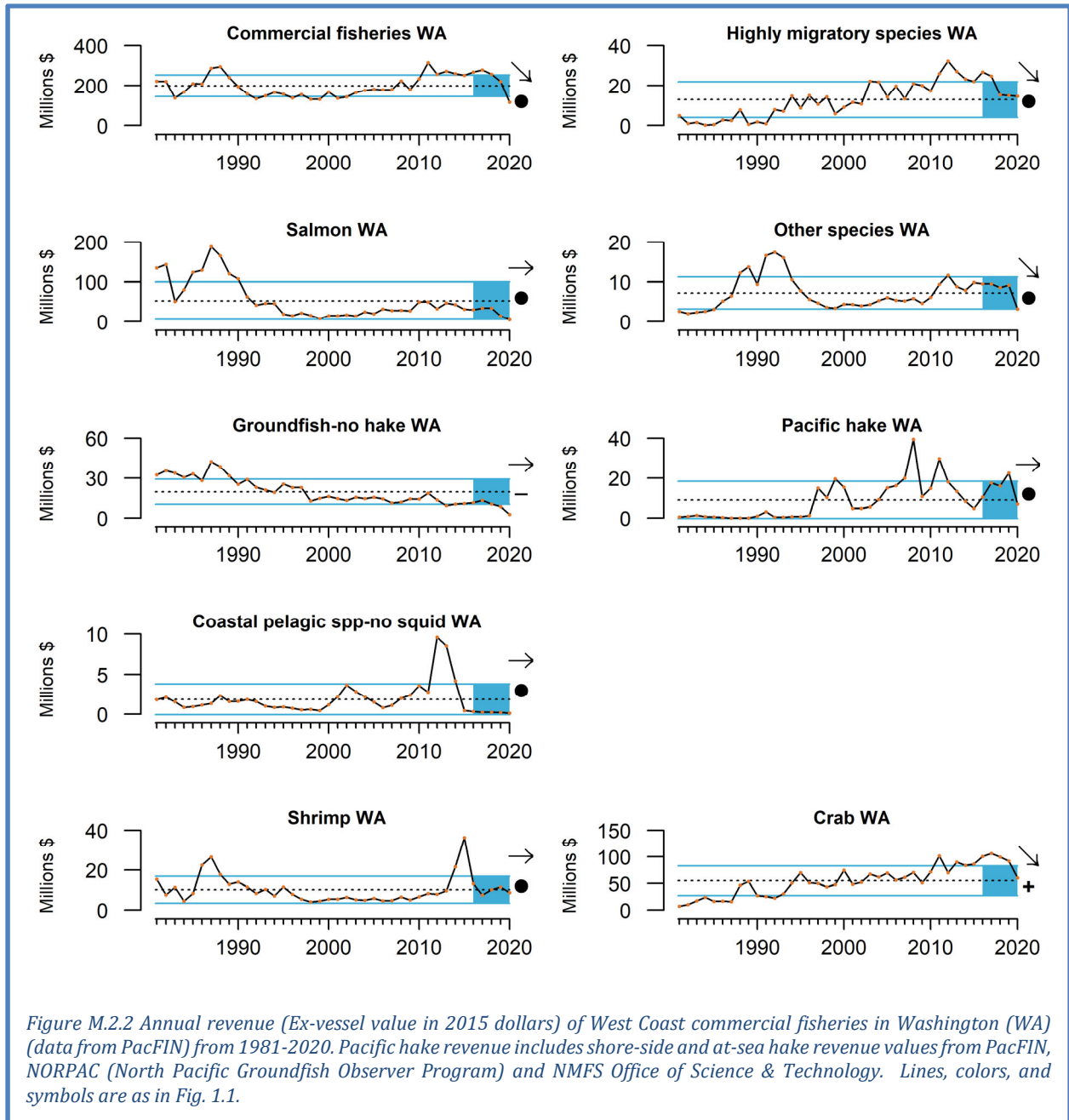
M.2 COMMERCIAL FISHERY REVENUES

Total revenue across U.S. West Coast commercial fisheries decreased from 2016 to 2020 and was 23% lower in 2020 than in 2019, based on data currently available (Figure M.2.1). This pattern was driven primarily by recent decreases in revenue from crab, Pacific hake and groundfish (excluding hake) fisheries. Ocean conditions, wildfires, compressed Dungeness crab fishing seasons, and COVID-related effects on supply and demand all likely contributed to the overall decrease in revenue observed in 2020. Revenue from crab has declined for the last 3 years, although 5-year mean crab revenue was still >1 s.d. above the long-term average. Five-year mean revenue from Pacific hake landings also was >1 s.d. above the long-term average, whereas revenue from CPS finfish was consistently >1 s.d. below long-term averages from 2016 to 2020. Market squid revenue has declined substantially over the past 5 years. Revenues from other individual fisheries showed no recent trends

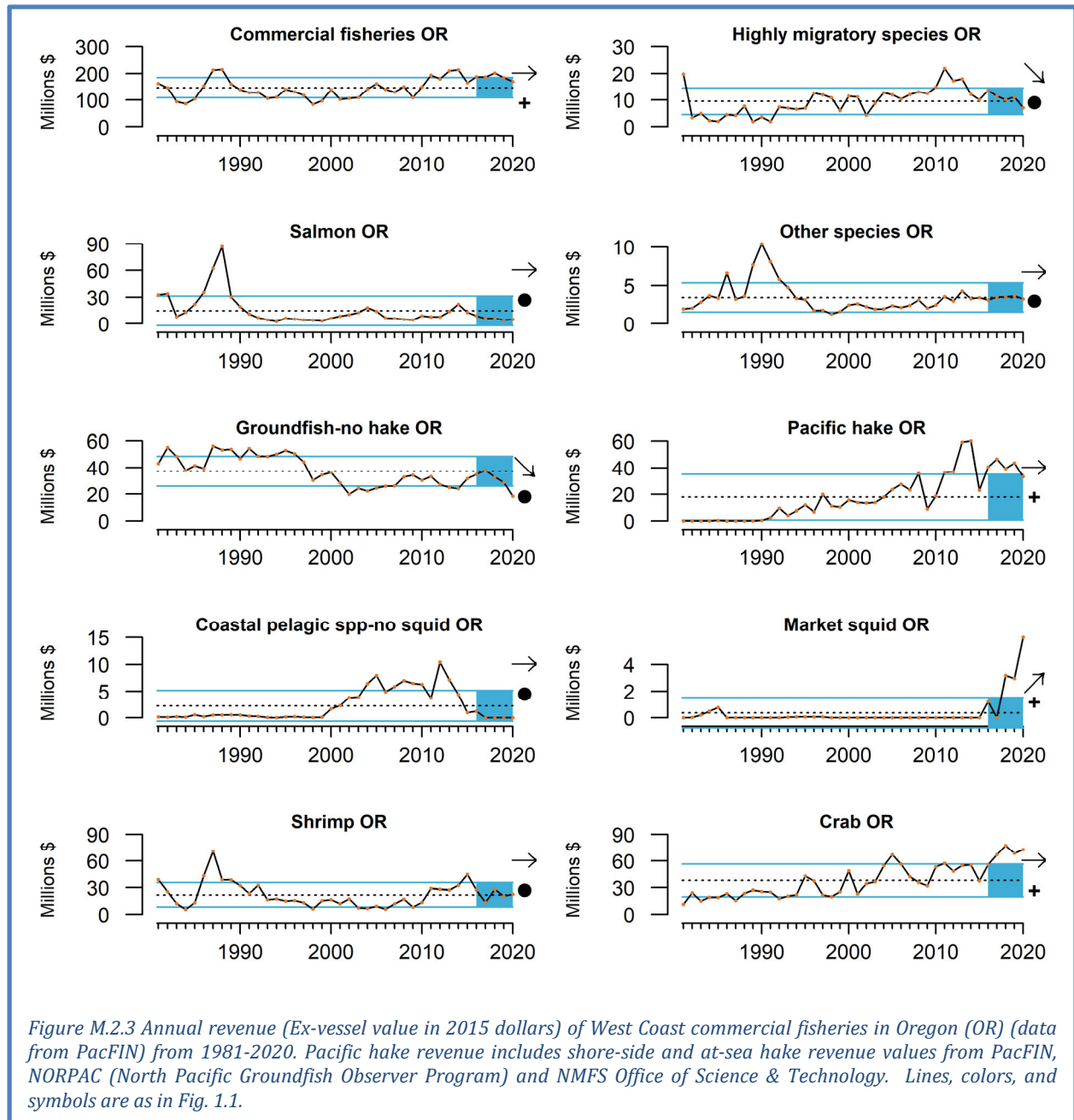


and were within ± 1 s.d. of long-term averages, but revenue from salmon, groundfish (excluding hake), HMS and other species were nearing the lowest levels of their respective time series.

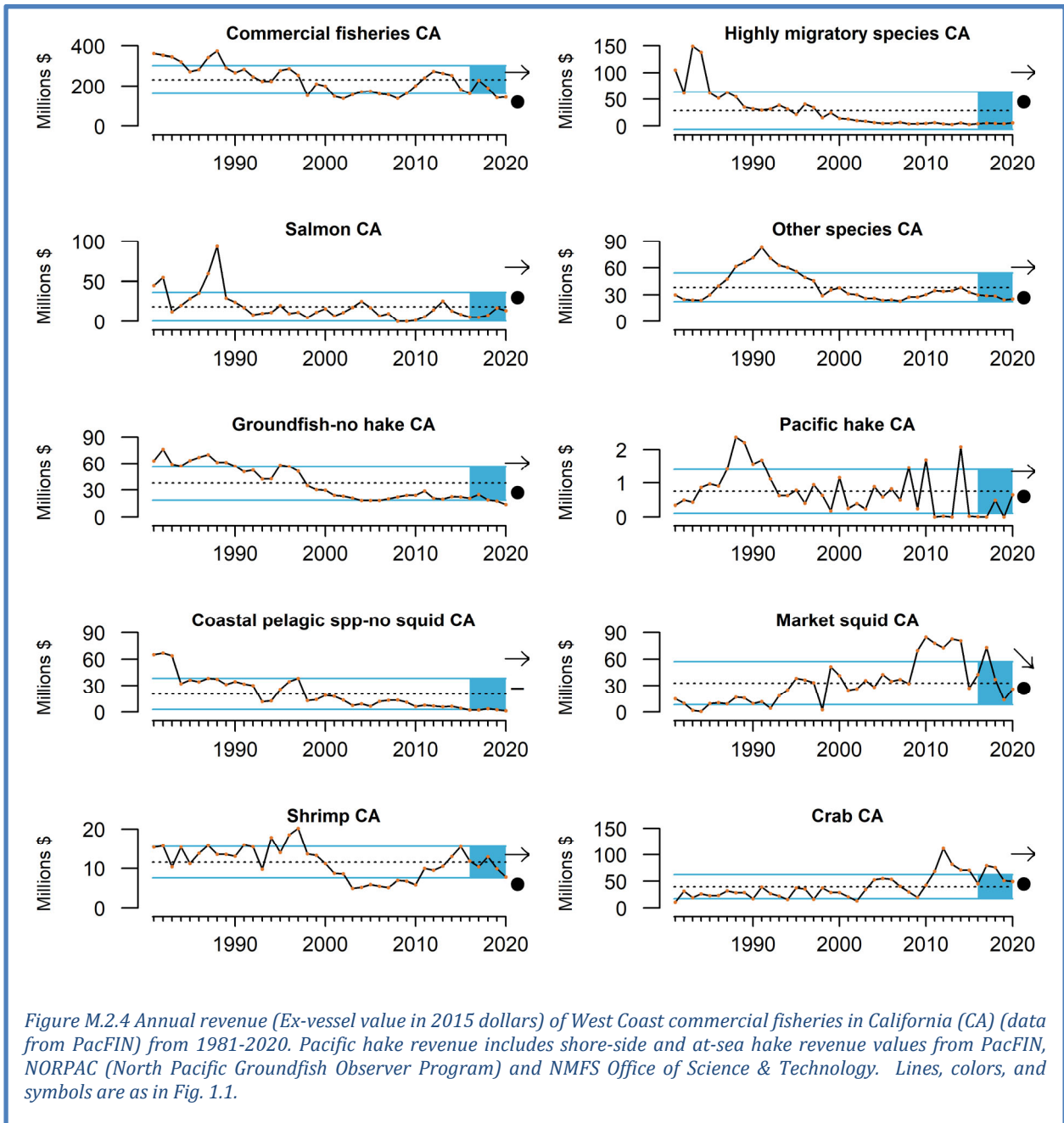
Total revenue across commercial fisheries in Washington decreased from 2016 to 2020, with a 47% drop from 2019 to 2020 based on data available at the time of the report (Figure M.2.2). This pattern was driven by decreases in revenue for nearly every fishery. Revenue from HMS, other species and crab fisheries decreased over the last 5 years, although 5-year mean crab revenue remained >1 s.d. above the long-term average. Revenue from groundfish (excluding hake) fisheries was >1 s.d. below the long-term average. Revenues from all other fisheries showed no trends and were within ± 1 s.d. of long-term averages over the last 5 years, although revenue from CPS finfish was consistently near the lowest level of the time series, as was salmon revenue in 2020.



Total revenue across commercial fisheries in Oregon decreased from 2016 to 2020 (Figure M.2.3). Based on data received to date, revenues in Oregon were down 15% in 2020 relative to 2019, driven by decreases in revenue from groundfish (excluding hake), Pacific hake, and HMS fisheries. Mean revenues for crab, hake and market squid have been >1 s.d. above the time series average for the past 5 years (including in 2020), and revenue from market squid continued to increase in Oregon. Based on current data, groundfish revenue in 2020 was the lowest of the time series for Oregon. All other fisheries showed no recent trends, and recent means were within ± 1 s.d. of long-term revenue averages, although revenue from CPS finfish fisheries was consistently near the lowest levels of the time series.



Total revenue across commercial fisheries in California varied close the lower range of long-term values from 2016–2020, although it increased slightly from 2019 to 2020 (Figure M.2.4). Market squid was the second most lucrative California fishery in 2020, but has decreased over the last 5 years. Revenue from other individual fisheries showed no five-year trends and were within ± 1 s.d. of long-term averages from 2016–2020, with the exception of revenue for CPS finfish, which was >1 s.d. below the long-term average. Revenue from groundfish (excluding hake) in 2020 was the lowest value of the entire time series and revenue from other species fisheries were near the lowest levels of their time series.



Appendix N FISHING GEAR CONTACT WITH SEAFLOOR HABITAT

Here we present updates to our ongoing temporal and spatial representations of the status and trends of federally managed, limited-entry bottom trawl gear contact with the seafloor as a function of distances trawled. These indicators provide complementary data to inform management of specific human activities that affect seafloor habitat. These estimates may also be helpful in evaluating potential tradeoffs with future non-fishing activities along the West Coast, including offshore renewable energy development. Estimates of coastwide distances exposed to federally managed bottom trawl fishing gear from 1999–2019 were calculated based on set and haul-back locations. Data come from logbooks analyzed by NOAA’s West Coast Groundfish Observer Program.

We first present time series of the data at a coastwide scale and broken out by ecoregion (Northern, Central and Southern CCE), substrate (hard, mixed, soft) and depth zone (shelf, upper slope, lower slope). At the scale of the entire coast, bottom trawl gear contact with seafloor habitat remained consistently at historically low levels from 2015–2019 (Figure N.1, top). During this period, the vast majority of bottom trawl gear contact occurred in soft, upper slope and soft, shelf habitats (Figure N.1, bottom). The Northern ecoregion has seen the most bottom trawl fishing gear contact with seafloor habitat, with nearly five times the magnitude as observed in the central ecoregion in soft, upper slope habitat. Little to no bottom trawling occurred in the Southern ecoregion during this time series.

A shift in trawling effort from shelf to upper slope habitats was observed during the mid-2000’s, which in part corresponded to depth-related spatial closures implemented by the Council. This difference has narrowed over the past decade. With new spatial closures and openings that began in 2020, this indicator will be of interest to monitor over the next few years for changes in bottom trawl fishing effort. Reduced bottom trawl gear contact may not coincide with recovery times of habitat depending on how fast recovery happens, which is likely to differ among habitat types (e.g., hard and mixed habitats will take longer to recover than soft habitat).

To illustrate spatial variation in bottom trawling activity, we estimated total distance trawled on a 2x2-km grid from 2002-2019 (Figure N.2). For each grid cell, we mapped the 2019 total distance trawled, the 2019 distance anomaly from the long-term mean and the most recent 5-year trend. Off Washington, cells where distance trawled was above average and increasing tended to be in central waters (Figure N.2 center and right, red cells), while northern and southern cells mostly experienced

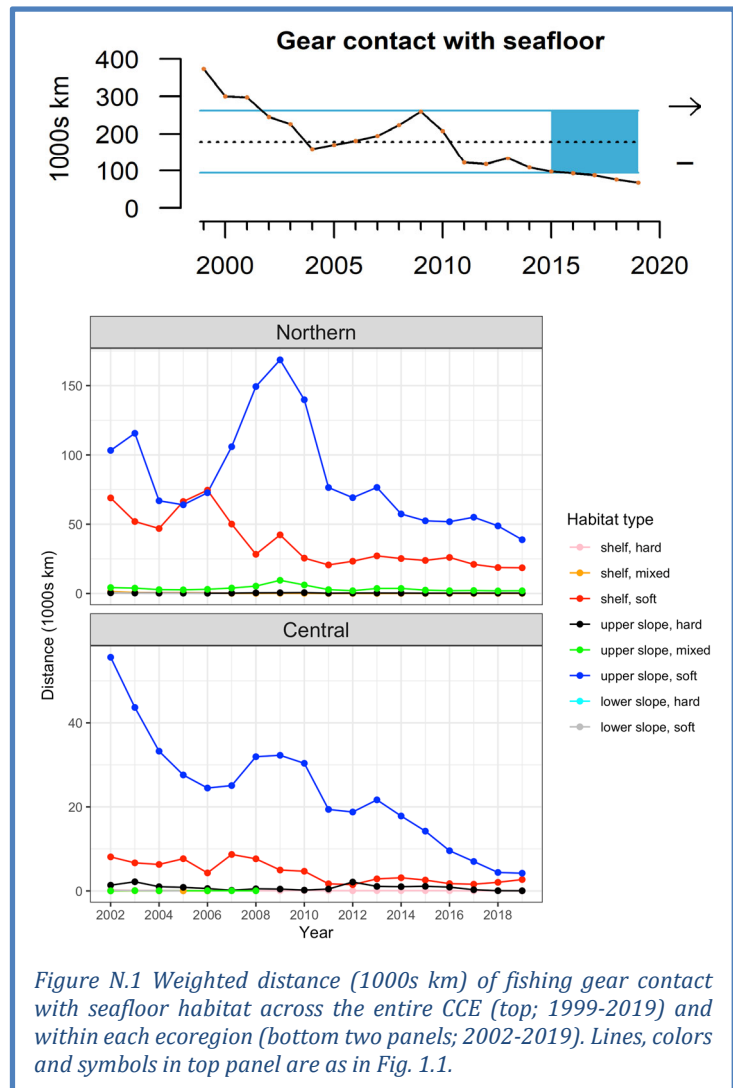


Figure N.1 Weighted distance (1000s km) of fishing gear contact with seafloor habitat across the entire CCE (top; 1999-2019) and within each ecoregion (bottom two panels; 2002-2019). Lines, colors and symbols in top panel are as in Fig. 1.1.

average or below-average bottom contact, with decreasing trawl contact in southern, nearshore waters (Figure N.2 center and right, red cells blue cells). Off Oregon, above-average bottom contact (red cells) in 2019 and increasing trends over the last five years were observed in several patches, the largest of which were off Central Oregon, while below-average anomalies in 2019 and decreasing trends were most concentrated to the south. Off California, the most notable patches of above-average bottom contact in 2019 and increased trawling over the last five years were just north of Cape Mendocino, while cells near the CA/OR border and just north of San Francisco Bay showed areas of below-average and decreasing trends in bottom contact in recent years. These spatial indicators provide more context and information about local conditions than the coastwide aggregated time series which showed bottom trawl gear contact at historically low levels and no trend from 2015 to 2019 (Figure N.1).

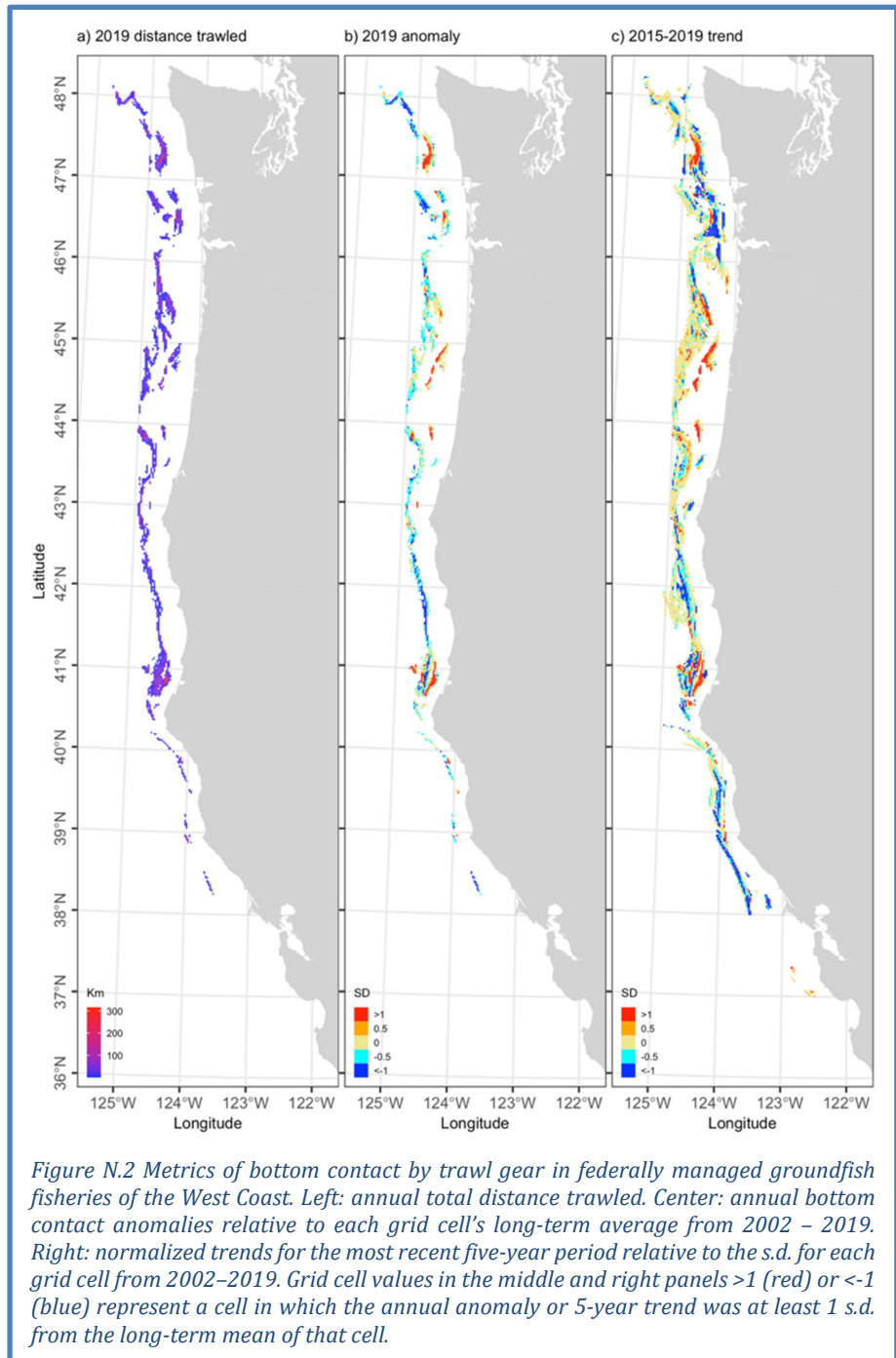
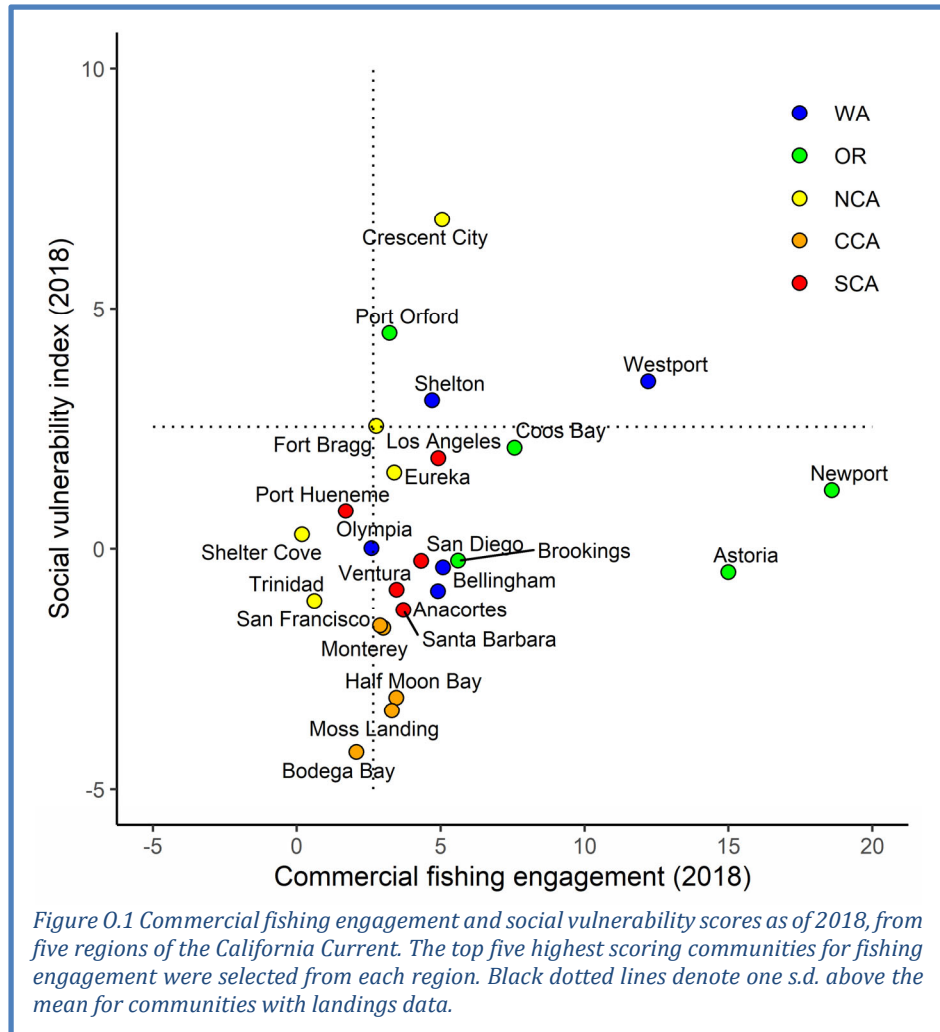


Figure N.2 Metrics of bottom contact by trawl gear in federally managed groundfish fisheries of the West Coast. Left: annual total distance trawled. Center: annual bottom contact anomalies relative to each grid cell's long-term average from 2002 – 2019. Right: normalized trends for the most recent five-year period relative to the s.d. for each grid cell from 2002–2019. Grid cell values in the middle and right panels >1 (red) or <-1 (blue) represent a cell in which the annual anomaly or 5-year trend was at least 1 s.d. from the long-term mean of that cell.

Appendix O SOCIAL VULNERABILITY OF FISHING-DEPENDENT COMMUNITIES

In Section 6.1 of the main report, we present information on the Community Social Vulnerability Index (CSVI) as an indicator of social vulnerability in coastal communities that are dependent upon commercial fishing. Fishery *dependence* can be expressed in terms of engagement, reliance, or by a composite of both. *Engagement* refers to the total extent of fishing activity in a community; it can be expressed in terms of commercial activity (e.g., landings, revenues, permits, processing, etc.) or recreational activity (e.g., number of boat launches, number of charter boat and fishing guide license holders, number of charter boat trips, number of bait and tackle shops, etc.). *Reliance* is the per capita engagement of a community; thus, in two communities with equal engagement, the community with the smaller population would have a higher reliance on its fisheries activities.

In the main body of the report, Figure 6.1.1 plots CSVI in 2018 against commercial reliance for the five most reliant communities in each sector from each of five regions of the CCE. Here, we present a similar plot of CSVI relative to commercial fishing engagement scores from 2018. Figure 0.1 shows commercial fishing-engaged communities and the corresponding social vulnerability results. Communities above and to the right of the dashed lines are at least 1 s.d. above the coastwide averages of both indices. Of note are fishing-oriented communities like Westport, Crescent City, Fort Bragg, Shelton, and Port Orford, which have relatively high commercial fishing engagement results and also a high CSVI composite result.



Information on community-level recreational fishing engagement (number of boat launches, number of charter boat and fishing guide license holders, total charter boat trips, bait shops, etc.) has not been updated beyond 2016. Thus we do not have updated comparisons of CSVI with recreational fishing reliance or engagement.

Appendix P FLEET DIVERSIFICATION INDICATORS FOR MAJOR WEST COAST PORTS

Catches and prices from many fisheries exhibit high interannual variability, leading to high variability in fishermen’s revenue, but variability can be reduced by diversifying activities across multiple fisheries or regions (Kasperski and Holland 2013). It should be noted that there may be good reasons for individuals to specialize, including reduced costs or greater efficiency; thus while diversification may reduce income variation, it does not necessarily promote higher average profitability. Kasperski (AFSC) and Holland (NWFSC) examined diversification of fishing revenue for more than 28,000 vessels fishing off the West Coast and Alaska over the last 39 years. As a measure of diversification, we use the effective Shannon index (ESI). ESI increases as revenues are spread across *more* fisheries, and as revenues are spread more *evenly* across fisheries; ESI = 1 when a vessel’s revenues are from a single species group and region; ESI = 2 if revenues are spread evenly across 2 fisheries; ESI = 3 if revenues are spread evenly across 3 fisheries; and so on. If revenue is not evenly distributed across fisheries, then the ESI value is lower than the number of fisheries a vessel enters.

As is true with individual vessels, the variability of landed value at the port level is reduced with greater diversification of landings. Diversification of fishing revenue has declined over the last 20 years for some ports (Figure P.1). Examples include Seattle and most but not all ports in Southern Oregon and California. However, a few ports have become more diversified including Bellingham Bay and Westport in Washington. Diversification in Astoria, Oregon had been increasing but has decreased in recent years while Brookings has had an erratic trend. Diversification scores are highly variable year-to-year for some ports, particularly those in Southern Oregon and Northern California that depend heavily on the Dungeness crab fishery, which has highly variable landings.

(Note: These indices and plots in Figure P.1 do not include income from recreational charter fleets, which may be an important component of diversification for some ports.)

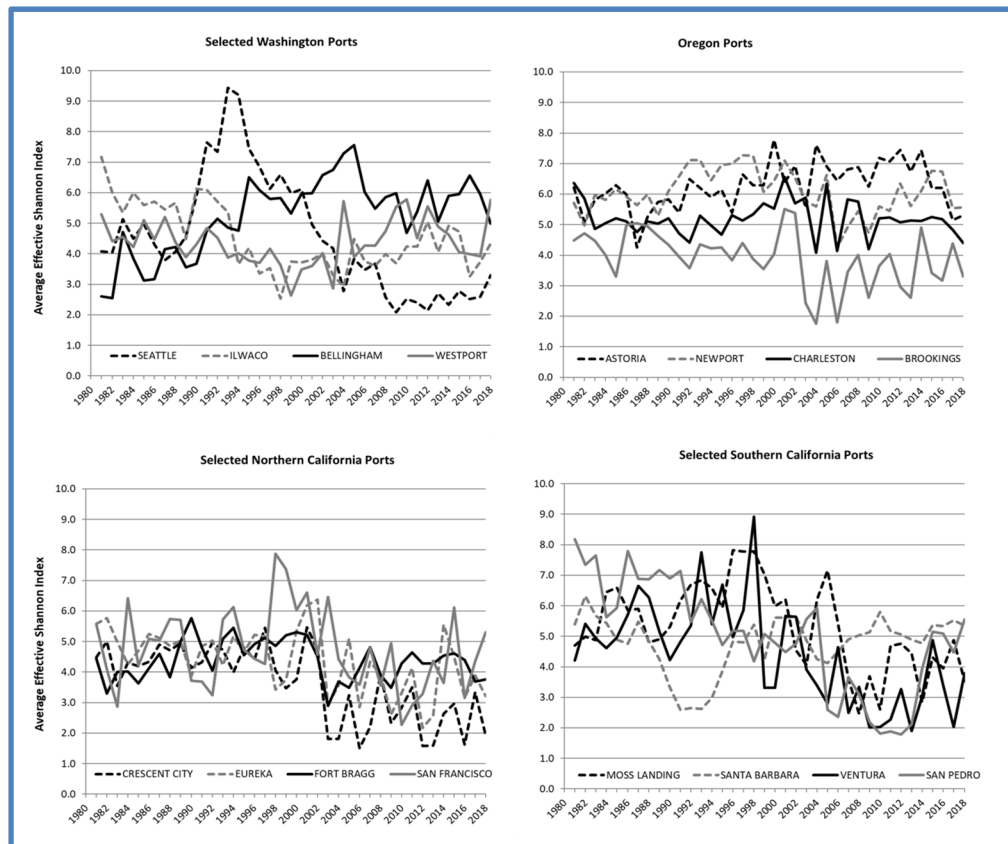


Figure P.1 Trends in fishery revenue diversification in major west coast ports by state. Data from D. Holland (NMFS/NWFSC) and S. Kasperski (NMFS/AFSC).

Appendix Q THEIL INDEX OF FISHERY REVENUE CONCENTRATION

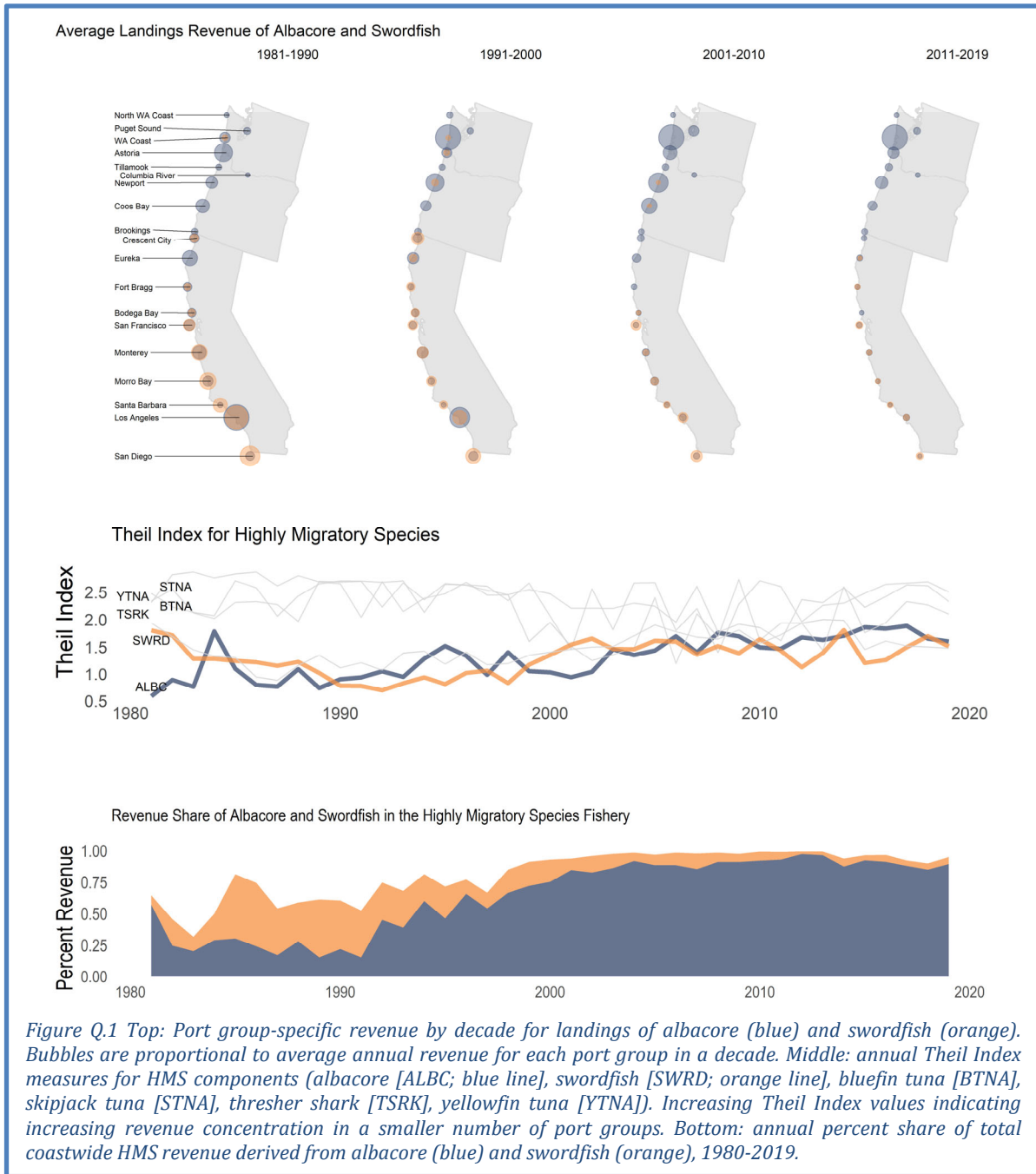
At the request of the Ecosystem Advisory Subpanel, we are working to develop indicators relevant to National Standard 8 (NS-8) of the Magnuson-Stevens Act. NS-8 states that: “Conservation and management measures shall, consistent with the conservation requirements of this Act (including the prevention of overfishing and rebuilding of overfished stocks), take into account the importance of fishery resources to fishing communities by utilizing economic and social data that meet the requirement of paragraph (2) [i.e., National Standard 2], in order to (a) provide for the sustained participation of such communities, and (b) to the extent practicable, minimize adverse economic impacts on such communities.” (NS-2 states that “Conservation and management measures shall be based upon the best scientific information available.”)

In last year’s report we presented a simple exploratory analysis of ex-vessel fishery revenue consolidation in ports on the West Coast, as an initial means of indicating if fishery access opportunities are changing within and across ports and/or FMPs. Following further discussions with the SSC-Ecosystem Subcommittee, we updated our methodology to use the Theil Index (Theil 1967) as an annual measure of geographic concentration of fishery revenue. Though it typically measures economic inequality, the Theil Index may be developed and applied in varying contexts. Here, we use the Theil Index as an estimate of how observed revenue is concentrated within ports, relative to what revenues would be if they were distributed with perfect equality across those ports.

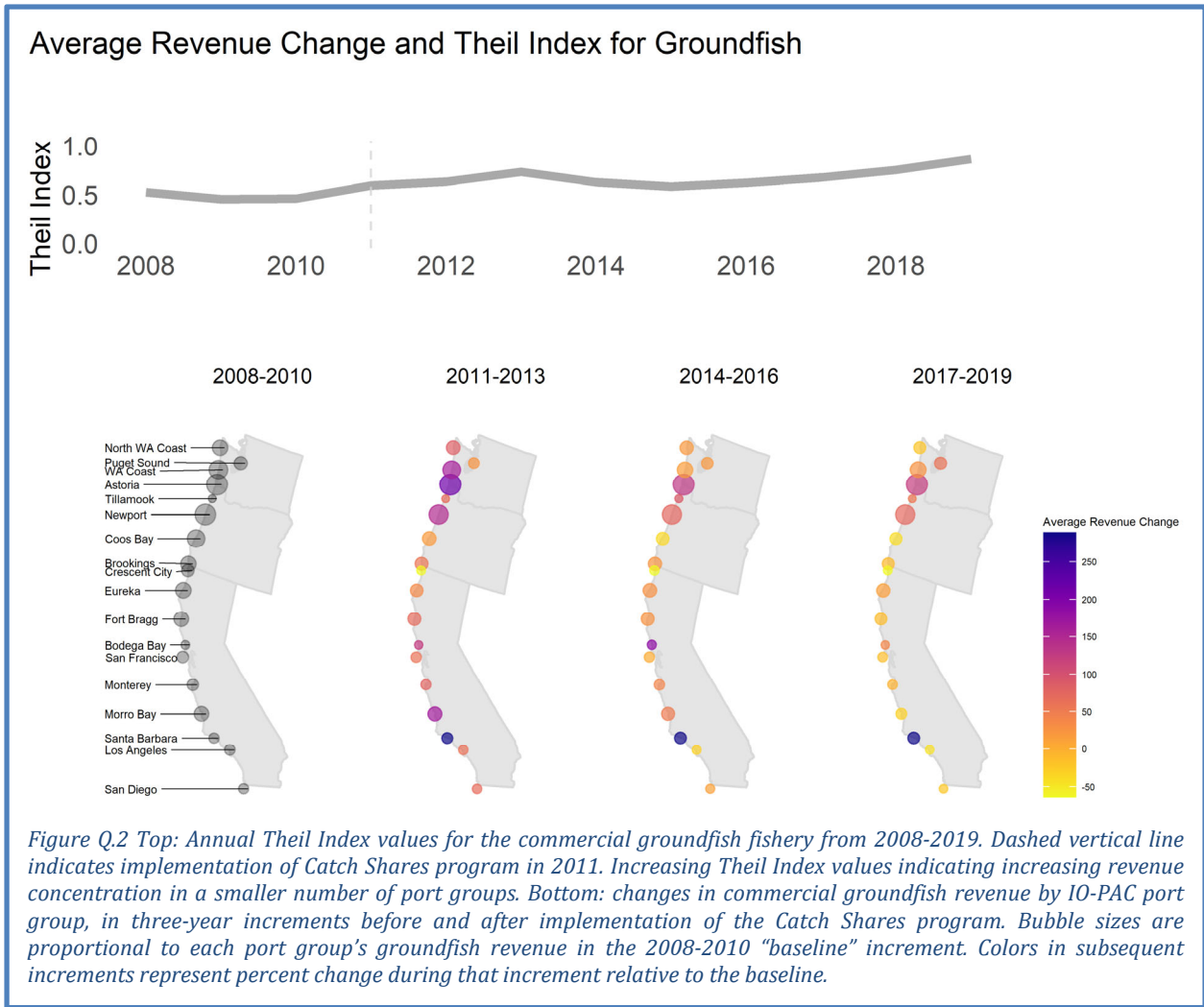
The Theil Index is a single annual measure of geographic concentration of revenue for a particular fishery or group of fisheries. We calculated the annual Theil Index from 1981-2019 for all West Coast commercial fisheries combined, eight broad fishery management groups, and, finally, at the level of individual species within those fishery management groups. The eight management groups are: All Commercial Fisheries; Coastal Pelagic Species; Salmon; Groundfish; Highly Migratory Species; Crabs; Shrimps and Prawns; and Other Species. We calculated the Theil Index to estimate revenue concentration across West Coast ports, at the level of the port-groups established with the input-output model for Pacific Coast fisheries (IO-PAC; Leonard and Watson 2011). The IO-PAC approach aggregates 97 fisheries landing locations to 21 port groups over the 1981-2019 time period.

In the main body, we showed how the Theil Index for All Fisheries has not exhibited high levels or extended trends of geographic concentration, but that different fishery management groups demonstrated clearer patterns of high variability over the study period, extended trends of decreasing or increasing concentration, or both (Figure 6.3.1). Here, we more closely examine annual changes in the Theil Index for two important West Coast fishery management groups in more depth.

First, as was shown in Figure 6.3.1, Theil Index values for HMS generally decreased from 1981 to 2002, indicating movement toward more equal distribution of HMS revenues across West Coast port groups, but then returned to higher annual values from 2003 to 2019, suggesting increased concentration of HMS revenue across fewer ports. In examining the annual Theil index measures for the individual species in the HMS category, we see evidence that shifts in HMS revenue concentration are largely due to changes in revenue distribution of two important species, swordfish and albacore. Swordfish, which contributed to HMS revenues in the early portion of the time series and were concentrated in the south, were replaced in more recent years by albacore, the revenues for which have come to dominate the HMS category (Figure Q.1). Landings revenues for swordfish and albacore are averaged over ten year periods and mapped to West Coast ports at the top of Figure Q.1. The Theil Index for HMS has generally increased over the past decade as the revenue share of albacore increased within the management group. Accordingly, greater geographic concentration of HMS revenues have corresponded with a shift in revenues to more northern ports, where albacore landings have recently been concentrated.



Our second case study is groundfish. In Figure Q.2, we focus on Theil Index values for groundfish beginning in 2008, three years prior to implementation of the Pacific Coast Trawl Catch Shares Program in 2011. As shown in the main report in Figure 6.3.1, Theil Index values for groundfish have been trending fairly continuously toward increased geographic concentration of revenues over the full time period, both prior to and after the 2011 change in the structure of groundfish management. While groundfish revenues have been increasingly concentrated across fewer West Coast ports, some research suggests this increasing concentration is not distinct from trends for other, non-groundfish fisheries (Speir and Lee 2021). In general, increased concentration of groundfish revenues has occurred in northern ports, as demonstrated by the map at the bottom of Figure Q.2. The maps indicate changes in groundfish revenues averaged over three year periods through 2019, with



groundfish revenue shares for 2008-2010, on the far left, presented as a baseline.

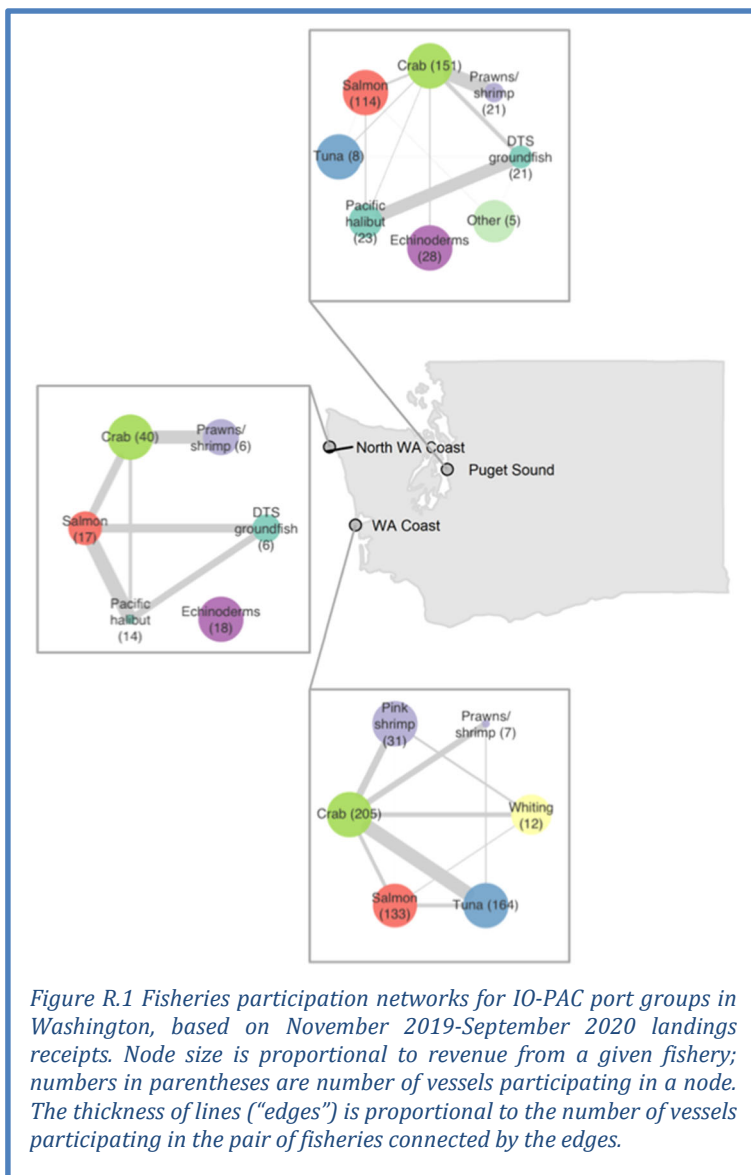
We will continue to develop these analyses for all fishery groups, in consultation with Council advisory bodies. We have made no effort yet to attribute changes in revenue concentration with management actions, environmental changes, food web changes, or changes within coastal communities. It is therefore premature to conclude that this is an effective indicator in the context of NS-8, or what changes in the index mean in terms of potential Council considerations. We also note that by pooling coastal communities into IO-PAC port groups, we are aggregating many communities at coarser scales than are appropriate for NS-8 considerations, which are attuned to communities rather than port groups. Community-scale estimation of the Theil Index is possible, and we should anticipate different qualitative and quantitative outcomes than those presented here once the scale is refined to the community level. Community-scale estimation will increase the complexity of data analysis, presentation and visualization, which will be an important discussion point between the IEA team and the Council if we continue to present this metric.

Appendix R FISHERIES PARTICIPATION NETWORKS

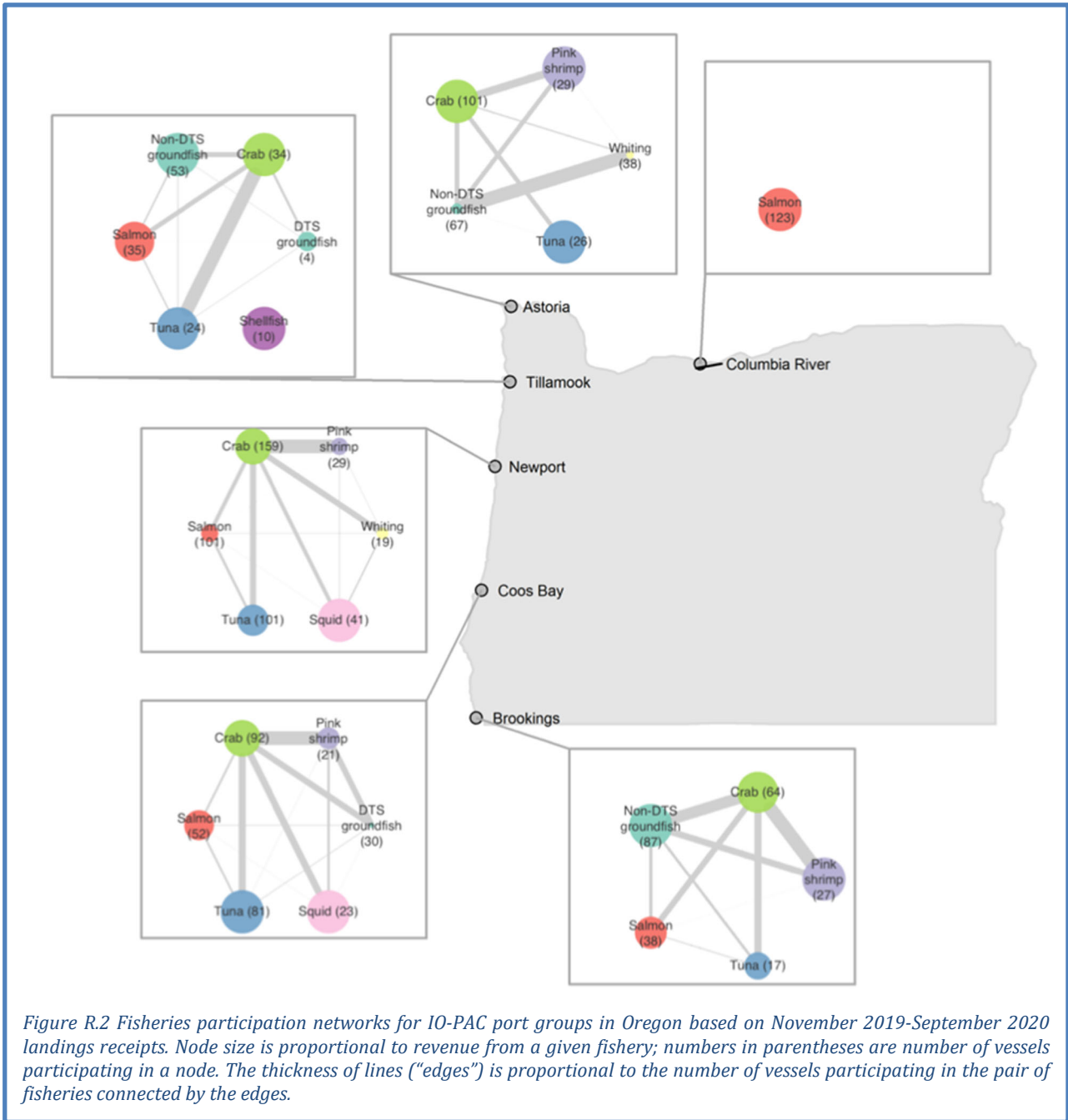
The connectivity reflected in fisheries participation networks reflects alternative sources of income from fisheries in different places—or community portfolios. These portfolios can be described on a variety of spatial and temporal scales (Fuller et al. 2017, Anderson et al. 2017, Addicott et al. 2018,

Beaudreau et al. 2019, Kroetz et al. 2019, Frawley et al. 2020, Fisher et al. 2021). These networks provide insights complementary to those of time series of landings, revenue, and diversification, by revealing place-based patterns of cross-fishery participation for individual vessels. They also provide refined information about how component fisheries contribute to geographic variation in the fishing reliance index. In so doing, fisheries participation networks offer one way to respond to requests from the Ecosystem Advisory Subpanel and Ecosystem Workgroup for deeper characterization of the social and economic conditions in U.S. West Coast fishing communities, and information relevant to the implementation of NS-8 under the Magnuson-Stevens Act.

Here we present illustrations of fisheries participation networks for IO-PAC port groups in Washington (Figure R.1), Oregon (Figure R.2), Northern and Central California (Figure R.3), and Southern California (Figure R.4) (except for Other Coastal WA and Unknown Ports). The fisheries participation networks presented here rely upon landings receipts from November 2019 through October 2020, aggregated into the 21 IO-PAC port groups. Nodes in these networks represent fisheries, organized based on the species groupings used in the diversification index time series (as in Section 6.2 and Appendix P; from Kasperski and Holland 2013), with node size scaled according to the amount of revenue generated by a fishery in each port group. The lines connecting pairs of nodes, or edges, indicate vessels that participate in both fisheries, and the widths of these edges scale with the number of vessels exhibiting this behavior. To maintain confidentiality, we include only fisheries with at least 3 vessels participating in a port group. Furthermore, a given fishery must contribute to at least 10% of a vessel's seasonal revenue for that vessel and fishery to be included in the network. Vessels are represented in all port groups for which their landings meet these conditions.



The networks presented here and in the main report, along with those for years 2004-2019, can be viewed at https://github.com/jameals/cciea_networks/tree/main/data/networks/participation.



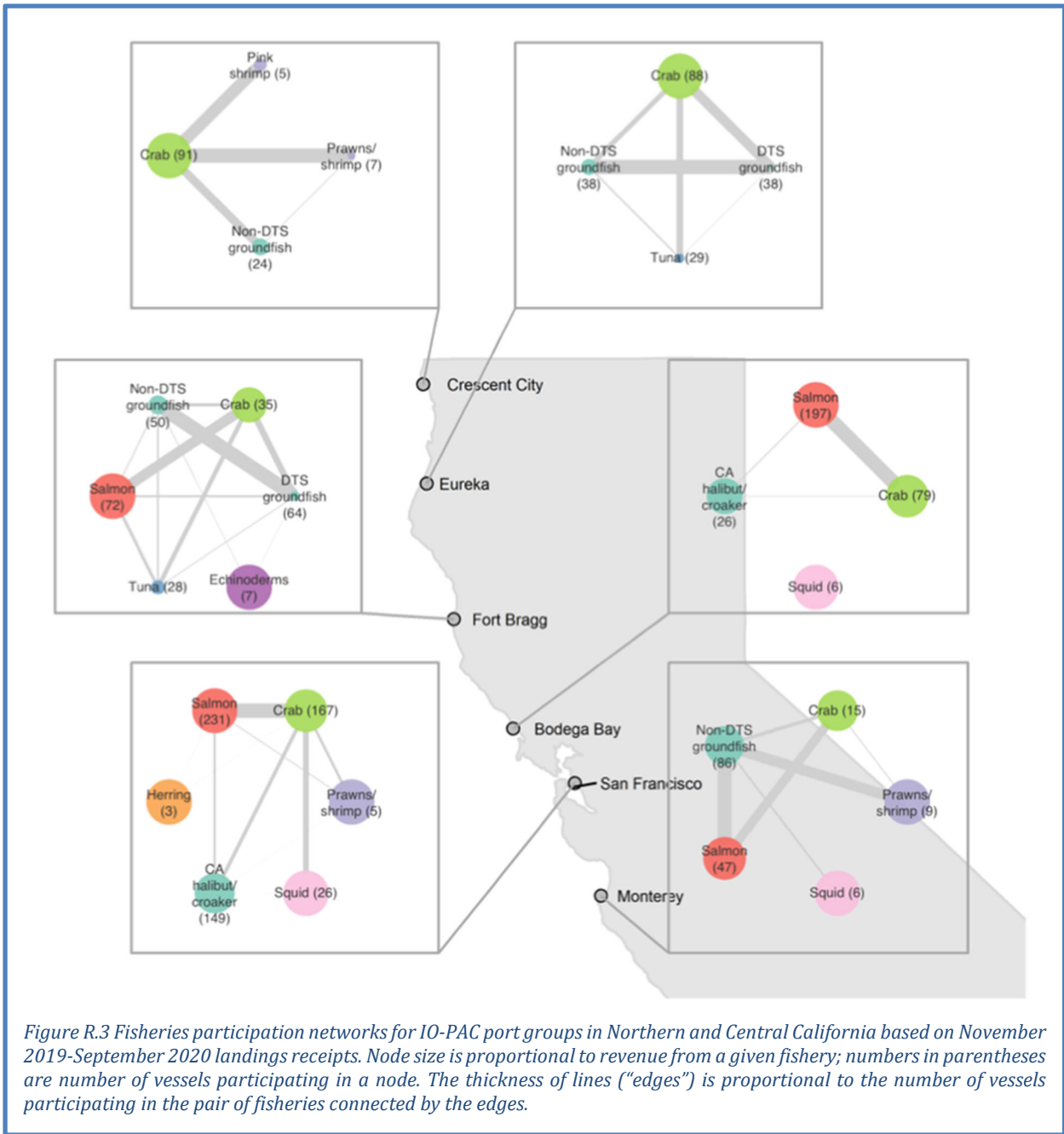
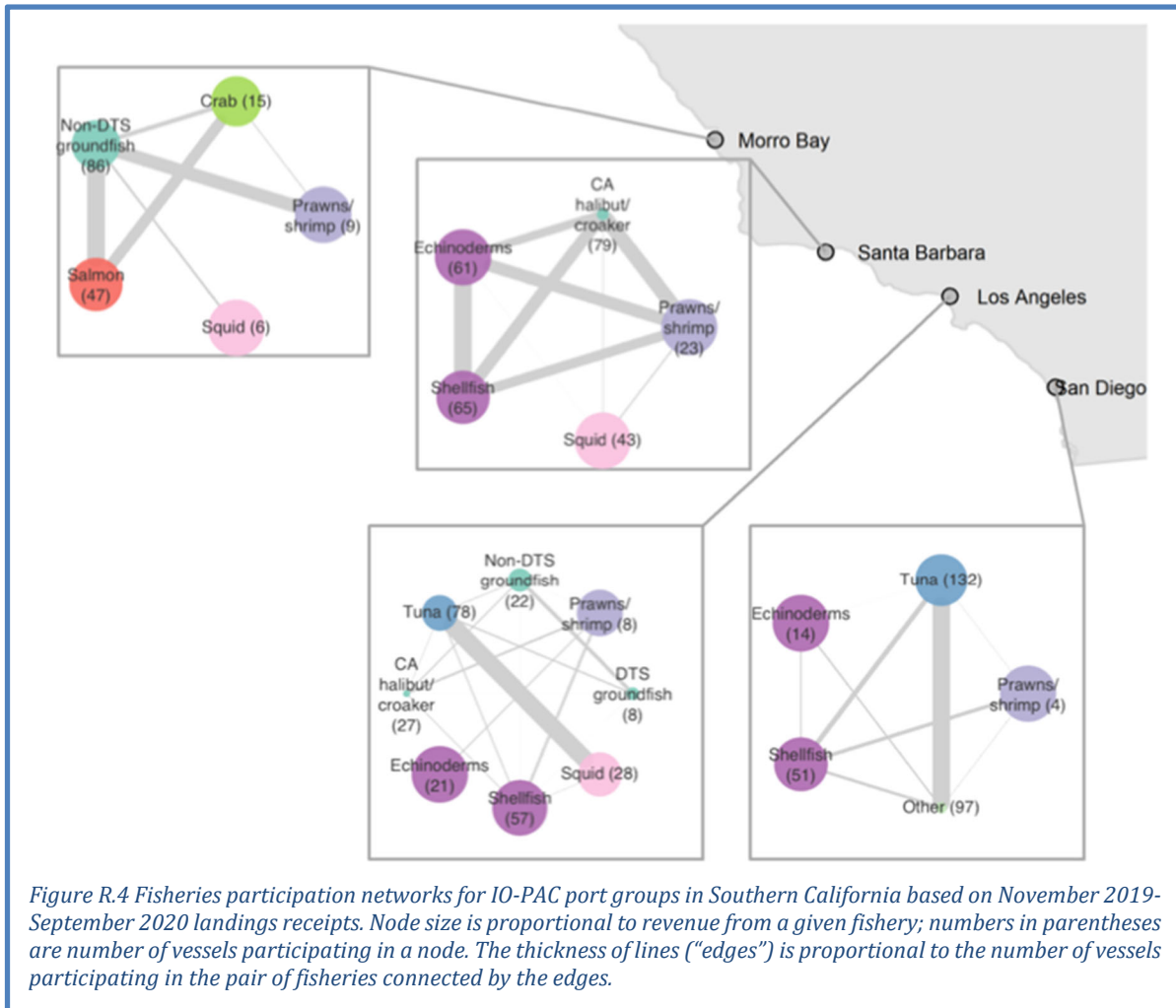


Figure R.3 Fisheries participation networks for IO-PAC port groups in Northern and Central California based on November 2019-September 2020 landings receipts. Node size is proportional to revenue from a given fishery; numbers in parentheses are number of vessels participating in a node. The thickness of lines ("edges") is proportional to the number of vessels participating in the pair of fisheries connected by the edges.



Appendix S REFERENCES

- Abell, R., *et al.* 2008. Freshwater ecoregions of the world: A new map of biogeographic units for freshwater biodiversity conservation. *BioScience* 58:403-414.
- Addicott, E.T., *et al.* 2018. Identifying the potential for cross-fishery spillovers: a network analysis of Alaskan permitting patterns. *Canadian Journal of Fisheries and Aquatic Sciences* 76:56–68.
- Anderson, S.C., *et al.* 2017. Benefits and risks of diversification for individual fishers. *Proceedings of the National Academy of Sciences* 114:10797-10802.
- Beaudreau, A.H., *et al.* 2019. Thirty years of change and the future of Alaskan fisheries: shifts in fishing participation and diversification in response to environmental, regulatory and economic pressures. *Fish and Fisheries* 20: 601-619.
- Bednaršek, N., *et al.* 2020. Exoskeleton dissolution with mechanoreceptor damage in larval Dungeness crab related to severity of present-day ocean acidification vertical gradients. *Science of the Total Environment*, article no. 136610.
- Brodeur, R.D., *et al.* 2019. Major shifts in pelagic micronekton and macrozooplankton community structure in an upwelling ecosystem related to an unprecedented marine heatwave. *Frontiers in Marine Science* 6:212.
- Burke, B.J., *et al.* 2013. Multivariate models of adult Pacific salmon returns. *PLoS One* 8:e54134.
- Chan, F., *et al.* 2008. Emergence of anoxia in the California Current large marine ecosystem. *Science* 319:920-920.

- DeLong, R.L., *et al.* 1973. Premature births in California sea lions: Association with high organochlorine pollutant residue levels. *Science* 181:1168-1170.
- DeLong, R.L., *et al.* 1991. Effects of the 1982-1983 El Niño on several population parameters and diet of California sea lions on the California Channel Islands. Pages 166-172 in F. Trillmich and K. A. Ono, editors. *Pinnipeds and El Niño: Responses to environmental stress*. Springer-Verlag, Berlin.
- DeLong, R.L., *et al.* 2017. Age-and sex-specific survival of California sea lions (*Zalophus californianus*) at San Miguel Island, California. *Marine Mammal Science* 33:1097-1125.
- Dyson, K., and Huppert, D.D. 2010. Regional economic impacts of razor clam beach closures due to harmful algal blooms (HABs) on the Pacific coast of Washington. *Harmful Algae* 9: 264-271.
- Feely, R.A., *et al.* 2008. Evidence for upwelling of corrosive "acidified" water onto the continental shelf. *Science* 320:1490-1492.
- Fisher, J.L., *et al.* 2015. The impact of El Niño events on the pelagic food chain in the northern California Current. *Global Change Biology* 21:4401-4414.
- Fisher, M.C., *et al.* 2021. Climate shock effects and mediation in fisheries. PNAS 118.
- Frawley, T.H., *et al.* 2021. Changes to the structure and function of an albacore fishery reveal shifting social-ecological realities for Pacific Northwest fishermen. *Fish and Fisheries* (in press).
- Friedman, W.R., *et al.* 2019. Modeling composite effects of marine and freshwater processes on migratory species. *Ecosphere* 10:e02743.
- Fuller, E.C., *et al.* 2017. Characterizing fisheries connectivity in marine social-ecological systems. *ICES Journal of Marine Science* 74:2087-2096.
- Gilmartin, W.G., *et al.* 1976. Premature parturition in the California sea lion. *Journal of Wildlife Diseases* 12:104-115.
- Goldstein, T., *et al.* 2009. The role of domoic acid in abortion and premature parturition of California sea lions (*Zalophus californianus*) on San Miguel Island, California. *Journal of Wildlife Diseases* 45:91-108.
- Hall, J.E., *et al.* 2018. Large river habitat complexity and productivity of Puget Sound Chinook salmon. *PLoS One* 13(11), p.e0205127.
- Harvey, C.J. *et al.* 2020. Ecosystem status report of the California Current for 2019-20: a summary of ecosystem indicators compiled by the California Current Integrated Ecosystem Assessment team (CCIEA). NOAA Tech. Memo. NMFS-NWFSC-160.
- Hobday, A.J., *et al.* 2016. A hierarchical approach to defining marine heatwaves. *Progress in Oceanography* 141:227-238.
- Iverson, S. J., *et al.* 1991. The effect of El Niño on pup development in the California sea lion (*Zalophus californianus*). Pages 180-184 in F. Trillmich and K. A. Ono, editors. *Pinnipeds and El Niño: Responses to environmental stress*. Springer-Verlag, Berlin.
- Jacox, M.G., *et al.* 2017. On the skill of seasonal sea surface temperature forecasts in the California Current System and its connection to ENSO variability. *Climate Dynamics* 53:7519-7533.
- Jacox, M.G., *et al.* 2018. Coastal upwelling revisited: Ekman, Bakun, and improved upwelling indices for the U.S. west coast. *Journal of Geophysical Research: Oceans* 123:7332-7350.
- Jacox, M.G., *et al.* 2020. Thermal displacement by marine heatwaves. *Nature* 584:82-86.
- Jager, H.I., *et al.* 1997. Modelling the linkages between flow management and salmon recruitment in rivers. *Ecological Modelling* 103:171-191.
- Jepson, M., and L.L. Colburn. 2013. Development of social indicators of fishing community vulnerability and resilience in the U.S. Southeast and Northeast Regions. NOAA Tech. Memo. NMFS-F/SPO-129.
- Jordan, M.S. 2012. Hydraulic predictors and seasonal distribution of *Manayunkia speciosa* density in the Klamath River, CA, with implications for ceratomyxosis, a disease of salmon and trout. MS thesis, Oregon State University, 79 pp.
- Kasperski, S., and D.S. Holland. 2013. Income diversification and risk for fishermen. *Proceedings of the National Academy of Sciences* 110:2076-2081.
- Keister, J.E., *et al.* 2011. Zooplankton species composition is linked to ocean transport in the Northern California Current. *Global Change Biology* 17:2498-2511.
- Kroetz, K., *et al.* 2019. Defining the economic scope for ecosystem-based fishery management. *Proceedings of*

- the National Academy of Sciences* 116:4188–4193.
- Laake, J.L., *et al.* 2018. Population growth and status of California sea lions. *Journal of Wildlife Management* 82:583-595.
- Lefebvre, K.A., *et al.* 2002. From sanddabs to blue whales: the pervasiveness of domoic acid. *Toxicon* 40:971-977.
- Leising, A.W., in revision. Marine heatwaves of the North East Pacific from 1982-2019: a Blobtrospective. *Journal of Geophysical Research: Oceans*.
- Leonard, J., and P. Watson. 2011. Description of the input-output model for Pacific Coast fisheries. NOAA Tech. Memo. NMFS-NWFSC-111.
- Limm, M.P. and M.P. Marchetti. 2009. Juvenile Chinook salmon (*Oncorhynchus tshawytscha*) growth in off-channel and main-channel habitats on the Sacramento River, CA using otolith increment widths. *Environmental Biology of Fishes* 85:141-151.
- Lindgren, F., and H. Rue. 2015. Bayesian spatial modelling with R-INLA. *Journal of Statistical Software* 63:1-25.
- Lyons, E., *et al.* 2005. Seasonal prevalence and intensity of hookworms (*Uncinaria* spp.) in California sea lion (*Zalophus californianus*) pups born in 2002 on San Miguel Island, California. *Parasitology Research* 96:127-132.
- McCabe, R.M., *et al.* 2016. An unprecedented coastwide toxic algal bloom linked to anomalous ocean conditions. *Geophysical Research Letters* 43:10366-10376.
- McKibben, M., *et al.* 2017. Climatic regulation of the neurotoxin domoic acid. *Proceedings of the National Academy of Sciences* 114:239-244.
- Melin, S.R., *et al.* 2008. The effects of El Niño on the foraging behavior of lactating California sea lions (*Zalophus californianus californianus*) during the nonbreeding season. *Canadian Journal of Zoology* 86:192-206.
- Melin, S.R., *et al.* 2010. Unprecedented mortality of California sea lion pups associated with anomalous oceanographic conditions along the central California coast in 2009. *CalCOFI Reports* 51:182-194.
- Melin, S.R., *et al.* 2012a. California sea lions: an indicator for integrated ecosystem assessment of the California Current system. *CalCOFI Reports* 53:140-152.
- Melin, S.R., *et al.* 2012b. Age-specific recruitment and natality of California sea lions at San Miguel Island, California. *Marine Mammal Science* 28:751-776.
- Morgan, C.A., *et al.* 2019. Recent ecosystem disturbance in the northern California Current. *Fisheries* 44:465-474.
- Morley, J.W., *et al.* 2018. Projecting shifts in thermal habitat for 686 species on the North American continental shelf. *PLoS One* 13:e0196127.
- Munsch, S.H., *et al.* 2019. Warm, dry winters truncate timing and size distribution of seaward-migrating salmon across a large, regulated watershed. *Ecological Applications* 29:p.e01880.
- Munsch, *et al.* 2020. Science for integrative management of a diadromous fish stock: interdependencies of fisheries, flow, and habitat restoration. *Canadian Journal of Fisheries and Aquatic Sciences* 77:1487-1504.
- Neveu, E., *et al.* 2016. An historical analysis of the California Current circulation using ROMS 4D-Var: system configuration and diagnostics. *Ocean Modelling* 99:131-151.
- NMFS, 2021. West coast fisheries impacts from COVID-19. US Department of Commerce.
- Nye, J.A., *et al.* 2009. Changing spatial distribution of fish stocks in relation to climate and population size on the Northeast United States continental shelf. *Marine Ecology Progress Series* 393:111-129.
- Peterson, W.T., *et al.* 2014. Applied fisheries oceanography ecosystem indicators of ocean condition inform fisheries management in the California Current. *Oceanography* 27:80-89.
- Ralston, S., *et al.* 2013. Interannual variation in pelagic juvenile rockfish (*Sebastes* spp.) abundance—going with the flow. *Fisheries Oceanography* 22:288-308.
- Reis, G.J., *et al.* 2019. Clarifying effects of environmental protections on freshwater flows to—and water exports from—the San Francisco Bay Estuary. *San Francisco Estuary and Watershed Science* 17(1).
- Ritzman, J., *et al.* 2018. Economic and sociocultural impacts of fisheries closures in two fishing-dependent communities following the massive 2015 US West Coast harmful algal bloom. *Harmful Algae* 80:35-45.
- Robertson, R.R., and E.P. Bjorkstedt. 2020. Climate-driven variability in *Euphausia pacifica* size distributions off northern California, *Progress in Oceanography* 188:102412.

- Rudnick, D.L., *et al.* 2017. A climatology using data from the California Underwater Glider Network - Dataset. Scripps Institution of Oceanography. doi: 10.21238/S8SPRAY7292
- Samhoury, J.F., *et al.* 2017. Defining ecosystem thresholds for human activities and environmental pressures in the California Current. *Ecosphere* 8:e01860.
- Santora, J.A., *et al.* 2020. Habitat compression and ecosystem shifts as potential links between marine heatwave and record whale entanglements. *Nature Communications* 11:536.
- Satterthwaite, W.H., *et al.* 2014. Match-mismatch dynamics and the relationship between ocean-entry timing and relative ocean recoveries of Central Valley fall run Chinook salmon. *Marine Ecology Progress Series* 511:237-248.
- Scannell, H.A., *et al.* 2020. Subsurface evolution and persistence of marine heatwaves in the Northeast Pacific. *Geophysical Research Letters* 10.1029/2020GL090548.
- Selden, R.L., *et al.* 2020. Coupled changes in biomass and distribution drive trends in availability of fish stocks to US West Coast ports. *ICES Journal of Marine Science* 77:188-199.
- Speir, C. and Lee, M. 2021. Geographic distribution of commercial fishing landings and port consolidation following ITQ implementation. *Journal of Agricultural and Resource Economics* 46:152-169.
- Strange, J.S., 2012. Migration strategies of adult Chinook salmon runs in response to diverse environmental conditions in the Klamath River basin. *Transactions of the American Fisheries Society* 141:1622-1636.
- Sturrock, A.M., *et al.* 2019. Eight decades of hatchery salmon releases in the California Central Valley: factors influencing straying and resilience. *Fisheries* 44:433-444.
- Sykes, G.E., *et al.* 2009. Temperature and flow effects on migration timing of Chinook salmon smolts. *Transactions of the American Fisheries Society* 138:1252-1265.
- Theil, H. 1967. *Economics and Information Theory*. Rand McNally, Chicago.
- Thompson, A.R., *et al.* 2019a. Indicators of pelagic forage community shifts in the California Current Large Marine Ecosystem, 1998–2016. *Ecological Indicators* 105:215-228.
- Thompson, A.R., *et al.* 2019b. State of the California Current 2018-19: a novel anchovy regime and a new marine heatwave? CalCOFI Reports 60:1-65.
- Thorson, J.T. 2019. Guidance for decisions using the Vector Autoregressive Spatio-Temporal (VAST) package in stock, ecosystem, habitat and climate assessments. *Fisheries Research* 210:143-161.
- Wells, B.K., *et al.* 2008. Relationships between oceanic conditions and growth of Chinook salmon (*Oncorhynchus tshawytscha*) from California, Washington, and Alaska, USA. *Fisheries Oceanography* 17:101-125.